

**CHARACTERIZATION OF SMOOTH MUSCLE CELL PHENOPTYPE AND  
FUNCTIONALITY FOR POTENTIAL TISSUE ENGINEERING APPLICATIONS**

by

**Sanket N. Patel**

B.S., North Carolina State University, 2006

Submitted to the Graduate Faculty of  
Swanson School of Engineering in partial fulfillment  
of the requirements for the degree of  
Master of Science

University of Pittsburgh

2009

UNIVERSITY OF PITTSBURGH  
SWANSON SCHOOL OF ENGINEERING

This thesis was presented

by

Sanket N. Patel

It was defended on

July 24, 2009

and approved by

Bridget M. Deasy, Ph.D., Assistant Professor, Departments of Orthopedic Surgery and  
Bioengineering

Claudette M. St.Croix, Ph.D., Assistant Professor, Department of Environmental and  
Occupational Health

Thesis Advisor: David A. Vorp, Ph.D., Professor, Departments of Surgery and  
Bioengineering

Copyright © by Sanket N. Patel

2009

# **CHARACTERIZATION OF SMOOTH MUSCLE CELL PHENOTYPE AND FUNCTIONALITY FOR POTENTIAL TISSUE ENGINEERING APPLICATIONS**

Sanket N. Patel, M.S.

University of Pittsburgh, 2009

Smooth muscle cell (SMC) embedded scaffolds have possible applications in treating diseased tissues that are rich in SMCs. Stress urinary incontinence (SUI) is an example of a disease that can be caused due to SMC dysfunction within the urinary sphincter.

The goal of this thesis was to create a SMC-populated tissue engineered urethral wrap (TEUW) using autologous urethral SMCs (uSMCs), to be used as a cuff around the native urethra to integrate with the host tissue for providing mechanical and functional reinforcement to the diseased urethra. uSMCs were isolated from rat urethras. SMC phenotype was verified by immunofluorescence and western blotting. Isolation purity was assessed by staining uSMCs for skeletal muscle and urothelium markers since they are also present in the urethra. TEUWs were examined for SMC phenotype, apoptosis, mechanical and histological endpoints after culture.

This thesis also evaluated the functionality of differentiated SMCs (dSMCs), which were derived via mechanical stimulation of bone marrow-derived mesenchymal stem cell (BMMSCs). The long-term objective is to use BMMSCs as an autologous source for SMCs in order to create TEUW-like tubular constructs for treating SMC related dysfunctions including, but not limited to SUI. uSMCs and dSMCs were assessed and compared for intracellular  $Ca^{2+}$  activity (fura-2) and contractile responses (live-cell) to various stimuli.

Results of isolated uSMCs revealed expression of SMC markers and absence of skeletal and urothelium markers, suggesting isolation purity. uSMC-based TEUWs showed non-linear

pressure-diameter profiles like soft tissues, greater compliance than the native urethra, and burst pressures similar to stem-cell based TEUWs. Both, uSMCs and dSMCs, exhibited intracellular  $Ca^{2+}$  activity, with and without extracellular  $Ca^{2+}$ , vital for full SMC function. However, their failure to show morphological changes in the presence of agonists during contractility assessment indicated absence of mature SMCs.

In summary, this study demonstrates proficient uSMC isolation, which represents an important step towards TEUW development, and that uSMCs and dSMCs are not fully functional at the differentiation stage tested. Future work should focus on increasing contractile protein expression by using matrix-like culture systems and/or biochemical stimulants. Following a systematic examination, SMC-populated TEUWs could be tested in an animal model.

## TABLE OF CONTENTS

<b>NOMENCLATURE.....</b>	<b>XIV</b>
<b>PREFACE.....</b>	<b>XVII</b>
<b>1.0 INTRODUCTION.....</b>	<b>1</b>
<b>1.1 SMOOTH MUSCLE CELLS .....</b>	<b>2</b>
<b>1.1.1 SMC contraction .....</b>	<b>3</b>
<b>1.1.2 SMC markers .....</b>	<b>4</b>
<b>1.1.2.1 Smooth muscle <math>\alpha</math>-actin .....</b>	<b>5</b>
<b>1.1.2.2 Calponin.....</b>	<b>6</b>
<b>1.1.2.3 Myosin heavy chain .....</b>	<b>6</b>
<b>1.2 LOWER URINARY TRACT .....</b>	<b>7</b>
<b>1.2.1 Micturition.....</b>	<b>8</b>
<b>1.2.2 SMC role in urethral function .....</b>	<b>10</b>
<b>1.3 URETHRAL DYSFUNCTION .....</b>	<b>12</b>
<b>1.3.1 Stress urinary incontinence.....</b>	<b>12</b>
<b>1.3.1.1 Demographics.....</b>	<b>13</b>
<b>1.3.1.2 SUI mechanisms.....</b>	<b>14</b>
<b>1.3.1.3 Current treatments and their limitations .....</b>	<b>14</b>
<b>1.3.2 Diabetes mellitus .....</b>	<b>16</b>

1.3.3	Spinal cord injury .....	17
1.3.4	Vaginal distension .....	17
1.4	<b>THE PROMISE OF REGENERATIVE MEDICINE .....</b>	<b>18</b>
1.4.1	Cell sourcing .....	19
1.4.1.1	Stem cells .....	20
1.4.2	Scaffolds .....	25
1.4.2.1	The use of fibrin as a scaffold in regenerative medicine .....	26
2.0	<b>HYPOTHESIS AND SPECIFIC AIMS.....</b>	<b>29</b>
3.0	<b>CHARACTERIZATION OF ISOLATED AND CULTURED URETHRAL SMOOTH MUSCLE CELLS .....</b>	<b>32</b>
3.1	<b>METHODS.....</b>	<b>32</b>
3.1.1	Animals .....	32
3.1.2	Tissue Isolation.....	33
3.1.3	Cell isolation and culture.....	34
3.1.4	Immunofluorescence.....	37
3.1.5	Western blotting.....	38
3.2	<b>RESULTS .....</b>	<b>40</b>
3.2.1	Morphology .....	40
3.2.2	Immunofluorescence.....	40
3.2.3	Western blotting.....	45
3.3	<b>DISCUSSION.....</b>	<b>47</b>
4.0	<b>INCORPORATION OF URETHRAL SMOOTH MUSCLE CELLS INTO A TISSUE ENGINEERED URETHRAL WRAP.....</b>	<b>51</b>

<b>4.1</b>	<b>METHODS.....</b>	<b>52</b>
4.1.1	Fabrication of a TEUW .....	52
4.1.2	Immunofluorescence.....	53
4.1.3	Apoptosis.....	53
4.1.4	Histology .....	54
4.1.5	Mechanical testing .....	55
4.1.6	Statistics .....	57
<b>4.2</b>	<b>RESULTS.....</b>	<b>58</b>
4.2.1	Immunofluorescence.....	58
4.2.2	Apoptosis.....	58
4.2.3	Histology .....	61
4.2.3.1	Hematoxylin and eosin .....	61
4.2.3.2	Masson't trichrome .....	62
4.2.3.3	Picrosirius red .....	63
4.2.4	Mechanical testing .....	63
4.2.4.1	Pressure-diameter relationship .....	64
4.2.4.2	Compliance.....	65
4.2.4.3	Burst pressure .....	66
<b>4.3</b>	<b>DISCUSSION.....</b>	<b>67</b>
<b>5.0</b>	<b>FUNCTIONALITY OF ISOLATED URETHRAL SMOOTH MUSCLE CELLS AND DIFFERENTIATED SMOOTH MUSCLE CELLS.....</b>	<b>71</b>
<b>5.1</b>	<b>METHODS.....</b>	<b>72</b>
5.1.1	Cell source and characterization .....	72

5.1.2	Cyclic stretch apparatus.....	73
5.1.3	Morphology .....	74
5.1.4	Immunofluorescence.....	75
5.1.5	Calcium imaging .....	75
5.1.6	Contraction assessment .....	77
5.2	RESULTS .....	78
5.2.1	Morphology .....	78
5.2.2	Immunofluorescence.....	80
5.2.3	Calcium imaging .....	83
5.2.4	Contraction assessment .....	85
5.3	DISCUSSION.....	86
6.0	CONCLUSIONS .....	90
7.0	FUTURE WORK.....	93
	APPENDIX A .....	95
	APPENDIX B .....	97
	BIBLIOGRAPHY.....	99

## LIST OF TABLES

Table 3-1: Recipe for Hank's Ca <sup>2+</sup> -free solution, solvent: ultrapure water.....	35
Table 3-2: Recipe for the tissue digestion medium, solvent: 5 mL Hank's solution.....	36
Table 3-3: Antibodies used for assessment of smooth muscle, skeletal muscle and urothelium markers by immunofluorescence.....	38
Table 5-1: Agonists used during calcium imaging studies.....	76
Table 5-2: Agonists used during contraction assessment.....	78

## LIST OF FIGURES

Figure 1-1: Regulation on SMC contraction [7].	4
Figure 1-2: Expression of SMC differentiation markers in developing SMCs. This is a hierarchical illustration of various markers starting with the synthetic SMC phenotype on the left to a fully differentiated contractile SMC phenotype on the right. Figure adapted from [5].	5
Figure 1-3: Components of the urinary system. Figure from [22].	7
Figure 1-4: Pelvic floor anatomy. Figure adapted from [25].	8
Figure 1-5: The micturition reflex during the reflex, stretch receptors fire (1), parasympathetic neurons fire and motor neurons stop firing (2), and smooth muscle contracts, internal sphincter passively pulls open, and external sphincter relaxes (3). Figure adapted from [6].	9
Figure 1-6: Cross-section of a human urethra distinguishing various components of a urethral wall using Masson's Trichrome histological stain [26]. L = lumen, scale = 0.5 mm.	10
Figure 1-7: An illustration of stress urinary incontinence. Figure adapted from [33].	13
Figure 3-1: Schematic illustrating the uSMC cell isolation. Cells not drawn to scale.	34
Figure 3-2: Phase contrast image of uSMCs in culture at passage 2. Image taken at 10x.	40
Figure 3-3: Immunofluorescence staining of rat urethra sections (positive control) for smooth muscle (A: SMA, B: CALP, C: MHC), skeletal muscle (D: SKEL) and urothelium (E: CK17) associated markers. Green = protein, blue = nuclei, L = lumen. Images taken at 10x.	42
Figure 3-4: Higher magnification of the immunofluorescence staining of rat urethra sections for skeletal muscle (A: SKEL, showing fine striations) and urothelium (B: CK17, showing polygonal shaped cells) associated markers. Green = protein, blue = nuclei, L = lumen. Images taken at 40x.	43
Figure 3-5: Immunofluorescence staining of SMA (A) and CALP (B) on uSMC monolayers. MHC (C), SKEL (D), and CK17 (E) stained negatively. The protein expression trend did not change with sequential passages. These are representative images taken at 20x.	44

Figure 3-6: MHC expression was maintained after treating the minced tissue with digestive enzymes (A) as well as media agitation (B) during the cell isolation protocol. Green = MHC, blue = nuclei. Images taken at 20x.....	45
Figure 3-7: Western blotting confirming the presence of SMC markers in protein extracted from healthy urethras. Std. = protein standard, MW = molecular weight.....	46
Figure 3-8: Western blot analysis of SMC marker expression in sequential passages of uSMCs. MHC was absent irrespective of the culture medium (A: DMEM, B: R311K) used. DMEM = DMEM media supplemented with FBS and pen-strep, R311K = commercially optimized rat smooth muscle specific media containing basal medium and growth supplements. Protein bands were not min/max calibrated. Ponceau red stain was used as an indicator of homogeneous protein loading.....	47
Figure 4-1: Schematic illustrating the fabrication of TEUW.....	53
Figure 4-2: Schematic showing the in vitro mechanical testing system. Figure adapted from [137].....	56
Figure 4-3: Immunofluorescence staining of uSMC embedded TEUW cryosections (A: SMA, B: CALP). MHC, SKEL, CK17 stained negatively. Green = protein, blue = nuclei, L = lumen. These are representative images taken at 10x.....	58
Figure 4-4: TUNEL staining for assessing apoptosis in TEUWs (A: positive control, B: negative control, C: TEUWs). Green = apoptosis, blue = nuclei, L = lumen. These are representative images taken at 10x.....	60
Figure 4-5: H&E staining of sections of uSMC-populated TEUW cultured for 5 days (A) and native urethra (B). Black/blue = nuclei, pink/red = fibrin (in A) and cytoplasm/connective tissue (in B). These are representative images.....	61
Figure 4-6: MT staining of sections of uSMC-populated TEUW cultured for 5 days (A) and native urethra (B). Black/dark brown = nuclei, red = fibrin (in A) and muscle/cytoplasm (in B), greenish blue = collagen, L=lumen. These are representative images. ....	62
Figure 4-7: PSR staining of sections of uSMC-populated TEUW cultured for 5 days (A) and native urethra (B). Red/orange = mature collagen fibers, green/yellow = immature collagen. These are representative images. ....	63
Figure 4-8: Pressure-diameter response curves for uSMC-based TEUWs (n = 4), stem cell-based TEUWs (n = 4), and native urethra (n = 1). Stem cell-based TEUW and native urethra data was obtained from [31]. ....	65
Figure 4-9: Compliance for uSMC-based TEUWs (n = 4), stem cell-based TEUWs (n = 4), and native urethra (n = 1). Stem cell-based TEUW and native urethra data was obtained from [31]. 66	

Figure 4-10: Burst pressure values for uSMC-based TEUWs (n = 4), and stem cell-based TEUWs (n = 3). Stem cell-based TEUW data was obtained from [31].	67
Figure 5-1: Schematic illustrating cyclic stretch 5 day mechanical stimulation of BMMSCs at 10% strain and 1 Hz frequency. Cells not shown to scale.	74
Figure 5-2: Coomassie brilliant blue stained BMMSCs in CTRL (A, static culture) and CS groups (B: cyclic stretch). Arrow indicated the direction of stretch. These are representative images taken at 10x.	79
Figure 5-3: Coomassie brilliant blue stained BMMSCs in CTRL (A, static culture) and CS groups (B: cyclic stretch). Arrow indicates the direction of stretch. These images were obtained from [91], taken at 10x.	80
Figure 5-4: Immunofluorescence staining of smooth muscle markers SMA (A, D), CALP (B, E), and MHC (C, F) on BMMSCs in CTRL (A-C, static culture) and CS groups (D-F, dSMCs). Arrow indicates the direction of stretch. Green = protein, blue = nuclei. These are representative images taken at 20x.	81
Figure 5-5: Immunofluorescence staining of smooth muscle markers SMA (A, D), CALP (B, E), and MHC (C, F) on BMMSCs in CTRL (A-C, static culture) and CS groups (D-F, dSMCs). Arrow indicates the direction of stretch. Green = protein, blue = nuclei. These images were obtained from [91], taken at 20x.	82
Figure 5-6: ATP-evoked $Ca^{2+}$ response in the presence ( $\approx 1.05$ ) and absence ( $\approx 0.62$ ) of extracellular $Ca^{2+}$ for uSMC monolayers. Averaged data from n = 12 cells.	83
Figure 5-7: ATP-evoked $Ca^{2+}$ response in the presence ( $\approx 0.50$ ) and absence ( $\approx 0.37$ ) of extracellular $Ca^{2+}$ for BMMSC monolayers obtained from stretched cultures (dSMCs). Averaged data from n = 13 cells.	84
Figure 5-8: ATP-evoked $Ca^{2+}$ response in the presence ( $\approx 0.35$ ) of extracellular $Ca^{2+}$ (but not absence) for BMMSC monolayers obtained from static cultures. Averaged data from n = 8 cells.	84
Figure 5-9: Representative images illustrating the change in spectral properties of fura-2 bound to intracellular $Ca^{2+}$ ions (pointed out in one cell with circles) before (A: baseline HBSS perfusion) and after (C: recovery using HBSS perfusion) an ATP-elicited response (B).	85
Figure 5-10: Montage (A: baseline media, B: agonist, C: recovery using media) illustrating failure of cells to contract in response to various agonists. This a representative montage for results obtained examining uSMCs, dSMCs, and BMMSCs obtained from static cultures. Images taken at 40x.	86

## NOMENCLATURE

$[Ca^{2+}]_{ex}$	Extracellular calcium
$[Ca^{2+}]_{in}$	Intracellular calcium
ADSC	Adipose derived-stem cell
ATP	Adenosine triphosphate
BMMSC	Bone-marrow derived mesenchymal stem cell
BSA	Bovine serum albumin
C	Compliance
$Ca^{2+}$	Calcium
CALP	Calponin
CK17	Cytokeratin 17
CS	Cyclic stretch
CTRL	Control
DAM	Donkey anti-mouse
DAPI	4, 6-diamino-2-phenylindole
DG	Diacylglycerol
DM	Diabetes mellitus
DMEM	Dulbecco's Eagle Modified Media
dSMC	Differentiated smooth muscle cell
ECM	Extracellular matrix

ERK	Extracellular signal-regulated kinase
FBS	Fetal bovine serum
H&E	Hematoxylin and eosin
HBSS	Hank's buffered salt solution
ID	Inner diameter
IP <sub>3</sub>	Inositol 1,4,5-triphosphate
JNK	c-jun amino terminal kinase
KCl	Potassium chloride
MAPK	Mitogen-activated protein kinase
MDSC	Muscle derived-stem cell
MHC	Myosin heavy chain
MLC	Myosin light chain
MT	Masson's trichrome
OD	Outer diameter
P	Pressure
PBS	Phosphate buffered saline
PE	Phenylephrine
PGA	Polyglycolic acid
PKC	Protein kinase C
PLA	Polylactic acid
PLGA	Poly (lactic-co-glycolic acid)
PSR	Picrosirius red
SCI	Spinal cord injury

SEM	Standard errors of means
SKEL	Fast-twitch skeletal myosin
SMA	Smooth muscle $\alpha$ -actin
SMC	Smooth muscle cell
SR	Sarcoplasmic reticulum
SUI	Stress urinary incontinence
TEUW	Tissue engineered urethral wrap
TGF- $\beta$	Transforming growth factor-beta
uSMC	Urethral smooth muscle cell
VD	Vaginal distension

## PREFACE

My graduate school experience has been an outgrowth of much reading, travel, reflection on science and life, and fruitful conversations with my colleagues, friends, and family, but it has also been a product of passion. My passion has provided me with the drive and motivation to work with great vigor. Despite this, in order to successfully complete my work, it took help, patience, and indulgence from others.

To begin with, I would like to thank my research advisor, Dr. David Vorp, for providing me the opportunity to work in his lab. I also thank him for initiating valuable collaborations for the purpose of my thesis. Aside from research-related endeavors, Dr. Vorp also tailored several key prospects for me while keeping my needs, personality and ambition in mind. I am very glad that I seized those opportunities presented to me, and will be forever grateful to him for his kind and thoughtful gestures.

I would also like to thank the remaining members of my defense committee: Dr. Bridget Deasy and Dr. Claudette St.Croix. I greatly appreciate Dr. Deasy's agreement in becoming my committee member and offering her feedback and advice. I sincerely express my gratitude to Dr. St.Croix, as well. Not only did she graciously agree to become a part of my defense committee, she was also as an excellent collaborator. Her intellect and warm, welcoming nature made her very approachable and enjoyable to work with.

The members of the Vascular Bioengineering Lab have been a class act, and I thank each one of them for their generosity with time and energy in thinking through my ideas and knowledge for this thesis. In alphabetical order, I thank: Douglas Chew, Deborah Cleary, Dr. Mohammad El-Kurdi, Diana Gaitan, Donna Haworth, Dr. Wei He, Dr. YuShin Kim, Dr. Timothy Maul, Roberta Melick, Brian Morelli, Melissa Morgan, Joseph Muthu, Dr. Salvatore Pasta, Dr. Lorenzo Soletti, Maggie Stevenson, Garret Viglione, and Anton Xavier. I would also like to recognize Paula Bernal, Drs. Simon Watkins, Deb Artim, and William deGroat for their generous collaborative efforts in my studies, the lab members of Drs. Yoshimura and Badylak for the provision of rats to isolate tissue, and Jennifer DeBarr for her help with histology.

To Dr. Harvey Borovetz and the department of Bioengineering, I thank you for having the faith in me and being willing to accept me in this prestigious program despite my reluctance to pursue a PhD. To Lynette Spataro and Joan Williamson, I thank you for helping me stay on the right track by ensuring all the administrative details were taken care of.

On a personal level, I would like to extend my special thanks to Anton, Brian, Garret, Joseph, Lorenzo, and Wei for being good friends and for maintaining a fun-filled, yet productive working tempo. To Gilliane, I am forever obliged for providing me with the moral support when negativity loomed. Both, Gilliane and the members of the computational lab were indispensable to my mental sanity in completing this work. They made my day-to-day work a very pleasant experience, and helped me manage the acrobatics of grad school routine with great serenity.

I would like to thank my family: two sisters, maternal aunt and uncle, and parents. I have gained so much from the insights of these six individuals. I have benefited from a lifetime of wisdom, encouragement, and support. Without their help, I would not have the peace of mind and mental stamina to achieve great things in life. I thank them all for their unconditional love.

Finally, I would like to mention my parents one more time. They remain the ultimate source of inspiration for me. They are always happy and in high spirit, never tired and exhausted, they never sigh or complain, but perform their chores with feelings of elation and happiness. I will forever be in debt to them for the supreme sacrifices they have made by migrating to America. I do realize how much they have sacrificed for our (their children) sake and I will do my best to give the best possible attention to all their wishes. *Mummy* and *pappa* – you are precious. I love you!

## 1.0 INTRODUCTION

Smooth muscle cells (SMCs) reside in various locations throughout the human body, including in vascular (in the blood vessel walls), gastrointestinal (in the walls of digestive tract and organs such as the esophagus), respiratory (in the airway passages), reproductive (in the uterus and other reproductive organs), ocular (in the eye), and urinary (in the walls of the bladder, urethra, and ureters) tissues [1-7]. SMCs have differing specialized functions in each tissue in which they are found. For instance, they are responsible for the alterations in the volume and diameter of hollow organs, enabling them to generate pressure and move contents; they adjust the shape of the lens and the diameter of the pupil in the eye; they produce erections of the hairs in the body; they control the passage of food through the gut and excretion of waste products; and they determine the movement of sperm cells, eggs and the delivery of a fetus [2, 6]. With these SMC functions in mind, it is not difficult to imagine that many common ailments can occur due to an alteration in SMC function.

For example, over 58 million people in the United States suffer from the malfunction of cardiovascular tissues, such as blood vessels [4]. Regenerative medicine tools involving cell therapy and/or tissue engineering provides an alternative to tissue transplantation, and could provide an inexhaustible supply of new tissues to replace lost or malfunctioning smooth muscle containing tissues and organs [8-10] .

Cell therapy involves cell injection methods that avoid the complications of a surgery by allowing the replacement of only those cells that supply the needed tissue function. However, cell mass sufficient to replace the lost or damaged tissue is difficult to achieve and its application for replacing the functions of structural tissues is rather limited [11].

Tissue engineering strategies involve the propagation of cells *in vitro* and combining them with a biomaterial to form a tissue construct. This practice employs merging cells with a scaffold, thereby enabling their manipulation prior to implantation in order to achieve the desired cell density, cell orientation, incorporation of capillary networks, degradation rate, and mechanical properties [4, 11].

The focus of this thesis has been on the smooth muscle of the lower urinary tract (urethra), which is a target tissue for reconstructive tissue engineering [12]. The knowledge obtained from this study may not only lead to better understanding for creating tissue engineered biological substitutes for the urethra, but it can also prove beneficial for other muscular tubes within the body.

## **1.1 SMOOTH MUSCLE CELLS**

There are three types of muscle tissue in the human body: skeletal muscle, cardiac muscle, and smooth muscle. Skeletal muscles make up the bulk of muscle content in the body. They are responsible for the positioning and moving of the skeleton. Cardiac muscle is only found in the heart and is responsible for moving blood in the circulatory system. Smooth muscle is the primary muscle of internal organs and tubes such as the stomach, bladder, urethra, blood vessels, and esophagus. Its primary function is to influence the movement of material into, out of, or

within the body by means of contraction [2, 6, 7, 13]. The following sections examine SMC contraction mechanism and phenotypic markers.

### 1.1.1 SMC contraction

The principal function of a mature SMC is contraction. **Figure 1-1** illustrates the regulation of the SMC contraction mechanism. Succinctly, once various agonists bind to specific receptors, the SMC contraction mechanism becomes activated. Following this, the classic cell response is to produce two second messengers, diacylglycerol (DG) and inositol 1,4,5-triphosphate (IP<sub>3</sub>), as a result of an increase in phospholipase C activity upon coupling by way of a G protein. IP<sub>3</sub> binds to specific receptors on the sarcoplasmic reticulum (SR), causing an increase in Ca<sup>2+</sup> within the cytosol. Ca<sup>2+</sup> ions can also enter the cell from the extracellular fluid via voltage (due to action potentials) or receptor (stretch dependent) gated ion channels. DG along with the intracellular Ca<sup>2+</sup> activates protein kinase C (PKC), which in turn promotes phosphorylation of Ca<sup>2+</sup> channels or other proteins that regulate cross-bridge cycling. Ca<sup>2+</sup> binds to calmodulin, activating myosin light chain kinase (MLC kinase). MLC kinase phosphorylates light chains in myosin heads and increases myosin ATPase activity. Energy released from ATP by myosin ATPase activity results in cycling of the myosin cross-bridges with actin for contraction. Along with ATP, phenylephrine (PE) and potassium chloride (KCl) were used in this thesis to assess SMC functionality. PE can trigger the SMC contraction mechanism by binding to the  $\alpha$ 1-adrenergic receptors on the SMC membrane. KCl can depolarize a SMC cell causing an influx of calcium ions through calcium channels, which can facilitate actin-myosin generated contractile force as mentioned above [7].

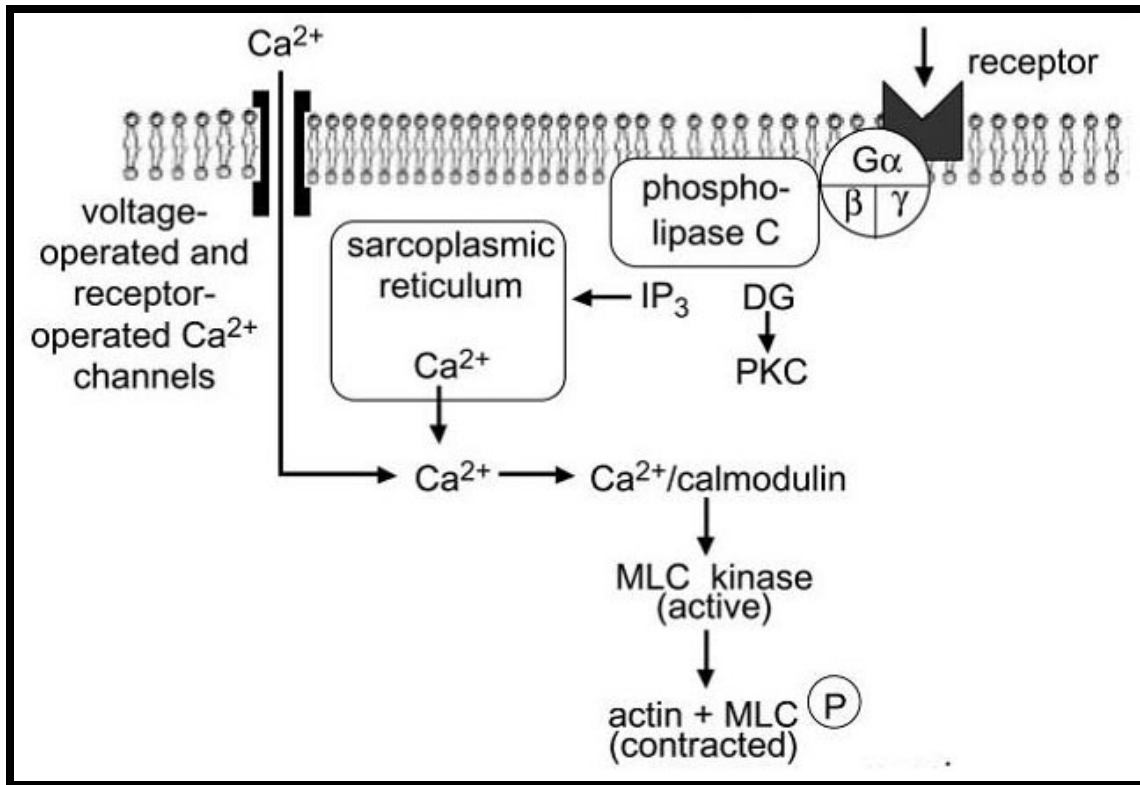
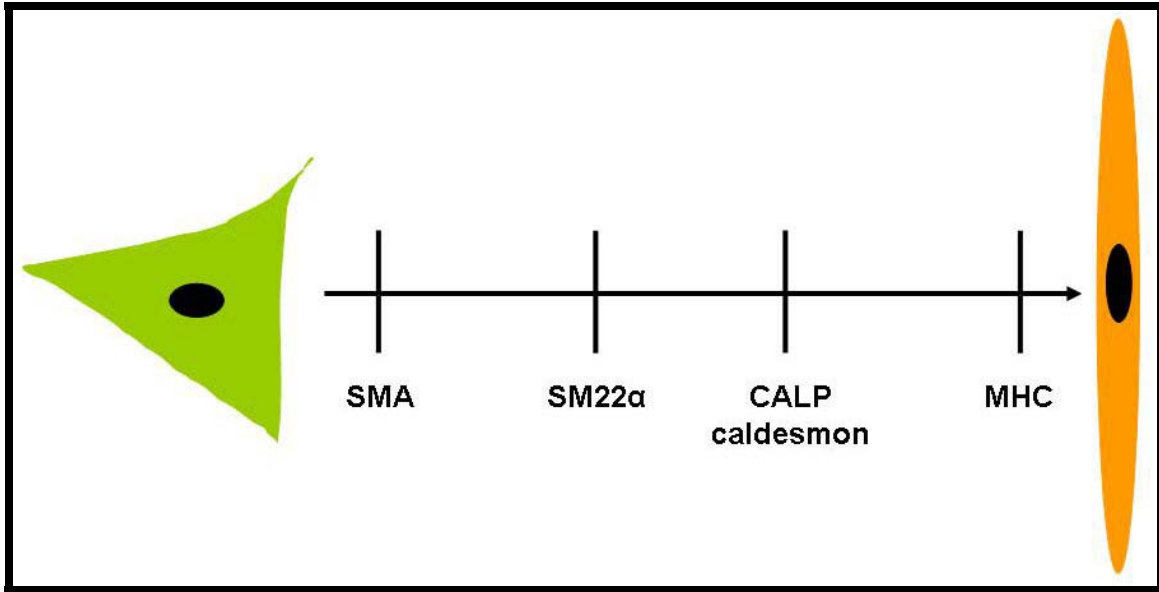


Figure 1-1: Regulation on SMC contraction [7].

### 1.1.2 SMC markers

Although the principal function of a mature SMC is contraction, the function of a SMC can vary at different developmental stages (**Figure 1-2**). Therefore, it is important to distinguish proteins that are characteristic of a given stage or state of SMC differentiation or maturation. The following section examines different marker proteins that are characteristic of different phenotypic states of a SMC.



**Figure 1-2: Expression of SMC differentiation markers in developing SMCs. This is a hierarchical illustration of various markers starting with the synthetic SMC phenotype on the left to a fully differentiated contractile SMC phenotype on the right. Figure adapted from [5].**

### 1.1.2.1 Smooth muscle $\alpha$ -actin

Smooth muscle  $\alpha$ -actin (SMA), a 42 kDa protein, is one of the six isoactins expressed in mammalian cells. It is the most abundant of the actin isoforms in a fully differentiated SMC [14]. It is also the single most abundant protein constituting 40% of total cell protein and over 70% of total actin content [15]. The high  $\alpha$ -actin content is required for generating greater forces [3]. In the past, it was thought that SMA was exclusively expressed by SMCs; however, it is now known that it is transiently expressed by a variety of cells. For example, SMA is expressed by myofibroblasts during wound healing [16] or tumor genesis [17]. Thus, SMA expression alone does not provide definitive evidence for SMC lineage.

### **1.1.2.2 Calponin**

Calponin (CALP) is a 28- to 34- kDa protein, encoded as l- and h<sub>1</sub>-calponin indicative of their low and high molecular weights, respectively [5]. CALP has been proposed to function as a regulator of SMC contraction because it interacts with filamentous actin (f-actin) and tropomyosin independently of Ca<sup>2+</sup>, and has been found to inhibit actin activated Mg<sup>2+</sup>-ATPase activity of myosin [18]. Unlike h<sub>2</sub>-calponin, a newly identified CALP isoform [5], l- and h<sub>1</sub>-calponin are exclusive to SMCs; including expression in developing and adult human aortic smooth muscle [19].

### **1.1.2.3 Myosin heavy chain**

Mature SMCs express a number of myosin isoforms, each representing an essential component of the contractile mechanism in muscle and non-muscle cells [5]. Multiple isoforms of myosin have been found in different tissues depending on its function and the developmental stage. Out of all the isoforms, myosin heavy chain (MHC) SM-1 (204 kDa) and -2 (200 kDa) are the most rigorous markers for differentiated SMCs [5, 19, 20]. Miano *et al.* demonstrated the expression of MHC restricted to smooth muscle tissue in a developing aorta as early as 10.5 days postcoitum, but no MHC was detected in the developing brain, heart, or skeletal muscle [21]. The preceding results establish that smooth muscle MHC is a highly specific marker for SMC lineage.

## 1.2 LOWER URINARY TRACT

The lower urinary tract is composed of two major organs: the bladder and urethra. Urine travelling through hollow tubes called ureters, originating from the kidneys, enters at the base of the bladder (**Figure 1-3**). The bladder expands and fills with urine until, by reflex action, it contracts and expels urine through a single tube, the urethra. The urethra in the males exits the body through the shaft of the penis. In females, the urethral opening is found anterior to the opening of the vagina and anus. This section details the process of urine discharge and the role of SMCs in urethra for maintaining a normal outflow tract.

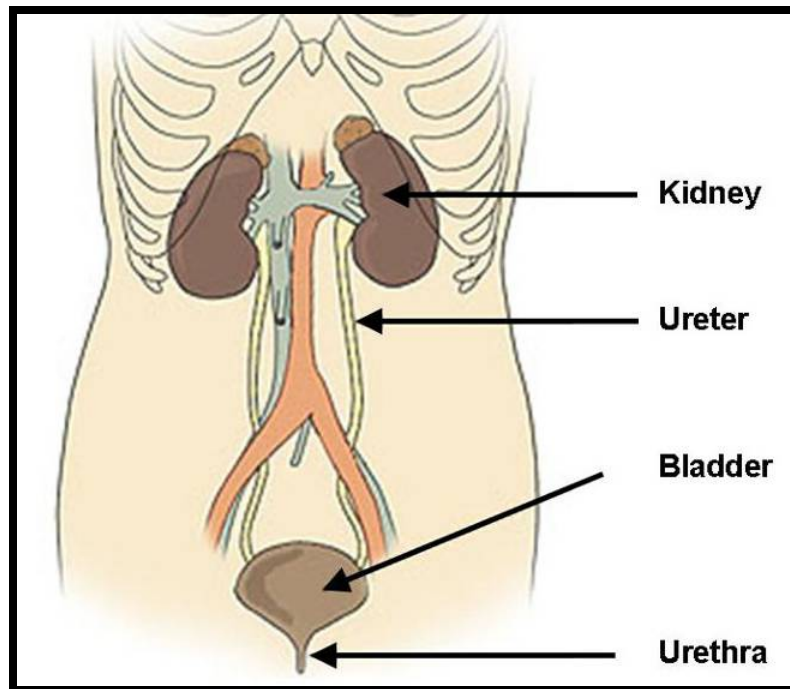


Figure 1-3: Components of the urinary system. Figure from [22].

### 1.2.1 Micturition

The process by which urine is excreted or removed from the body is called urination, and more formerly, micturition. The bladder, which is a hollow organ, can hold up to 500 mL of fluid volume in a human body [23]. The distal neck of the bladder is continuous with the urethra, through which the urine passes to reach the external environment. There are two rings of muscle between the bladder opening and urethra's orifice, which are identified as sphincters (**Figure 1-4**). The internal sphincter is a continuation of the bladder wall and consists of smooth muscle. Its normal tone keeps it contracted. The external sphincter is a ring of skeletal muscle controlled by somatic motor neurons. Stimulation from the central nervous system maintains contraction of the external sphincter except during urination [24].

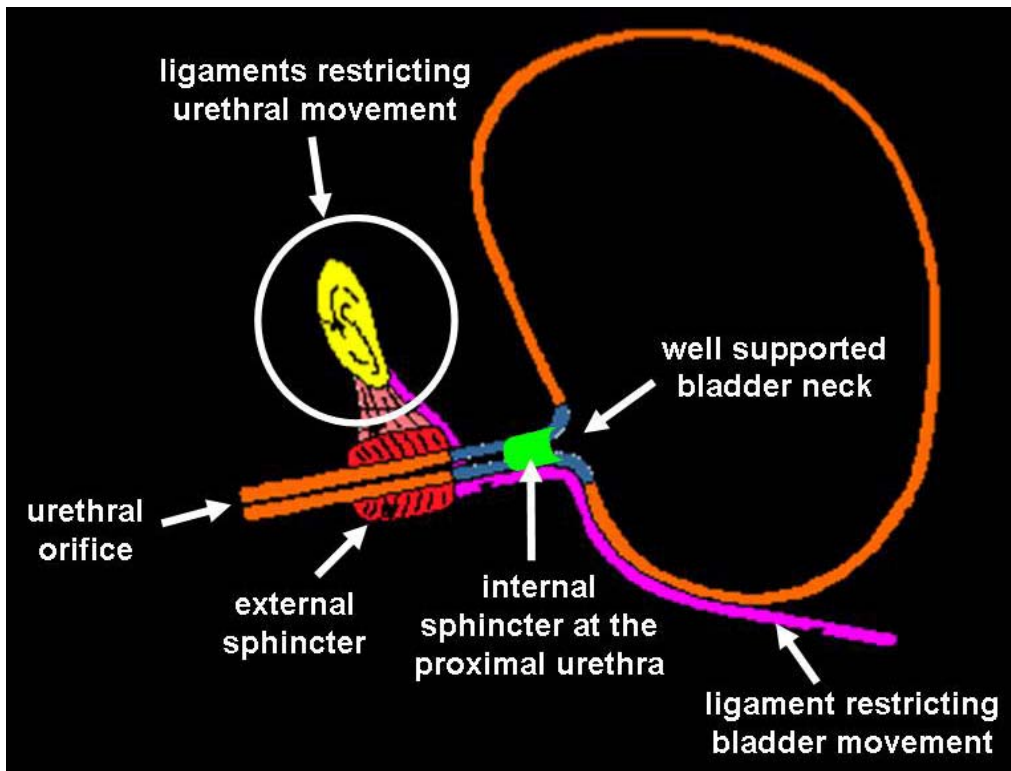
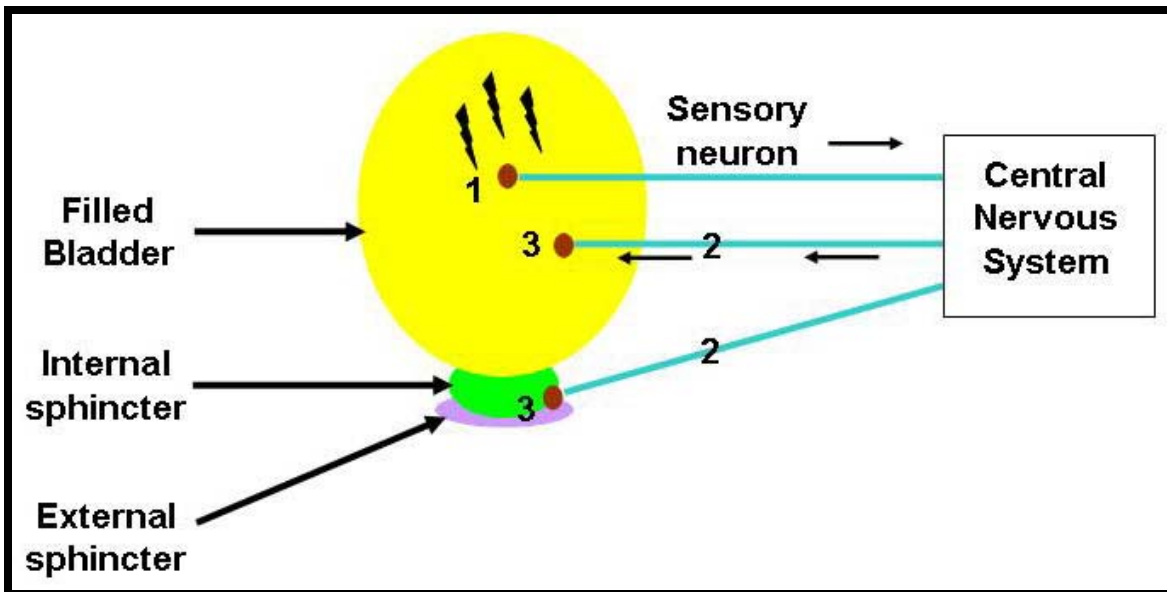


Figure 1-4: Pelvic floor anatomy. Figure adapted from [25].

Micturition is a simple spinal reflex that is subject to both conscious and unconscious control from the brain. As the bladder fills with urine and its walls expand, stretch receptors send signals via sensory neurons to the spinal cord (**Figure 1-5**). There, the information is integrated and transferred to two different set of neurons. The stimulus of a full bladder excites the parasympathetic neurons that control the smooth muscle in the bladder wall. The smooth muscle contracts, increasing the pressure on the bladder contents. Simultaneously, somatic motor neurons leading to the external sphincter are inhibited. Contraction of the bladder pushes urine downwards to the urethra. Pressure exerted by urine forces the internal sphincter open while the external sphincter relaxes [6]. Urine passes into the urethra and out of the body, aided by gravity.



**Figure 1-5: The micturition reflex during the reflex, stretch receptors fire (1), parasympathetic neurons fire and motor neurons stop firing (2), and smooth muscle contracts, internal sphincter passively pulls open, and external sphincter relaxes (3). Figure adapted from [6].**

### 1.2.2 SMC role in urethral function

During bladder filling, the main function of urethra is to prevent leakage of urine by generating a urethral closure pressure greater than the bladder's intravesical pressure. During micturition, the urethral pressure drops and the urethra relaxes its muscles, shortens in length, allowing the urine to flow out. Smooth muscle is found through out the length of a female urethra and up to the membranous part within the male urethra [13]. The urethral wall is composed of various layers: urothelium, lamina propria, circumferential and longitudinal smooth muscle, and striated muscle (Figure 1-6).

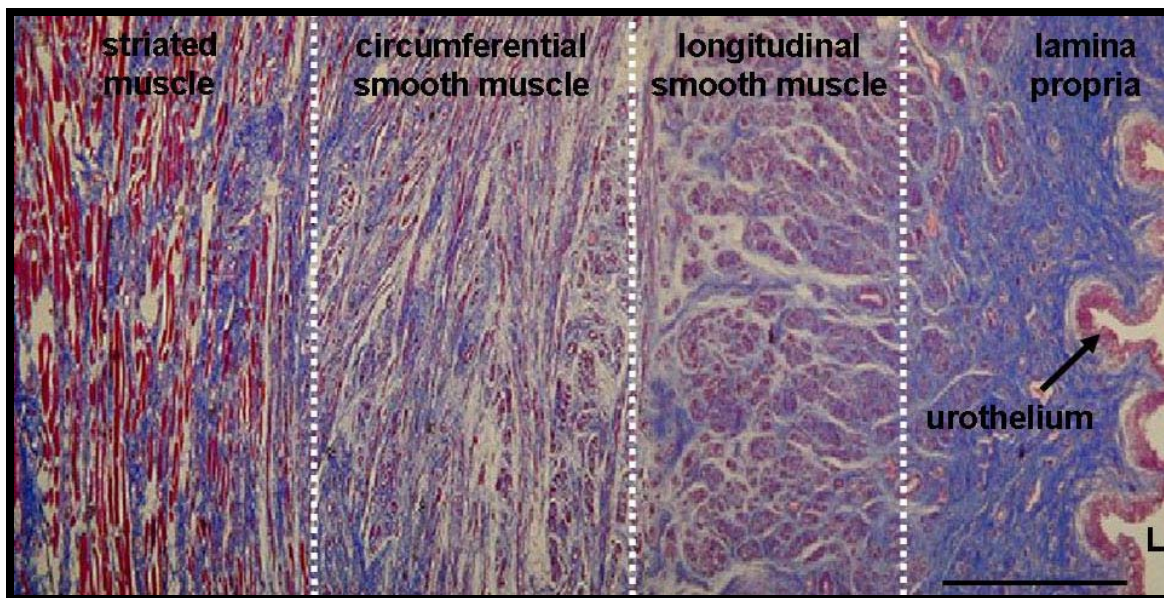


Figure 1-6: Cross-section of a human urethra distinguishing various components of a urethral wall using Masson's Trichrome histological stain [26]. L = lumen, scale = 0.5 mm.

Lining the lumen of the urethra is the urothelium. It acts as the permeability barrier protecting the underlying tissue from noxious urine components while also stretching in response to urine pressure. The next layer is the submucosal layer of the lamina propria. It is highly

vascular and also contains some longitudinal smooth muscle cells within the extracellular matrix between blood vessels and longitudinally arranged elastic fibers. It has a passive role in mediating pressure and preventing urine entering the urethra [13]. The outermost layer is composed of striated (skeletal) muscle. It plays little role in generating the resting urethral pressure because of its anatomic location within the distal external sphincter. The slow twitch skeletal fibers contribute to sustain urethral pressures during bladder filling, however; it is the fast twitch skeletal fibers that are involved in generating transient contractions to elevate urethral tone when the intra-abdominal pressure rises [13].

In between the lamina propria and striated muscle is the smooth muscle layer arranged in both the circumferential and longitudinal orientations. The circumferential smooth muscle layers throughout the urethra. It has been shown that the contraction of circumferential smooth muscle contributes to sphincteric function, in a high pressure zone of a urethra, containing no striated muscle [27]. Studies have shown that blockage of  $\alpha$ -adrenoceptors reduces the urethral pressure, but does not completely abolish it, suggesting that the myogenic tone of urethral smooth muscle also contributes to the resting pressure [28, 29]. The size of smooth muscle responses to applied agonists also vary depending on the position along the urethra as well as the density of innervation [30]. Thus, overall the circumferential smooth muscle plays an important role in maintaining urethral pressure during filling, and the activation of nervous system may contribute to functions such as the enhancement of urethral pressure once the bladder is full. The role of longitudinal smooth muscle is less clear. Contraction of longitudinal smooth muscle may shorten the urethra and open it during micturition [13]. Given the importance of circumferential smooth muscle in maintaining continence, the long-term goal of the urethral smooth muscle-based tissue engineered urethral wrap (TEUW) is to take place of this layer *in vivo*. This can be facilitated by

injecting  $\alpha$ -bungarotoxin, which would block the neuromuscular transmission of the adventitial layer of skeletal muscle (by binding to its nicotinic receptors), adjacent to which the TEUW would be implanted as a cuff around the proximal urethra [31].

### **1.3 URETHRAL DYSFUNCTION**

Urethral dysfunction is a common complication associated with medical conditions including diabetes mellitus, spinal cord injury, and vaginal distension during childbirth. This section summarizes them

#### **1.3.1 Stress urinary incontinence**

Stress urinary incontinence (SUI) is the involuntary loss of urine as a result of increased abdominal pressure, in the absence of bladder contraction [32]. In people who suffer from this condition, exertions such as laughing, sneezing, coughing, or lifting have the unpleasant consequence of urine leakage (**Figure 1-7**). This leads to fear of unpleasant accidents, loss of self confidence and ultimately to a restricted ability to go about daily lifestyle.

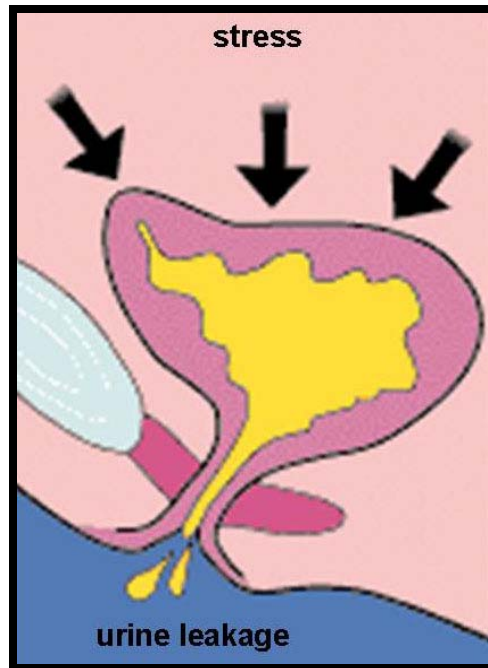


Figure 1-7: An illustration of stress urinary incontinence. Figure adapted from [33].

### 1.3.1.1 Demographics

The majority of SUI sufferers are women. SUI affects approximately 25 million women within the United States. 25% premenopausal women and 40% postmenopausal women report urine leakage. However, only 10% of middle-aged women report the condition as bothersome, reducing their quality of life including sexual well-being [34]. Given the embarrassing nature of SUI, not all women seek help to receive an appropriate treatment. As such, the true cost of treating SUI must be greater than the current \$16.3 billion estimation [23]. The peak age of an SUI episode is reported between the ages of 45 and 49 years [34]. The onset of symptoms can be monitored by keeping a diary to study voiding patterns and thereby defining the amount of discomfort, fluid intake, drug use, recent surgery, and illness in an individual's routine life, before beginning a treatment regimen [23].

### **1.3.1.2 SUI mechanisms**

There are three different mechanisms by which SUI can take place. First, the intrinsic urethral pressure generated by smooth muscle and striated muscle populated sphincters can be affected, leading to urine leakage under minimal stress than under normal conditions. This is known as intrinsic sphincter deficiency. Second, the presence of a hypermobile urethra descending with pressure cannot guard the equally distributed abdominal pressure onto the bladder and urethra, allowing urine to leak. Furthermore, nerve damage to the pelvic floor muscles can also compromise the guarding reflex of urethra. The third factor in SUI is an external problem such as obesity, chronic lung disease and recreational stress. These three factors can not only affect the pressure exerted on the lower urinary tract, but with time can progressively damage the urethral innervation and muscular support [24].

### **1.3.1.3 Current treatments and their limitations**

There are four treatments currently available for patients suffering from SUI: exercising, vaginal inserts, pharmacotherapy, and surgery.

Pelvic floor muscle training includes Kegel exercises which aim at strengthening the pelvic muscle tone by contracting and relaxing the local musculature. In order to experience efficient results, an intense training session is required on a regular basis, usually involving a health care professional. What makes these exercises wasteful is that the patients do not perform them correctly, regularly and for an adequate amount of time [24].

Intravaginal devices such as pessaries have knobs that sit under the urethra to increase urethral support. The risk associated with this therapeutic option is minimal but includes vaginal tissue erosion and discharge [34]. Pessaries require manual dexterity for use and periodic

removal for cleaning them in order to prevent infection. As such, even if used correctly, they only offer temporary comfort.

Attempts to increase urethral tone using medication have traditionally involved  $\alpha$ -agonists and estrogen. However, randomized trials using these drugs worsened baseline conditions and these drugs are no longer recommended [35]. More recently, the Food and Drug Administration withdrew phenylpropanolamine from the market because of severe side effects leading to hemorrhagic strokes in women [36]. Other possible agonists are being investigated for their role in treating SUI.

Minimally invasive sling (tension-free vaginal tape) procedures have been more recently introduced, which can be surgically placed under local anesthesia with reduced recovery time. It is designed to increase urethral support. As with all surgical interventions, they are subject to failure and life-threatening complications. Patients undergoing such procedures have suffered from abdominal hernia and bladder injury [37]. Moreover, the chances of infection and secondary interventions are always a peril.

Due to issues that accompany the current treatments available in a primary healthcare setting, many researchers have explored the use of regenerative medicine to restore normal urethral function. For example, periurethral bulking agents such as cross-linked collagen, microbeads, and autologous fat have been used under cytoscopic control. Despite their interim success, this approach has been mired by reabsorption, the need for multiple injections, and allergic responses [38]. Muscle-derived stem cells (MDSCs) have been isolated from skeletal muscle tissue and injected into the urethral wall, because of their ability to differentiate into both myogenic and non-myogenic lineages [39, 40]. The initial results of a clinical trial show that pure cell therapy with MDSCs facilitate objective and subjective improvement of SUI in female

patients [39]. Another report showed that adipose-derived stem cells (ADSCs) can also be used for the treatment of urinary incontinence. When injected into the bladder and urethra of rats, ADSCs remained viable within the lower urinary tract and demonstrated morphological and phenotypic evidence of smooth muscle incorporation and differentiation [41]. Despite these encouraging results, the current limitations of such techniques lie in the small amount of cells which can be produced for injection. In another study, Atala *et al.* used acellular collagen matrices derived from the bladder submucosa with cells obtained from the urethral tissue for tubularized replacements in rabbits. Cell-seeded matrices were successfully replaced, but lacked the demonstration of contractile function. Moreover, unseeded matrices led to poor tissue formation and graft collapse due to stricture formation [42].

### **1.3.2 Diabetes mellitus**

More than 18 million Americans are diagnosed with diabetes mellitus (DM), a condition identified by the body's inability to properly produce insulin to process sugar, resulting in high blood sugar levels [43]. Patients suffering from diabetes mellitus have a greater risk for developing urethral dysfunction [44]. Urethral dysfunction with DM encompasses symptoms such as urinating urgency and frequent voiding. The exact mechanism by which diabetes causes such dysfunction is not completely known. However, it is known that high blood sugar can cause an increase in the amount of urine produced, resulting in urgency, frequent urination, and possibly incontinence [45].

DM-associated complications such as autonomic neuropathy can cause nerve damage leading to a loss of sensation of in bladder fullness, thus reducing the ability to sense the need to urinate. Since urine storage and bladder emptying is a precise coordination, the abnormal voiding

regimen causes innervation damage to the urethra and directly impairs striated and smooth muscle within the sphincter, thereby degrading the voiding function by impairing urethra-bladder reflexes [46].

### **1.3.3 Spinal cord injury**

In the United States alone, approximately 11,000 people suffer from a spinal cord injury (SCI) each year [47]. SCI usually disables and paralyzes an individual below the site of an injury due to an unexpected accident [48].

The majority of SCI patients develop urologic complications due to abnormal micturition reflex. Following SCI, damage to sacral and lumbar segments of the spinal cord affect how well the bladder, urethral sphincter and brain work together [36]. The afferent impulses from the bladder fail to traverse the pelvic nerves to the sacral segment, and in turn fail to stimulate the lumbar segment of the spinal cord to release hormones, which cause the bladder to relax and the internal urethral sphincter to constrict. Subsequently, with a sudden increase in abdominal pressure, the guarding reflex of the urethra is also absent due to SCI-induced damage. The action potentials from the bladder do not transmit along the sensory neurons directly from the brain to pudendal nerve, leading to failure of hormonal release that aid in increasing urethral tone to prevent urine leakage [36, 49].

### **1.3.4 Vaginal distension**

With millions of babies born each year, vaginal distension (VD) associated with childbirth is an important causal factor of SUI. It is proven that that vaginal delivery can cause disruption to the

anatomical support of the female patient. For instance, our lab has shown that VD alters the biomechanical properties of the urethra [50]. Others have shown that the descent of the fetus through the pelvis causes muscle stretching and connective tissue damage within the pelvic floor [51, 52]. It may also cause extensive nerve damage, leading to a weakened and compromised urethral sphincter. In some cases, the severity of the nerve damage can cause extensive muscular weakness and poor transmission of abdominal pressure changes to the proximal urethra, leading to SUI [51, 53].

#### **1.4 THE PROMISE OF REGENERATIVE MEDICINE**

Regenerative medicine is the practice of creating living, functional tissues to repair or replace tissue or organ function that is lost due to age, disease, damage, or congenital defects. It is a rapidly growing field, which holds great promise of regenerating damaged tissues and organs in the body by stimulating previously irreparable organs to heal themselves [54]. Most notably, regenerative medicine has the potential to solve the organ shortage dilemma we face with the increasing number of patients that require life-saving organ transplants.

Advances in the application of regenerative medicine for SMC-rich tissues and organs are abundant. Such advances are demonstrated in the study by Kofler *et al.* who successfully engineered smooth muscle cells in a hybrid culture with esophageal epithelial cells in a complex effort to tissue engineer an esophagus [55]. In another study, Baker *et al.* developed a potential strategy to prevent modulation of differentiated smooth muscle cells to a synthetic phenotype after seeded onto 3D scaffolds for creating functional tissue substitutes [56]. Researchers have made such steady progress with regenerative medicine approaches that they have been able to

expand their applications to include clinical trials in humans. The study by Atala *et al.* demonstrates that after achieving desirable bladder fluid-holding capacity results in dogs implanted with urothelial and SMC-seeded biodegradable scaffolds, they have been able to focus their efforts on clinical trials in humans for bladder augmentation [57]. For the tissue engineering of blood vessels, Opitz *et al.* showed that the vascular smooth muscle cells exposed to shear stress after seeding on a tubular matrix regained the physiological functionality by switching from synthetic (undifferentiated) to a contractile (differentiated) phenotype [58]. Given the immense challenges faced in mimicking a complex native tissue, these are exciting results.

To continue to meet these challenges, we will need to continue combining our experience in biology, engineering, material science and other disciplines to improve current regenerative medicine approaches. Only then we will match all the promises made in press, particularly for the clinical translation of regenerative medicine using techniques such as cell therapy and tissue engineering.

Cell therapy involves injection of specific cells capable of replacing lost function in targeted tissues and organs. Tissue engineering, in its most frequent paradigm, entails stimulating living cells to develop biological substitutes for the restoration or replacement of tissues, with or without scaffolds (biomaterials). The following section discusses two fundamental aspects of tissue engineering: cells and scaffolds. For the purpose of this thesis, particular attention has been given to bone-marrow derived mesenchymal stem cells and fibrin (scaffold).

#### **1.4.1 Cell sourcing**

Cells used in regenerative medicine come from a variety of sources including human donors (allogenic), animal sources (xenogenic), or application-specific differentiated cells from the

patients themselves (autologous). In using, allogenic and xenogenic sources, there is a risk that the cells may be subjected to immunorejection. Cell-surface modulation offers a possible solution to this problem by deleting immunogenic sites, which therefore prevents host rejection [11]. The use of isolated, dissociated autologous cells eliminates the possibility of immune rejection. When injected or transplanted using a scaffold, they use the vascular supply and stroma provided by the host environment for attachment and remodeling [11]. However, the use of such cells also has limitation such as the possibility of an association with the same pathologically diseased target tissue. Stem cells offer a viable alternative to this dilemma because they are easily obtainable from different tissue sources. The following discussion addresses the use of stem cells, with a specific focus on adult stem cells (adipose, muscle and bone marrow-derived), and the use of bone-marrow derived mesenchymal stem cells in tissue engineering-based therapies.

#### **1.4.1.1 Stem cells**

According to the National Institutes of Health, a stem cell is a cell that has the ability to self replicate for an indefinite period, often throughout the lifetime of an organism. Given right conditions, stem cells can differentiate to the many different cell types that make up the organism. In other words, stem cells have the ability to develop into mature cells that have specialized functions, such as heart, skin, or nerve cells [59]. The term pluripotent is often used to describe cells originating from all three embryonic germ layers: mesoderm, endoderm, and ectoderm. Embryonic stem cells (derived from embryos) can self-replicate and are pluripotent. They can give rise to cells derived from all the three germ layers. Adult stem cells are undifferentiated cells, found amongst differentiated cells in a tissue or an organ, such as blood, brain, gut, skeletal muscle, skin, liver, and bone-marrow, to name a few. Pluripotent adult stem

cells are rare, but can be found in tissues such as the umbilical cord. However, adult stem cells can renew themselves and can differentiate into numerous cell types of the tissue or an organ [60].

Given the ethical dilemmas surrounding embryonic stem cell research, adult stem cells have been given tremendous attention to make scientific progress [61]. An important aspect of adult stem cell research is that a patient's own cells could be expanded in culture, differentiated into a specific cell type, and then reintroduced into the patient. This would also mean that the cells are less likely to be rejected by the host immune system [59].

#### ***1.4.1.1.1 Adipose-derived stem cells***

Adipose tissue (human fat) is a source of multi-lineage cell population called ADSCs. These cells are present in abundance in a human body and can be easily procured by local excision or liposuction [62]. Many believe that ADSCs are a viable alternative to bone marrow-derived stem cells because bone marrow-procurements can be painful requiring spinal anesthesia, and may yield low cell numbers upon processing. However, there is a need to compare these two populations more accurately [62]. Nonetheless, the promise of ADSCs as a cell source is unquestioned, as it has been used in a number of tissue-specific applications. For instance, Erickson *et al.* demonstrated the chondrogenic potential of ADSC *in vitro* and *in vivo* by growing ADSCs in a chondrogenic media with an end goal of tissue engineering cartilage [63]. ADSCs have also been differentiated into hepatic lineage, which benefits liver transplantation efforts [64]. Furthermore, ADSCs have also shown differentiation potential for myogenic [65] and neural tissues [66]. Relevant to this work, rat ADSCs were differentiated into SMCs using chemically-defined media containing beta-mercaptoethanol *in vitro* [67]. Also, Jack *et al.*

demonstrated the feasibility of differentiating ADSCs into SMCs by seeding them on to a bladder composite nurtured with smooth muscle inductive media [41].

#### ***1.4.1.1.2 Muscle-derived stem cells***

Skeletal muscle may constitute a convenient source of stem cells for cell-mediated therapies. These cells appear to be distinct from the satellite cells and possess the ability to differentiate into various cell lineages. These cells are referred to as muscle-derived stem cells (MDSCs) [68, 69]. For MDSC procurement, only a small amount of muscle biopsy is harvested under a minimally invasive procedure that can be safely performed even in an ambulatory setting without affecting the patient's health [69]. MDSCs have been used as a cell source in a variety of tissue engineering applications. For instance, in bone tissue engineering, researchers were successful in co-localizing the implanted MDSCs within the newly formed bone [70]. Within urology, introduction of MDSCs in the bladder wall resulted in the formation of myotubes and myofibers in the smooth muscle layers of the lower urinary tract, demonstrating promise for treating bladder dysfunction [71]. Most relevant to this work is the use of MDSCs to treat stress urinary incontinence. After obtaining positive results in increasing leak point pressures in animal models of internal sphincter deficiency, efforts led by Huard and Chancellor have facilitated conducting clinical trials for treating females suffering from stress urinary incontinence [39, 40]. One-year follow-up suggests some symptomatic improvements; however, the researchers conclude that a deeper delivery of the MDSCs into the external sphincter might be required to see rapid improvements. Moreover, an appropriate dose of cells is yet to be determined and investigations for randomization and blinding studies are currently missing [39]. Nonetheless, it is evident that

skeletal muscle represents a viable source for MDSCs that may be continually used to further expand our efforts in regenerative medicine-based treatments.

#### ***1.4.1.1.3 Bone marrow-derived mesenchymal stem cells***

In the 1950s, researchers discovered that the bone marrow contains two kinds of stem cells. One population is called hematopoietic stem cells, which are capable of forming all of the blood cells in the body. The second population is called bone marrow-derived mesenchymal stem cells (BMMSCs; also known as non-hematopoietic stem cells or bone marrow stromal stem cells) [59]. Friedenstein *et al.* were the first to develop its cell isolation methods and protocols to test their differentiation potential [72]. Since then, BMMSCs have been shown to differentiate into multiple mesoderm-type cell lineages such as osteoblasts [70], chondrocytes [73], endothelial cells [74], and also into non-mesoderm-type lineages such as neuronal-like cells [75].

Currently, there are no markers exclusive to BMMSCs. Despite efforts to isolate a homogeneous cell population, current methods yield a heterogeneous cell population [76]. Morphologically, they are cuboidal, fibroblast-like cells. Their initial growth *in vitro* is characterized via a colony forming assay. They stain negative for hematopoietic surface markers [60]. An important characteristic of BMMSCs is their ability to differentiate into different lineages using different chemically-defined culture conditions [77, 78]. In the present culture conditions using fetal bovine serum, BMMSCs can exhibit senescence-associated growth arrest, after 25-40 population doublings *in vitro* [79].

#### ***1.4.1.1.3 The use of BMMSCs in regenerative medicine***

BMMSCs - being easy to obtain and grow - are prime candidates for use in the field of regenerative medicine. There are four areas of clinical therapy where the use of BMMSCs has been explored: local implantation, systemic transplantation, in combination with gene therapy, and in tissue engineering applications [80].

BMMSCs have successfully treated bone defects in rat studies [81, 82]. Clinically, local injections of expanded autologous BMMSCs were proficient in the treatment of large fracture defects in patients [73]. The use of BMMSCs has also been tried in patients with vascular ischemia. The results obtained were encouraging, but need to be confirmed using randomized trial involving adequate number of patients [74]. One human study examined the effects of systemic transplantation of BMMSCs. Children with osteogenic imperfections were injected with these cells. Results revealed homing of BMMSCs in bone and production of normal collagen [70]. Genetically modified BMMSCs have also shown promising results. They demonstrated the expression of endogeneous proteins for an extended amount of time after transplantation *in vitro* [83].

Many tissue engineering strategies have also surfaced targeting replacement or reconstruction of an assortment of tissues. For instance, rat and goat BMMSCs were cultured in osteogenic and chondrogenic medium before inoculating scaffold to produce multiple phenotypes in an effort to tissue engineer articular cartilage [84]. Porcine BMMSCs were differentiated into SMCs before inoculating acellularized porcine matrix to construct trachea [85]. Within cardiovascular tissue engineering, BMMSCs are being assessed to develop a trileaflet heart valve using polyglycolic acid-based scaffolds [86, 87]. Relevant to this work, in urology, Shukhla *et al.* differentiated BMMSCs into mature SMCs *in vitro* to support bladder

augmentation using small intestinal submucosa matrix [88]. Lastly, many groups, including ours, have been successful in differentiating BMMSCs towards a SMC phenotype in response to mechanical and/or chemical stimuli [89-93].

### **1.4.2 Scaffolds**

Most strategies in tissue engineering make use of a biomaterial as a scaffold to direct a specific cell type to organize into a 3D structure, performing differentiated function of the targeted tissue [8]. The isolated cells only have a limited capacity to reform a tissue structure by themselves, and need a temporary template (scaffold) that can guide tissue restructuring and remodeling by facilitating cell adhesion, proliferation, migration and differentiation [11].

Many classes of scaffolds have been used for cell-based tissue engineering. They can be categorized into naturally derived materials (e.g., collagen, fibrin), acellular tissue matrices (e.g., small intestinal submucosa, bladder submucosa), and synthetic polymers (e.g., polyglycolic acid [PLA], polylactic acid [PLA], poly (lactic-co-glycolic acid) [PLGA]) [94].

Collagen is the most abundant and ubiquitous structural protein in the body. It is known to exhibit minimal inflammatory response and has been approved by the Food and Drug Administration for many medical applications including wound healing and artificial skin [94]. Acellular tissue matrices are collagen-rich matrices that are prepared by removing cellular components from tissues. They slowly degrade upon implantation and are replaced and remodeled by the extracellular matrix synthesized by the ingrowing cells [11]. However, such collagen-based scaffolds often exhibit weak mechanical properties incapable of mimicking the strength of the native tissue structure [95]. Synthetic polymer materials are advantageous in that

their chemistry and material properties can be well controlled and reproduced on a larger scale. A drawback of synthetic polymers, however, is the lack of biological recognition [11].

The design and selection of a scaffold is critical in the development of engineering tissues. Generally, an ideal scaffold should be bioresorbable, in that it should be capable of complete degradation into the body's natural metabolites by simple hydrolysis. It must also enhance cellular attachment, proliferation and organized development of native structures [96]. The scaffold should be easily and reproducibly processed into a desired shape that can be maintained after implantation in order to define the ultimate shape of the regenerated tissue. An ideal scaffold should also have mechanical properties similar to the tissue or organs intended for regeneration and degrade as cells synthesize new extracellular matrix to over take load bearing [11]. Angiogenesis, the formation of new blood vessels, is another important concern for tissue engineering, and an ideal scaffold must support and facilitate this process, as it is essential to the function of regenerated tissue [96]. For the purpose of this thesis, the following section offers sequential insight into the makeup of fibrin and its use as a scaffold in tissue engineering.

#### **1.4.2.1 The use of fibrin as a scaffold in regenerative medicine**

In 1960, Wichterele *et al.* published a paper in *Nature* describing the polymerization of a hydroxyethyl methacrylate monomer and a cross-linking agent in the presence of water and other solvents [97]. This innovation led to the contact lens industry and to the modern field of biomedical hydrogels. One example of a biomedical hydrogel, which has been widely used, is a fibrin gel [98-100]. The following section offers sequential insight into the makeup of fibrin followed by fibrin-based biomedical applications.

Fibrin is a natural polymer of the monomer fibrinogen, resulting from the last step of the blood coagulation cascade. Fibrinogen is a 340 kDa soluble protein composed of three

polypeptide chains: A $\alpha$ , B $\beta$ , and  $\gamma$ . Fibrin is formed after an enzyme (thrombin) mediated cleavage of A and B peptides from the A $\alpha$  and B $\beta$  polypeptide chains. The resulting fibrin monomer has a tendency to self-associate and form insoluble fibrin. A stable fibrin network is formed once the insoluble fibrin forms covalent bonds with other plasma proteins such as lysine and glutamine. This produces the fibrin hydrogel, which can be broken down by an enzyme called plasmin (fibrinolysis), and be cleared by the kidneys and liver [11, 96].

Fibrin serves itself as a promising candidate in many tissue engineering applications. It offers some important advantages such as high seeding efficiency and uniform cell distribution [101], adhesion capabilities [102], ability to induce angiogenesis [103], sound mechanical properties [104], and controlled degradation rate [105]. Furthermore, it can be produced from the patient's own blood and used as an autologous scaffold to avert foreign body reaction [106].

Due to such advantages, fibrin has been widely used to replace a variety of different tissues and organs. In a tissue engineering approach to regenerate adipose tissue, fibrin hydrogels were used to encapsulate preadipocytes, demonstrating volume stable adipose tissue [107]. In the field of orthopedics, fibrin has been used as a scaffold for bone regeneration to treat tibial defects in rabbits [108]. Fibrin has also been investigated for tissue engineering of cartilage [109]. Within cardiac tissue engineering, Birla *et al.* suspended cardiac myocytes within fibrin gels and demonstrated myocardial tissue-like formation after implantation of the constructs around the femoral artery of a rat model [110]. For liver transplantation efforts, fibrin hydrogels were utilized to create fibrin-hepatocyte (human donated) constructs by mixing commercially available fibrinogen and thrombin [111]. Fibrin-based scaffolds have also been exploited to treat central and peripheral nerve injuries in rat and chicken models [112, 113]. Fibrin-based matrices served to treat many corneal diseases including corneal perforation and limbal cell deficiency in

humans [114, 115]. In an effort to improve skin grafts, fibrin seeded with keratinocytes and fibroblasts resulted in suitable epidermal structure [116]. These examples demonstrate fibrin's versatility to serve as a tissue engineering scaffold for different target tissues.

## 2.0 HYPOTHESIS AND SPECIFIC AIMS

Smooth muscle cells (SMCs) are a major component of many tissues and organs within the cardiovascular, gastrointestinal, reproductive, respiratory, ocular, and urologic systems of the human body. Therefore, it is important to create biological substitutes that would restore and maintain normal function in tissues that are diseased or injured due to SMC dysfunction. An example of a disease that can be caused due to SMC abnormality is stress urinary incontinence (SUI). Current SUI treatments such as pelvic floor muscle training, vaginal inserts, pharmacotherapy, and surgery are limited due to unsatisfactory therapeutic efficacy and/or complications that raise the need for repeated procedures [34]. Regenerative medicine based approaches seem to hold much promise for augmentation or replacement of diseased tissues [38, 117]. However, only a few approaches using cell therapy and tissue engineering have been reported for urethral applications. Most of the reported literature supports replacing a part or entire native urethra with a scaffold [1, 12, 118], which has resulted in issues such as scaffold constriction, insufficient mechanical strength, untimely scaffold degradation, and poor tissue growth and remodeling [42, 119, 120]. Instead of replacing a part or an entire urethra, we assert that a functional wrap (tubular geometry) can provide the mechanical stability and functional reinforcement to the impaired urethra. Bone marrow-derived mesenchymal stem cells (BMMSC)-based tissue engineered urethral wraps (TEUWs) are currently being placed as a cuff around the native urethra to integrate with the host urethral tissue allowing it to remain intact

[31]. This study explores the use of autologous urethral smooth muscle cells (uSMCs) as the functional component of the TEUW because there is no proven functional substitute for native uSMCs. It also serves as an *in vitro* control group to the BMMSC-based TEUW.

While the use of autologous cells helps avoid immune rejection, their harvest can cause an inflammatory response. More so, for patients suffering from an end-stage organ failure, a tissue biopsy may not yield a sufficient number of cells for expansion and transplantation. In these situations, adult stem cells may be a viable cell source from which SMCs can be derived and be used to populate our TEUWs. Adult stem cells such as the BMMSCs have been of great therapeutic interest in the field of regenerative medicine [121-124]. Recently, from our own laboratory, Dr. Timothy Maul's research presented a unified perspective on how physiologically relevant mechanical stimulation can be utilized to trigger BMMSCs differentiation towards SMCs [91]. However, functionality of these differentiated SMCs (dSMCs) remains questionable. As such, the current study also put forth an effort to assess the functionality of dSMCs. Ultimately, TEUWs populated with such dSMCs would be a more adaptable option in a clinical setting.

The hypothesis and corresponding specific aims are as follows:

**Hypothesis 1:** *A living smooth muscle-populated tubular construct can be fabricated in vitro, using autologous uSMCs within a fibrin scaffold.*

**Specific Aim 1:** To characterize the SMC phenotype of isolated and cultured uSMCs

**Specific Aim 2:** To incorporate uSMCs in a tubular construct and assess biological and mechanical endpoints

**Hypothesis 2:** *uSMCs and dSMCs demonstrate functionality in the presence of appropriate chemical stimuli.*

**Specific Aim 3:** To assess functionality of uSMCs and dSMCs.

This research project was broken into three major components for the three specific aims. For specific aim 1, the cell isolation technique was optimized to maximize the yield of viable, dissociated uSMCs. uSMCs were assessed for SMC phenotype by means of immunofluorescence and immunoblotting. For specific aim 2, uSMCs were incorporated into the fibrin-based TEUWs and cultured in a spinner-flask. TEUWs were then evaluated for SMC phenotype, apoptosis, histology, and mechanical properties. For the specific aim 3, BMMSCs were subjected to a cyclic stretch regimen to obtain the dSMCs, whose phenotype was assessed using immunofluorescence. dSMCs were then used along side uSMCs for functionality assessment by means of measuring intracellular  $Ca^{2+}$  activity and contractile response using fura-2  $Ca^{2+}$  imaging and live-cell contractility studies, respectively. The knowledge obtained from this project can further help elucidate induction of complete SMC function and ultimately aid in providing efficient therapies for SUI and other SMC related dysfunctions.

### **3.0 CHARACTERIZATION OF ISOLATED AND CULTURED URETHRAL SMOOTH MUSCLE CELLS**

In 1913, Champy *et al.* were the first to report SMCs in culture [125]. Since then, several groups have focused on SMC culture from different tissues. However, most studies reported in the literature focus on vascular [20, 126, 127], bronchial [128-130], and bladder SMCs [131-134]. In contrast, little is known with regards to the characteristics of cultured urethral SMCs [135, 136]. This clearly presents a problem. If we do not adequately characterize uSMCs *in vitro*, it is difficult to interpret results of studies utilizing these cells with regards to their significance to the intact *in vivo* state. Therefore, this chapter focuses on characterization studies that are essential to further our knowledge of native uSMC physiology using *in vitro* cultured uSMCs.

### **3.1 METHODS**

#### **3.1.1 Animals**

Adult female Sprague-Dawley rats (240-310 g, 9-15 wks of age; Charles Rivers Laboratories, Wilmington, MA) were used in all the studies. The animals were housed at the University of Pittsburgh and/or the McGowan Institute for Regenerative Medicine's animal facilities under the supervision of the Department of Laboratory Animal Resources. The policies and procedures of

the animal laboratory are in accordance with those detailed in the *Guide for the Care and Use of Laboratory Animals*, published by the US Department of Health and Human Services. Procedural protocols were approved by the University of Pittsburgh Institutional Animal Care and Use Committee.

### **3.1.2 Tissue Isolation**

Intact urethras were isolated as previously described [137]. Briefly, animals were first sacrificed by using urethane anesthesia or 100% CO<sub>2</sub> inhalation in an animal box. The bladder and urethra were then exposed via a lower midline incision. Intramedic<sup>TM</sup> Polyethylene-50 tubing (catheter, OD = 0.965 mm; Becton Dickinson, Sparks, MD) was inserted in the urethra until it reached the bladder dome, extending the entire axial length of the urethra. The tissue was secured to the tubing with 4-0 silk sutures at the midbladder and at the most distal portion of the urethra to maintain *in vivo* length after dissection. The ureters were ligated with sutures and served as an anatomic landmark to measure the *in vivo* urethral length. The pubic bone was cut at a position lateral to the urethra and then separated and resected. The exposed urethra was gently removed from the ventral vaginal wall and the whole bladder-urethra unit was isolated. Urethras were obtained by dissecting the bladder-urethra unit at two sites:  $\approx$ 3 mm below the ureter sutures (at the bladder neck) and the sutures at the most distal portion of the urethra.

### 3.1.3 Cell isolation and culture

**Figure 3-1** briefly illustrates the uSMC cell isolation protocol, which was similar to a previously described method [138]. The exposed urethras were placed in cold oxygenated Hanks'  $\text{Ca}^{2+}$ -free solution (**Table 3-1**), in which they were cut open longitudinally.

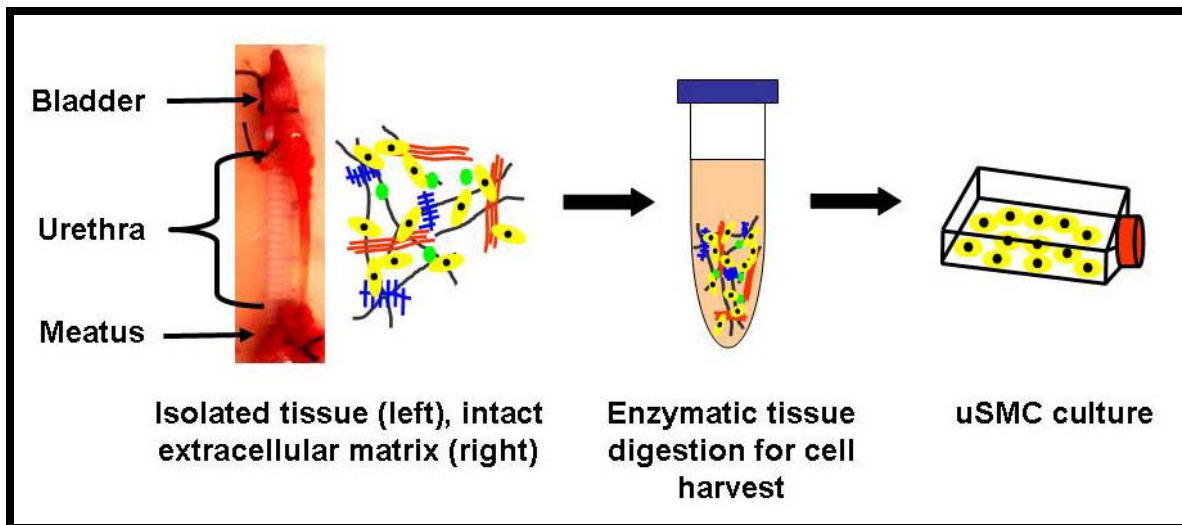


**Figure 3-1:** Schematic illustrating the uSMC cell isolation. Cells not drawn to scale.

**Table 3-1: Recipe for Hank's Ca<sup>2+</sup> -free solution, solvent: ultrapure water.**

<b>Chemical</b>	<b>Quantity (g/L)</b>	<b>Catalog Number</b>	<b>Manufacturer</b>
KCl	0.4	BP366-500	Fisher, Pittsburgh, PA
KH <sub>2</sub> PO <sub>4</sub>	0.06	3252-01	JT-Baker, Phillipsburg, NJ
NaHCO <sub>3</sub>	1.3	S233-500	Fisher, Pittsburgh, PA
NaCl	7.3	BP358-322	Fisher, Pittsburgh, PA
NaH <sub>2</sub> PO <sub>4</sub>	0.095	SX0710-1	Fisher, Pittsburgh, PA
HEPES	2.38	BP310-100	Fisher, Pittsburgh, PA

The urothelium layer was removed by scraping the lumen using a sterile stainless steel surgical blade (Sklar Instruments, Sheffield, UK) stainless steel scalpel. The tissue was then cut into tiny pieces ( $\approx 1 \text{ mm}^2$ ) followed by centrifugation in Hank's Ca<sup>2+</sup> -free solution for 10 minutes at 1200 rpm and 4°C. To enzymatically dissociate the tissue and isolate uSMCs from it, the tissue pellet was stirred in a dispersal medium (**Table 3-2**) using a small magnetic stir bar for 15 minutes at 37°C, 5% CO<sub>2</sub>. The tissue pellet was gently hand tapped after each minute to assist uSMC release and tissue matrix dissociation.

**Table 3-2: Recipe for the tissue digestion medium, solvent: 5 mL Hank's solution.**

<b>Chemical</b>	<b>Quantity (mg)</b>	<b>Catalog Number</b>	<b>Manufacturer</b>
Collagenase (type 1A)	15	C9891	Sigma-Aldrich, St.Louis, MO
Protease (type XXIV)	0.5	P8038	JT-Baker, Phillipsburg, NJ
Bovine Serum Albumin	10	BAH66-3300	Equitech-bio, Kerrville, TX
Trypsin Inhibitor	10	T9003	Sigma-Aldrich, St.Louis, MO

Following enzymatic dissociation, the tissue was centrifuged for 10 minutes at 1200 rpm and 4°C. After the removal of supernatant, release of uSMCs from the extracellular matrix was further facilitated by stirring the tissue pellet at room temperature for 15 minutes while suspended in complete media, which constituted Dulbecco's Eagle Modified Media (DMEM, Invitrogen, Carlsbad, CA) supplemented with 10% fetal bovine serum (FBS, Atlanta Biologicals, Atlanta, GA) and 1% penicillin-streptomycin (pen-strep, Invitrogen, Carlsbad, CA). The tissue was then centrifuged again at 1200 rpm for 10 minutes at 4°C and the supernatant removed. The cells were cultured on T-25 cm<sup>2</sup> flask in complete medium in a 37°C incubator at 5% CO<sub>2</sub>. Cells were grown until 90-95% confluency in a T-25 cm<sup>2</sup> flask for the first passage. Thereafter, all the cells were transferred to a T-75 cm<sup>2</sup> for passage 2. Following this, cells were grown until 85% confluency and split into 1:3 ratio for subculture using T-175 cm<sup>2</sup> flasks. Cells were detached by brief exposure to trypsin-EDTA (Invitrogen, Carlsbad, CA) solution followed by the addition of complete media, and then centrifuged at 1200 rpm for 5 min at 4°C. Media influence on SMC phenotype was assessed by means of immunofluorescence and western blotting by culturing a subset of isolated cells in an optimized, rat, SMC-specific media (R311K, Cell Applications, San Diego, CA). Unless otherwise noted, the complete media was composed of DMEM

supplemented with FBS and pen-strep. Media was changed every 2 days. Cells were cultured and used until passage 5.

### 3.1.4 Immunofluorescence

Immunofluorescence staining of cells was performed on a monolayer of cells grown on glass cover slips using a plating density of 5000 cells/cm<sup>2</sup>. Samples were first fixed in 4% paraformaldehyde (USB Corporation, Cleveland, OH), washed 5 times in phosphate buffered saline (PBS, Sigma-Aldrich, St. Louis, MO), and then incubated in 0.1% Triton X-100 (Fisher, Pittsburgh, PA) to permeabilize the cell membranes. Next, the samples were washed 5 times using a washing solution made of 0.5% bovine serum albumin (Equitech-bio, Kerrville, TX) and 0.15% glycine (Sigma-Aldrich, St. Louis, MO) in PBS. To prevent non-specific binding, samples were then blocked with 5% bovine serum albumin and 0.15% glycine in PBS for 45 minutes. Samples were rinsed again 5 times with the washing solution.

To confirm SMC phenotype, each sample was then incubated with monoclonal primary antibody such as  $\alpha$ -smooth muscle actin (SMA), calponin (CALP), and smooth muscle myosin heavy chain (MHC) for 1 hour. To check the purity of cell isolation, absence of striated muscle and urothelium was confirmed using fast-twitch skeletal myosin (SKEL) and cytokeratin 17 (CK17) as primary antibodies, respectively, for 1 hour. See **Table 3-3** for more details on primary antibodies used. The secondary antibody utilized for all primary antibodies was Alexa 488 conjugated donkey IgG fraction (DAM 488, 1:500, Invitrogen, Carlsbad, CA) to mouse immunoglobulins. Nuclei were counterstained with DAPI (4, 6-diamino-2-phenylindole, 1:1000). The samples were mounted using Fluoro-gel (Electron Microscopy Sciences, Hatfield, PA). The following day, images were taken under an epifluorescent microscope (Nikon Eclipse

E800, Glenshaw, PA) and qualitatively assessed. For our positive control, the same protocol was performed on cryosections (8  $\mu$ m thickness) of native urethral tissue.

**Table 3-3: Antibodies used for assessment of smooth muscle, skeletal muscle and urothelium markers by immunofluorescence.**

<b>Classification</b>	<b>Antibody</b>	<b>Dilution</b>	<b>Catalog Number</b>	<b>Manufacturer</b>
Smooth Muscle	$\alpha$ -SMA	1:500	A5228	Sigma-Aldrich, St.Louis, MO
Smooth Muscle	CALP	1:400	M3556	Dako, Capintaria, CA
Smooth Muscle	MHC	1:400	AB681	Abcam Inc., Cambridge, MA
Skeletal Muscle	SKEL	1:250	M1570	Sigma-Aldrich, St.Louis, MO
Urothelium	CK17	1:100	C9179	Sigma-Aldrich, St.Louis, MO

### **3.1.5 Western blotting**

To further confirm the SMC phenotype on protein extracted from cell monolayers, western blotting was performed. Whole cell lysates were obtained from cultures using Halt protease inhibitor cocktail (Thermo Scientific, Rockford, IL) and T-PER protein extraction reagent (Thermo Scientific, Rockford, IL) at 1:100 dilution. Lysates were sonicated, microcentrifuged and the protein concentration determined by BCA colorimetric assay. Protein samples (40-50  $\mu$ g per well) were resolved by electrophoresis on 4-15% Tris-HCl gels (Bio-Rad Laboratories,

Hercules, CA) at 200 V. Total protein separated by SDS-PAGE was electro-transferred to nitrocellulose membranes in a cold Tris-glycine buffer at 100 V for 1 hour. Membranes were blocked for 5% milk blocking buffer, incubated with primary antibody for 1 hour and then labeled with horse radish peroxidase conjugated secondary antibody (1:10000, Thermo Scientific, Rockford, IL) at ambient temperature. SMA, CALP, and MHC were used as primary antibodies using the same dilutions as shown in **Table 3-3**. Labeled proteins were visualized by chemiluminescent imaging using the Kodak Molecular Imaging Station (v.4.5.0, Kodak, Rochester, NY). Ponceau stain was used as a homogeneous protein loading control.

For the positive control, western blotting was performed on protein samples (200 µg per well) extracted from native urethras. Following tissue isolation, urethras were finely powdered in liquid nitrogen using a mortar and a pestle on dry ice. Upon evaporation of liquid nitrogen, the powdered tissue was quickly transferred to a tube containing the lysis buffer (in 1 mL ultrapure water: 1% raw Triton X-100, 1M Tris-HCl, 5 M NaCl, 0.05% Brij 35, 1 M NaN<sub>3</sub>) supplemented with protease inhibitor with one EDTA tablet (Roche Diagnostics, Mannheim, Germany), 2 mM serine protease inhibitor (PMSF; Sigma-Aldrich, St.Louis, MO) and 5 µg/mL cystein protease inhibitor in water (E-64; AG Scientific Inc., San Diego, CA). We used a new lysis buffer for the protein extracted from tissues because it is more effective in inhibiting the protease activity, which is more pronounced in a tissue than a cell monolayer. Apart from the protein extraction and the lysis buffer, the remaining blotting protocol was as described above for the cell monolayers.

## 3.2 RESULTS

### 3.2.1 Morphology

Cultures of uSMCs were mostly homogeneous, displaying a characteristic spindle-shaped morphology. Although, some cells exhibited a more spread out and flattened morphology (Figure 3-2).

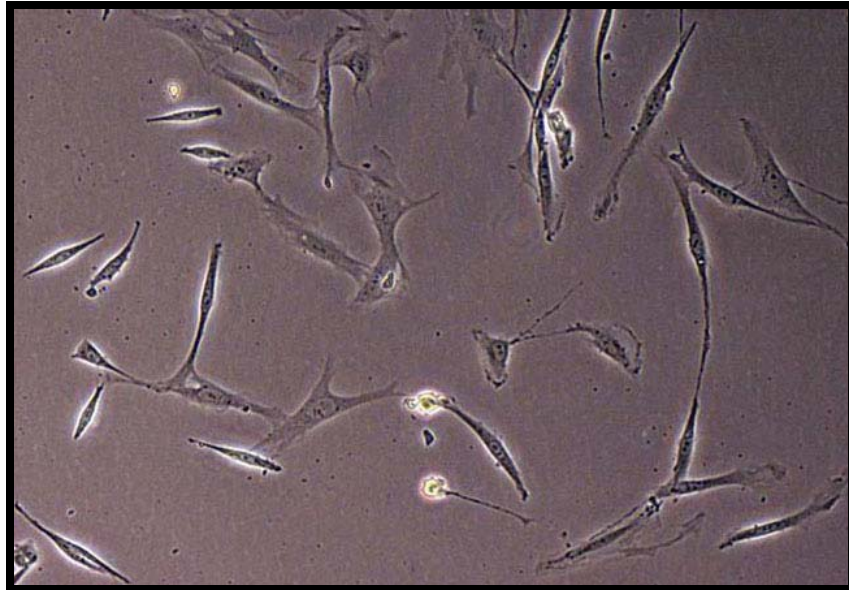
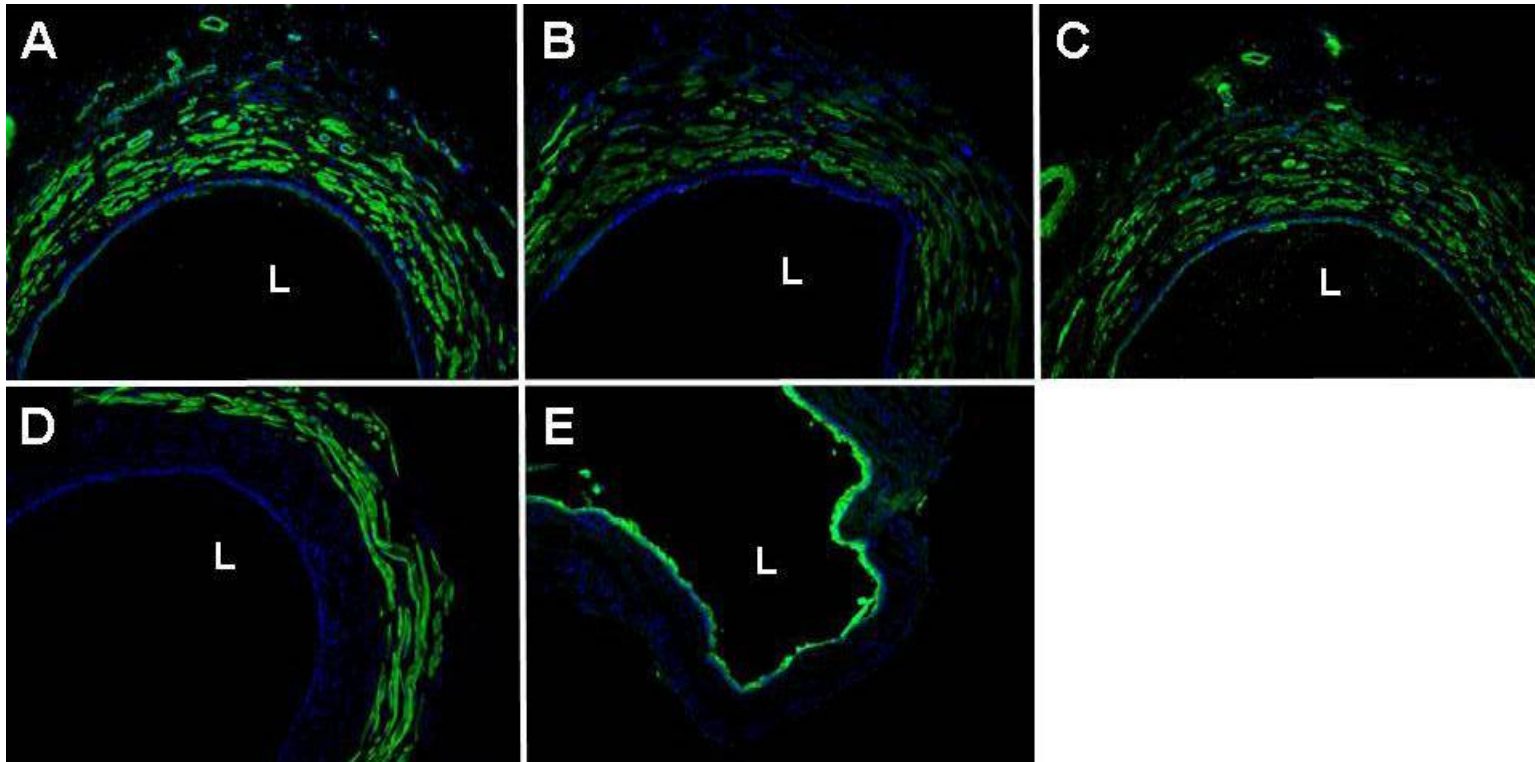


Figure 3-2: Phase contrast image of uSMCs in culture at passage 2. Image taken at 10x.

### 3.2.2 Immunofluorescence

A panel of antibodies selected as relevant to smooth muscle, skeletal muscle and urothelium was applied to sections of rat urethral tissue as positive control (Figure 3-3). Antibodies against SMA, CALP, and MHC reacted intensely with cells present within both the smooth muscle

bundles of the urethral wall and associated with small blood vessels (**Figure 3-3, A-C**). SKEL stained the adventitial layer of the urethral cross-sections, which is predominantly composed of skeletal muscle (**Figure 3-3, D**). A higher magnification (**Figure 3-4A**) clearly depicts striations within the skeletal muscle component of the urethra. CK17 labeled only the luminal urothelium lining of the urethral tissue (**Figure 3-3E**). A highly magnified image (**Figure 3-4B**) clearly illustrates the characteristic cuboidal shape of the cells within the basement membrane of the urothelium.



**Figure 3-3: Immunofluorescence staining of rat urethra sections (positive control) for smooth muscle (A: SMA, B: CALP, C: MHC), skeletal muscle (D: SKEL) and urothelium (E: CK17) associated markers. Green = protein, blue = nuclei, L = lumen. Images taken at 10x.**

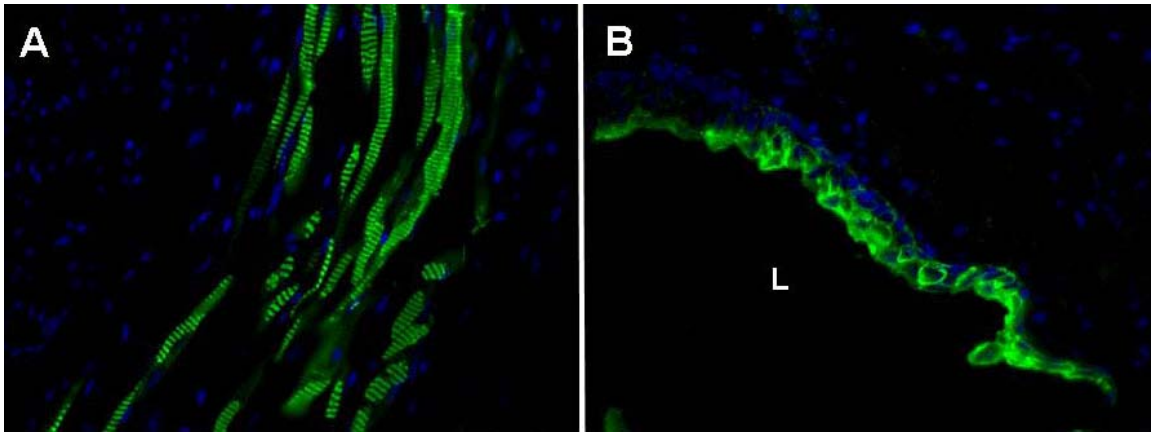


**Figure 3-4: Higher magnification of the immunofluorescence staining of rat urethra sections for skeletal muscle (A: SKEL, showing fine striations) and urothelium (B: CK17, showing polygonal shaped cells) associated markers. Green = protein, blue = nuclei, L = lumen. Images taken at 40x.**

Immunofluorescence staining was used to assess the different cell types within the culture. SMC markers such as SMA and CALP displayed cytoplasmic distribution and were arranged in filaments running longitudinally throughout the positive cells (**Figure 3-5, A-B**). However, expression of the contractile smooth muscle marker such as MHC was absent (**Figure 3-5C**). SKEL and CK 17 also stained negatively in the uSMC monolayer (**Figure 3-5, D-E**).

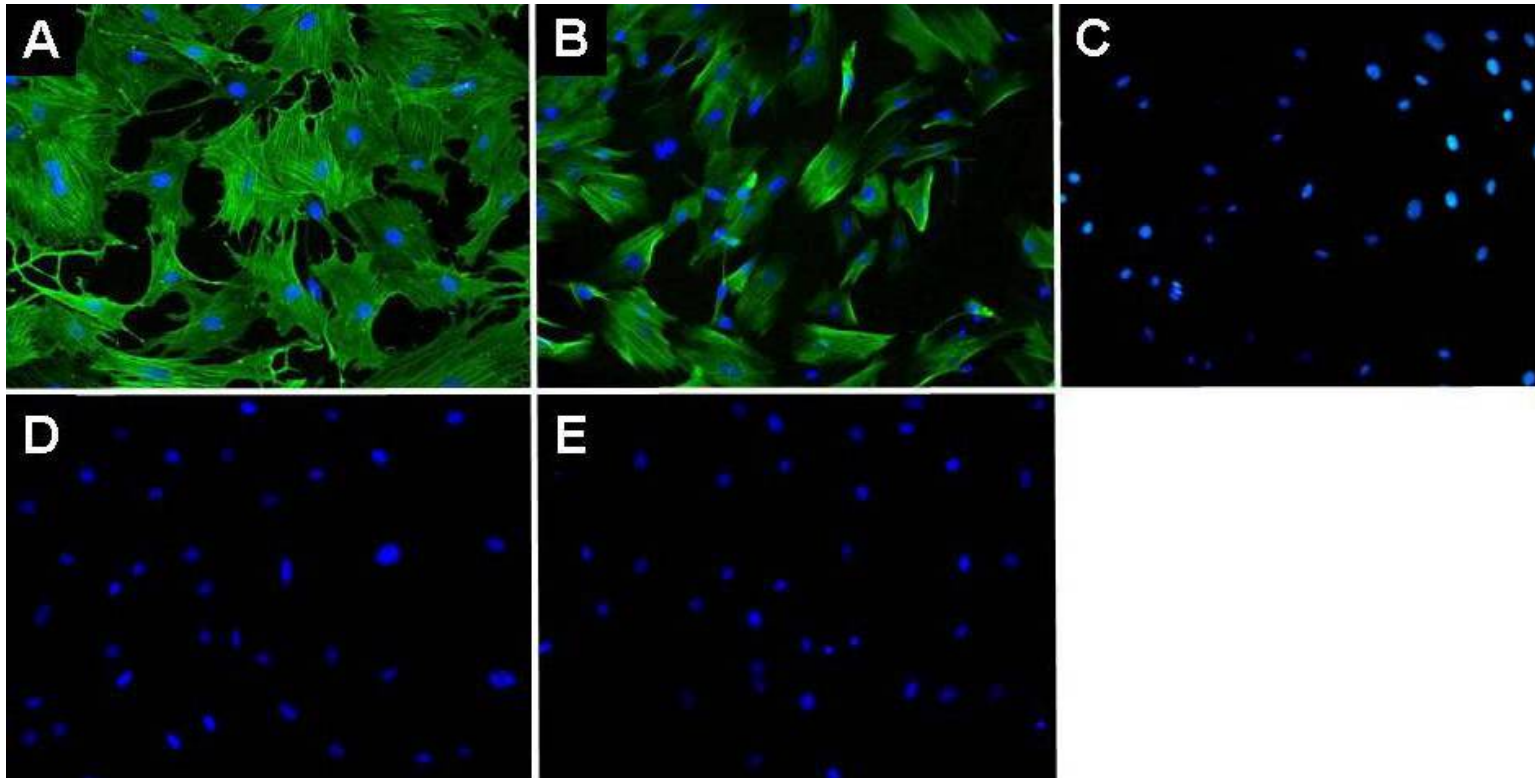


**Figure 3-5: Immunofluorescence staining of SMA (A) and CALP (B) on uSMC monolayers. MHC (C), SKEL (D), and CK17 (E) stained negatively. The protein expression trend did not change with sequential passages. These are representative images taken at 20x.**

Since MHC expression was absent in our uSMC cultures, we were thus interested in finding if the MHC expression was lost during any of our cell isolation steps. Therefore, immunofluorescence staining was performed on minced tissue pieces obtained after exposing the tissue to the enzymatic digestion step and subsequently stirring it in complete media to further aid in cell release. **Figure 3-6** shows that MHC was still present in the minced tissue pieces during these two steps of the cell isolation protocol. This finding was not confirmed by western blotting.

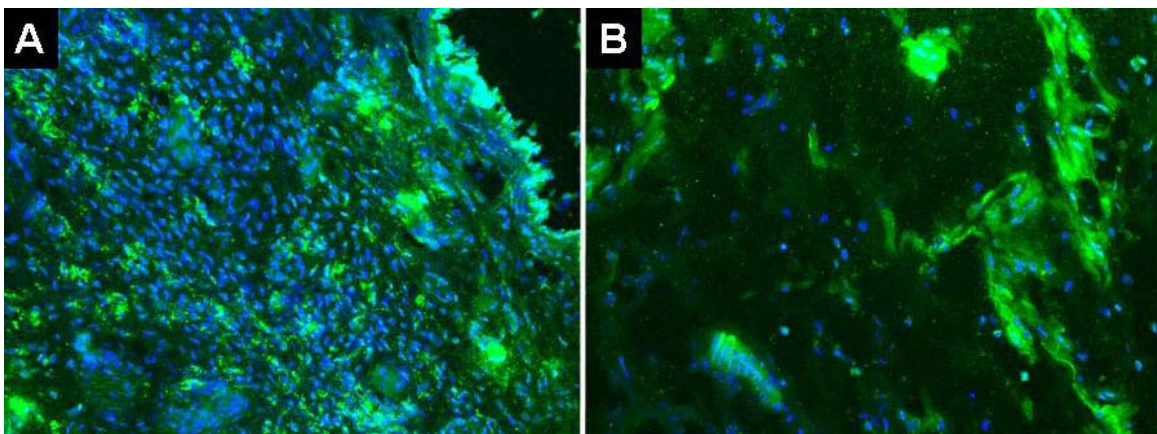


**Figure 3-6:** MHC expression was maintained after treating the minced tissue with digestive enzymes (A) as well as media agitation (B) during the cell isolation protocol. Green = MHC, blue = nuclei. Images taken at 20x.

### 3.2.3 Western blotting

Western blotting was used to confirm the SMC phenotype of the cell monolayers as shown by the immunofluorescence staining. **Figure 3-7** demonstrates the expression of smooth muscle associated markers in the native urethra (positive control). It also shows that our lysis buffer cocktail worked effectively in inhibiting the protease activity within the protein extracted from the native tissue facilitating maintenance and identification of SMC markers.

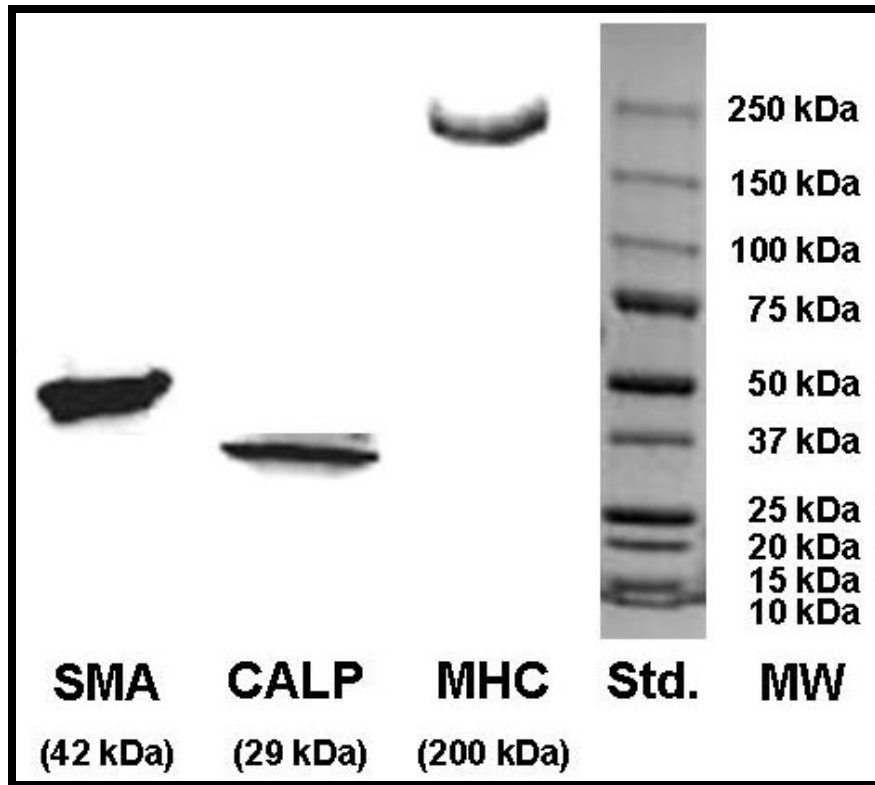


**Figure 3-7:** Western blotting confirming the presence of SMC markers in protein extracted from healthy urethras. Std. = protein standard, MW = molecular weight.

Assessment of smooth muscle protein expression by western blotting showed the expression of SMA and CALP, but not MHC. **Figure 3-8** shows that the protein expression for SMA and CALP does not seem to decrease over the number of passages tested (up to passage 5). **Figure 3-8A** illustrates this expression of SMA and CALP in sequential passages when uSMCs were cultured using DMEM media supplemented with 10% FBS and 1% pen-strep. The failure of MHC expression in our uSMC cultures led us to try a commercially optimized, rat specific smooth muscle cell media (R311K kit) on a fresh set of isolated uSMCs. We hoped that the combination of basal media along with the cocktail of growth supplements in the R311K kit would help maintain contractile marker such as MHC. However, no change in the protein expression of smooth muscle markers was seen in response to the R311K kit (**Figure 3-8B**). The

protein expression trend stayed exactly as seen while culturing uSMCs DMEM supplemented with FBS and pen-strep.

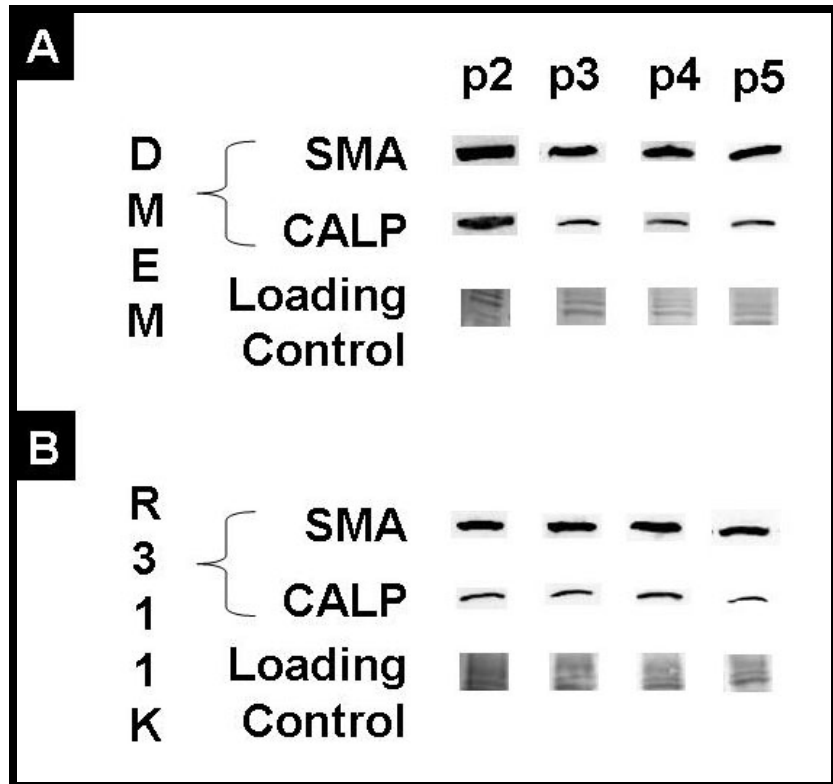


**Figure 3-8: Western blot analysis of SMC marker expression in sequential passages of uSMCs. MHC was absent irrespective of the culture medium (A: DMEM, B: R311K) used. DMEM = DMEM media supplemented with FBS and pen-strep, R311K = commercially optimized rat smooth muscle specific media containing basal medium and growth supplements. Protein bands were not min/max calibrated. Ponceau red stain was used as an indicator of homogeneous protein loading.**

### 3.3 DISCUSSION

Isolation and culture of uSMCs provides an *in vitro model* that may be useful in studying the physiology of uSMCs and aid in urethral reconstruction and regeneration. As such, it becomes

essential to be able to identify uSMCs cells using an objective criterion. Identification of our cell strains as uSMCs is based on cell morphology and phenotypic expression of SMA and CALP.

Methods for isolation of cells from tissue can be divided into explant and enzyme treatment methods. Explant methods, in which the finely minced tissue is grown in culture, have been used for their simplicity. But this method has a significant disadvantage of yielding insufficient cell numbers in a short period of time. On the other hand, enzyme treatment method yields morphologically well-differentiated isolated cells in the same timeframe as that of an explant method [20]. Although it can be difficult to determine suitable conditions from which to obtain cells with relatively high purity [139], we were successful in obtaining uSMCs using the enzyme treatment method. It appears that there was a good balance between various factors including enzyme concentrations, incubation times, and gentle agitation using magnetic stirring and hand-taps to effectively digest the extracellular matrix (ECM) proteins causing disruption of cell adhesion and consequently uSMC release.

uSMCs stained intensely for SMA and CALP, a trend unchanged for all subculture passages tested (up to passage 5, **Figure 3-8**) The high level of SMA expression might be due to the presence of myofibroblasts and/or abundant synthetic SMCs. CALP expression is a promising result because it suggests a trend towards the contractile SMC phenotype. But the lack of MHC (highly definitive contractile marker) expression was of concern. Therefore, it became imperative to check the time point at which we lost MHC expression to better understand what could be causing it. It appears that throughout the isolation protocol, MHC expression was maintained (**Figure 3-6**). However, in transitioning from 3D (native urethral tissue, **Figure 3-3**) to 2D (tissue culture flasks, **Figure 3-5**) culture environment, MHC expression was lost. As seen

in the western blot results, even the use of commercially available smooth muscle conditioned media did not alter this result.

While the lack of MHC indicated absence of full contractile machinery, the lack of SKEL and CK17, along with the presence of SMA and CALP suggested purity of our cell isolates. Using the enzymatic tissue dissociation method, we were successful in obtaining cells that were morphologically spindle-shaped and phenotypically positive for SMA and CALP as shown by the immunofluorescence and western blotting results. This study demonstrates proficient uSMC isolation, which represents an important step towards the development of a TEUW.

Any scientific study is bound to have limitations. The central limitation of this study is its inability to precisely identify what controlled the transition of a fully contractile SMC (expressing MHC, in the urethra) to a synthetic SMC (not expressing MHC, in the monolayers). Our speculation is that the variable loss of smooth muscle contractile marker (MHC) is due to absence of various components that foster the contractile state in a 3D physiologic environment. These possible components include, but are not limited to, extracellular matrix (ECM) surrounding, SMC-SMC interaction, SMC-urothelium interaction, hormone influence, and nerve signaling [2].

Even though it is difficult to mimic the complexity of a native tissue *in vitro*, it is possible to increase the contractile protein expression on cultured cells using a 3D tissue culture system such as Matrigel (a basement membrane matrix). Utilization of such ECM-like culture systems has shown a gradual reorganization of the structural proteins into architecture similar to their *in vivo* counterparts [140-142]. These structures hold cells together by providing physical support and a matrix to which cells can adhere, signal each other, and regulate intercellular communication similar to *in vivo* physiology [143]. Therefore, it is very likely that the lack of

such a supportive microenvironment caused uSMCs to lose the differentiated cells once isolated from tissue and removed from the native matrix.

In addition to ECM as a substratum for culturing uSMCs, the use of growth factors is also important in order to maximize phenotypic characteristics. For instance, transforming growth factor beta (TGF- $\beta$ ) is responsible for increasing matrix production by SMCs and helps to maintain an integrated wall in tubular organs by increasing integrin content [144]. Additionally, TGF- $\beta$  has shown to induce SMC phenotype in bone-marrow derived stem cells [90] and even non-muscle cells such as endothelial cells [145]. TGF- $\beta$ , therefore, plays an important role in determining SMC phenotype, and the use of this growth factor in our cell culture could prove to be beneficial in upregulating MHC expression, that is currently missing in the isolated uSMCs.

We believe that the individual and/or synergistic use of ECM-like substrates and growth factors such as TGF- $\beta$  have the potential to evoke changes in SMC phenotype in our cultures uSMCs, consistent with the native cells. This is strictly a hypothesis and further studies are needed in this important area.

#### 4.0 INCORPORATION OF URETHRAL SMOOTH MUSCLE CELLS INTO A TISSUE ENGINEERED URETHRAL WRAP

Various disorders of the urethra such as stress urinary incontinence (SUI) may lead to damage or loss of connective tissue, nerves, and muscle, often requiring tissue reconstruction [34]. Only a small amount of mucosa is available for grafting, and other sources of tissue such as skin flaps and buccal mucosa have been frequently used. Although the initial results were encouraging, the long-term results were accompanied with complications such as fistulas, hair growth, and graft constriction [42, 119, 120]. In an attempt to overcome this problem, many investigators used acellular biodegradable biomaterials; however, it led to the formation of strictures [1, 12, 42, 118]. To avoid this hindrance, we have attempted a tubularized repair using cells and scaffold to create a tissue engineered urethral wrap (TEUW), which when placed as a periurethral cuff would integrate with the host tissue and facilitate tissue regeneration and compatibility [31].

This study solely focuses *in vitro* assessment of a TEUW, composed of a natural biodegradable matrix (fibrin) as our scaffold, populated with urethral smooth muscle cells (uSMCs). uSMC-based TEUW will serve as an *in vitro* control group to a stem-cell based TEUW, which is currently being assessed in a rat model of SUI [31]. Our efforts in developing such a treatment option will provide a more thorough understanding of the therapeutic use of tissue engineering for smooth muscle-rich tubular organs such as the urethra.

## 4.1 METHODS

### 4.1.1 Fabrication of a TEUW

Fibrin-based tissue engineered urethral wraps (TEUWs) were fabricated by first combining 3 mg/mL bovine fibrinogen (Sigma-Aldrich, St. Louis, MO) with 0.5 units/mg thrombin (Sigma-Aldrich, St. Louis, MO) and  $1 \times 10^6$  uSMCs/mL. This mixture of cells and fibrin (cell suspension) was poured into a mold, made by placing a Teflon mandrel concentrically inside a glass sheath to produce a tubular geometry (**Figure 4-1**). Molds were placed in an incubator for 45 minutes at 37°C, 5% CO<sub>2</sub>. Upon gelation, constructs ( $\approx$  2.5 mm inner-diameter, 10 mm outer-diameter, 5 cm length, ) were freed from the mold and placed into a dynamic spinner flask culture containing Dulbecco's Eagle Modified Media (Invitrogen, Carlsbad, CA) supplemented with 10% fetal bovine serum (Atlanta Biologicals, Atlanta, GA), 1% penicillin-streptomycin (Invitrogen, Carlsbad, CA), 0.1 g/mL aminohexanoic (to inhibit fibrin degradation; Sigma-Aldrich, St. Louis, MO) and 50  $\mu$ g/mL ascorbic acid (to enhance collagen production; Sigma-Aldrich, St. Louis, MO) for 5 days. The fabrication parameters including chemical concentration, cell seeding density, culture method and duration were similar to those used in fabricating a stem-cell based TEUW [90].

At the end of the 5-day spinner flask culture, TEUW samples (n = 4) compacted to  $1.81 \pm 0.09$  ( $\pm$  standard error of means, see **Appendix A** for calculations) of its initial volume ( $\approx$  0.6 mm inner-diameter, 2.6 mm outer-diameter, 1.5 cm length). These samples were assessed by means of immunofluorescence, apoptosis, histology, and mechanical testing.

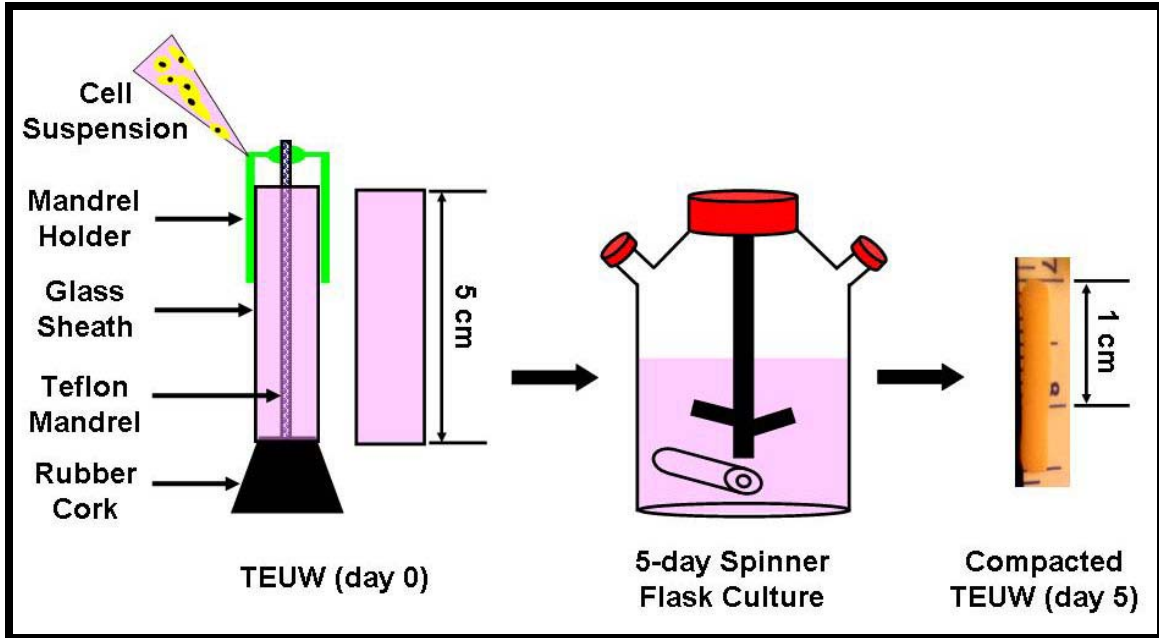


Figure 4-1: Schematic illustrating the fabrication of TEUW.

#### 4.1.2 Immunofluorescence

Following the 5-day spinner flask culture, TEUW samples were fixed in 4% paraformaldehyde (USB Corporation, Cleveland, OH) overnight followed by 24-hour incubation in 30% sucrose (Sigma-Aldrich, St.Louis, MO). Subsequently, they were embedded in TBS Tissue Freezing Medium (Fisher, Pittsburgh, PA), sectioned (8  $\mu\text{m}$  thickness), and mounted to slides to assess SMC phenotype via immunofluorescence staining as previously described in **Chapter 3.1.4**.

#### 4.1.3 Apoptosis

The TUNEL assay was carried out using a fluorescein, in situ cell death detection kit (Roche Diagnostics, Mannheim, Germany). Paraformaldehyde cryosections (8  $\mu\text{m}$  thickness) were washed 3 times in PBS for 10 minutes each. The cell membranes of the samples were then

permeabilized at room temperature for 10 minutes using 0.1% Triton X-100 (Fisher, Pittsburgh, PA) and 0.1% sodium citrate (Fisher, Pittsburgh, PA) in PBS. Each sample was then rinsed 3 times with PBS. The positive control samples were treated with a solution composed of DNase and bovine serum albumin/Tris-HCl in the ratio 1:2 for 10 minutes at room temperature. The negative controls and experimental groups were left in PBS. Following this, the negative control samples were treated with label solution (vial 1). In parallel, the positive control and experimental groups were treated with the TUNEL reaction mixture which constituted enzyme solution (vial 1) and label solution (vial 2) in the ratio of 1:9. All samples were incubated at 37°C humidified incubator for 25 minutes. The samples were then rinsed 3 times with PBS. Nuclei were counterstained with DAPI (4, 6-diamino-2-phenylindole, 1:1000). The samples were mounted using Fluoro-gel (Electron Microscopy Sciences, Hatfield, PA). The following day, images were taken under an epifluorescent microscope (Nikon Eclipse E800, Glenshaw, PA) and qualitatively assessed.

#### **4.1.4 Histology**

Following the 5-day spinner flask culture, TEUW samples were fixed in 4% paraformaldehyde overnight followed with a phosphate buffered saline (PBS, Sigma-Aldrich, St. Louis, MO) rinse. Subsequently, they were embedded in paraffin blocks, sectioned (8 µm thickness), and mounted to slides to evaluate collagen production via Masson's trichrome and picosirius red. TEUW thickness, cell distribution, and construct morphology were assessed via hematoxylin and eosin. Samples were viewed under brightfield microscopy (Nikon Eclipse E800, Glenshaw, PA), and images were qualitatively evaluated. Picosirius red stained samples require a light polarizer to measure the birefringence and were imaged using a Nikon Eclipse E600 scope (Glenshaw, PA).

To ensure that the staining protocols worked effectively, histology was also performed on paraffin-embedded sections of the native urethra.

#### **4.1.5 Mechanical testing**

Mechanical testing of the TEUWs was performed using an *ex vivo* testing chamber previously described [137]. TEUWs were mounted onto the stainless steel tees within the bathing chamber of the *in vitro* testing apparatus (**Figure 4-2**) using 4-0 sutures (Ethicon, Somersville, NJ). Medium 199 (Invitrogen, Carlsbad, CA) was used to fill the bathing chamber and the hydrostatic fluid reservoir (a calibrated ring stand). Manual displacement of the fluid reservoir along the ring stand provided variable intraluminal static pressure. After removal of air bubbles from the system, TEUWs were preconditioned (10-second cycles of 0-8 mm Hg for 3.5 minutes) to remove viscoelastic effects. Next, they were subjected to incremental increases in intraluminal pressure (2 mm Hg increments ranging from 0-20 mm Hg) while recording pressure (P) and outer diameter (OD) measurements using a laser micrometer. Each pressure increment step was maintained for 1 minute to take into account outer diameter deformation caused due to a time-dependent viscoelastic property called creep.

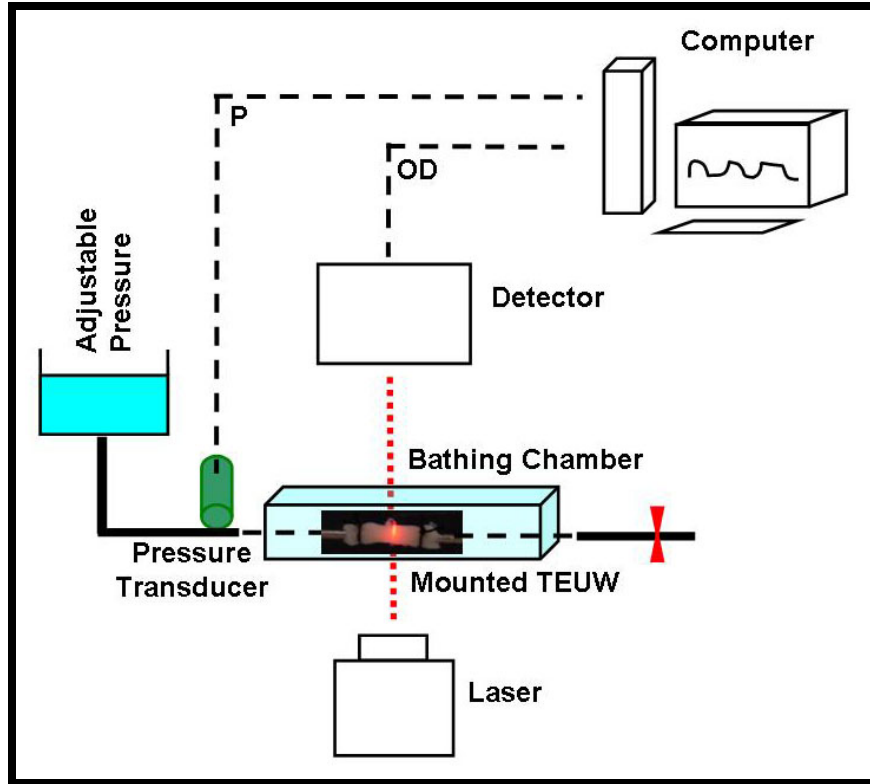


Figure 4-2: Schematic showing the in vitro mechanical testing system. Figure adapted from [137].

Histology and the assumption of incompressibility were used to determine loaded inner diameter from loaded outer diameter measurements. H&E images of TEUW were imported into Scion Imaging Software (v.4.0.3.2, Scion, Frederick, MD) for quantification of sample cross-section. Assuming constant length during testing, the inner diameter at zero pressure was calculated by subtracting twice the thickness from the measured outer diameter. The inner radius at all other pressures was calculated as shown below:

$$R_{i,P} = \sqrt{R_{o,P}^2 - R_{o,P0}^2 + R_{i,P0}^2}$$

where  $R_{i,P}$  and  $R_{o,P}$  are the inner and outer radius at any applied pressure,  $P$ , and  $R_{i,P0}$  and  $R_{o,P0}$  are the inner and outer radius at zero pressure [50]. Compliance ( $C$ ) was calculated using the following equation:

$$C = \frac{\left( \frac{D_{\max} - D_{\min}}{D_{\min}} \right)}{P_{\max} - P_{\min}}$$

where  $D_{\max}$  and  $D_{\min}$  represent the measured diameters corresponding to the maximum and minimum pressures,  $P_{\max}$  and  $P_{\min}$ , used to define the range over which the compliance is calculated [50]. Because the overall compliance parameter does not allow detection of the differential responses seen at lower pressures (0-6 mm Hg), stepwise compliance using smaller pressure ranges (2 mm Hg) was examined. Following pressure-diameter data acquisition, burst pressures were also measured on the TEUWs by steadily increasing the intraluminal pressure until a rupture was seen in the construct using a media-filled syringe pump. Pressure-diameter and compliance profiles of uSMC-based TEUWs were compared to those previously obtained for stem-cell based TEUWs and the native urethra [31]. Burst pressure comparisons were made between uSMC- and stem cell-based TEUWs [31].

#### 4.1.6 Statistics

Standard errors of means (SEM) are shown as error bars in figures for uSMC- and stem cell-based TEUWs. Comparisons are based on Student's *t-test* with significance levels set at  $p < 0.05$ . Statistical comparisons were not made with the native urethra data because of its low  $n$  value ( $n = 1$ ).

## 4.2 RESULTS

### 4.2.1 Immunofluorescence

Immunofluorescence staining was used to confirm the presence of SMC markers within the TEUWs after a 5-day spinner flask culture. **Figure 4-3** shows positive staining of  $\alpha$ -smooth muscle actin (SMA) and h1-calponin (CALP). Smooth muscle myosin heavy chain (MHC), fast-twitch skeletal myosin (SKEL) and cytokeratin 17 (CK17) stained negatively as expected based on the immunofluorescence staining of uSMC monolayer described **Chapter 3.2.2**.

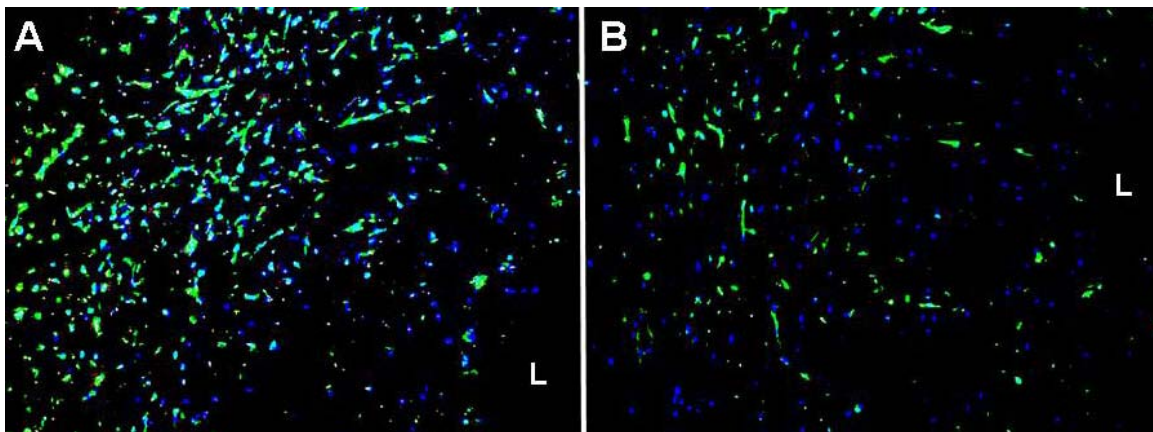


**Figure 4-3: Immunofluorescence staining of uSMC embedded TEUW cryosections (A: SMA, B: CALP). MHC, SKEL, CK17 stained negatively. Green = protein, blue = nuclei, L = lumen. These are representative images taken at 10x.**

### 4.2.2 Apoptosis

Qualitative assessment of apoptosis as seen in **Figure 4-4** suggests that the fibrin gel was not cytotoxic to uSMCs during their interactions over the course of 5 days in culture. **Figure 4-4A** depicts programmed cell death caused by preferential DNA cleavage during the TUNEL reaction

(positive control). The fragmented DNA in the positive control samples were tagged with a fluorescent probe called fluorescein, which is detected in green. In contrast, the negative controls (**Figure 4-4B**) and experimental controls (TEUW, **Figure 4-4C**) do not show signs of apoptosis. Neither negative controls nor experimental controls were exposed to DNase cleavage. Unlike negative controls, the experimental samples were exposed to the TUNEL reaction incorporated with fluorescein probe.

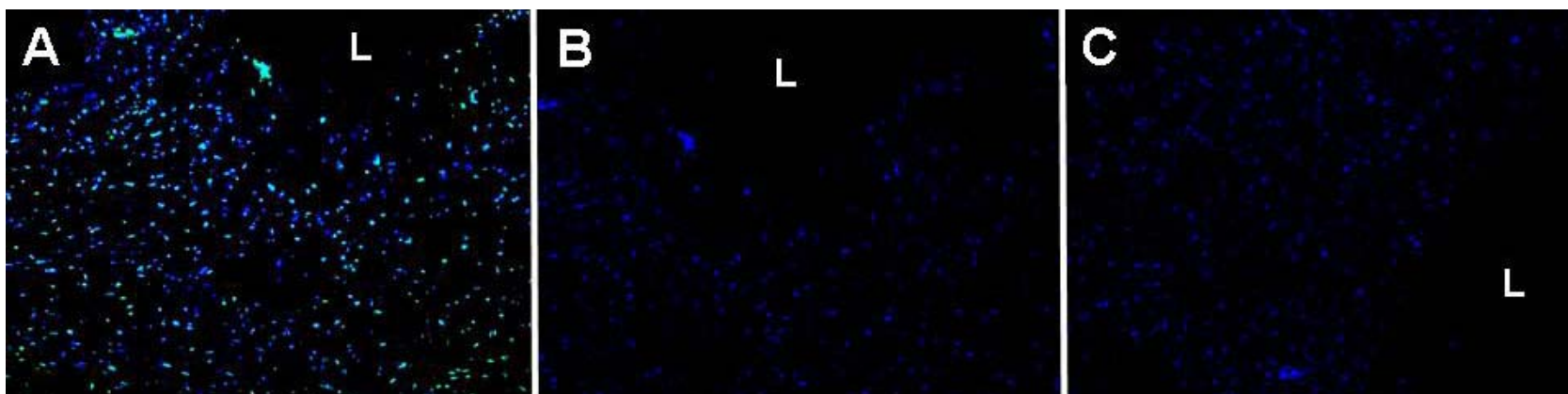
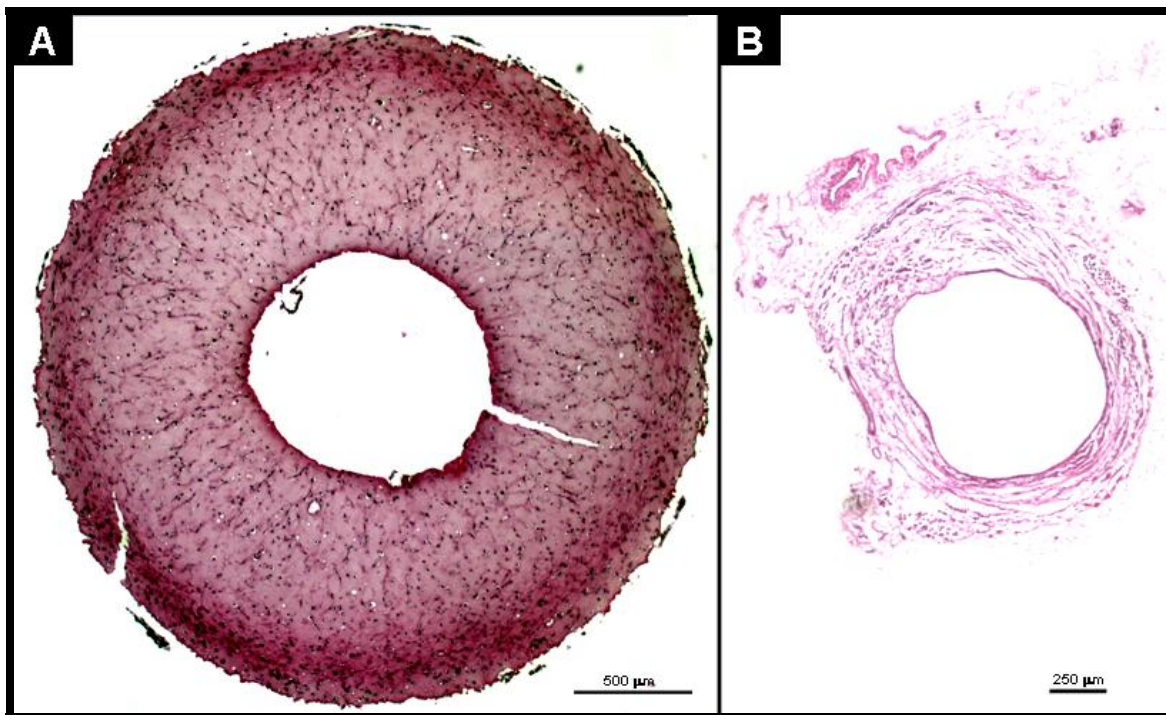


Figure 4-4: TUNEL staining for assessing apoptosis in TEUWs (A: positive control, B: negative control, C: TEUWs). Green = apoptosis, blue = nuclei, L = lumen. These are representative images taken at 10x.

### 4.2.3 Histology

#### 4.2.3.1 Hematoxylin and eosin

Hematoxylin and eosin (H&E) staining of the TEUW sections show uSMC nuclei in black/blue and the fibrin matrix in pink/red (**Figure 4-5A**). Qualitative assessment of this result indicates uniform cell distribution within the TEUW. Furthermore, it captures the tubular geometry of the TEUW. Such images were used to calculate TEUW thicknesses ( $0.99 \pm 0.04$  mm), which are essential in analyzing mechanical testing data. **Figure 4-5B** shows cell nuclei in dark blue, and the cytoplasm and connective tissue in pinkish red due to the eosin counterstain.



**Figure 4-5: H&E staining of sections of uSMC-populated TEUW cultured for 5 days (A) and native urethra (B). Black/blue = nuclei, pink/red = fibrin (in A) and cytoplasm/connective tissue (in B). These are representative images.**

#### 4.2.3.2 Masson's trichrome

Masson's trichrome (MT) staining was used to selectively stain nuclei, muscle/cytoplasm, and collagen fibers in TEUW sections and in native urethra (positive control). **Figure 4-6A** shows the absence of collagen fibers in TEUWs over a 5-day culture period despite the presence of ascorbic acid. **Figure 4-6B** clearly shows an abundant amount of collagen in the native urethra while clearly displaying muscle and cytoplasmic content in red. In both samples, nuclei are easy to detect by the dark brownish stain.

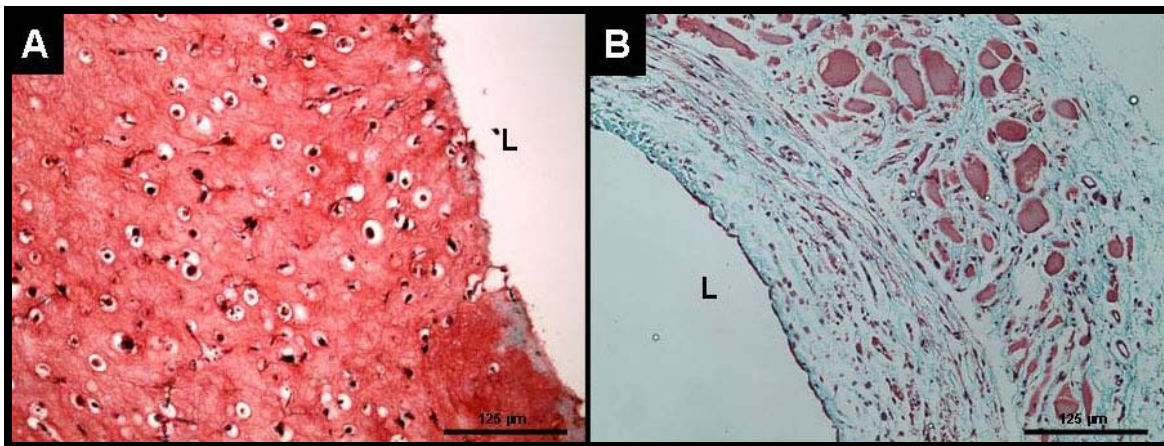


**Figure 4-6:** MT staining of sections of uSMC-populated TEUW cultured for 5 days (A) and native urethra (B). Black/dark brown = nuclei, red = fibrin (in A) and muscle/cytoplasm (in B), greenish blue = collagen, L=lumen. These are representative images.

#### 4.2.3.3 Picrosirius red

In addition to masson's trichrome, picrosirius red (PSR) was also used to assess collagen. It is one of the best understood techniques in collagen histochemistry. Using birefringence properties under a polarized microscope, PSR aids in distinguishing thicker, mature collagen fibers (red/orange) from thinner, immature collagen fibers (green/yellow). **Figure 4-7** confirms the absence and presence of collagen fibers in TEUWs (**Figure 4-7A**) and native urethra (**Figure 4-7B**), respectively.

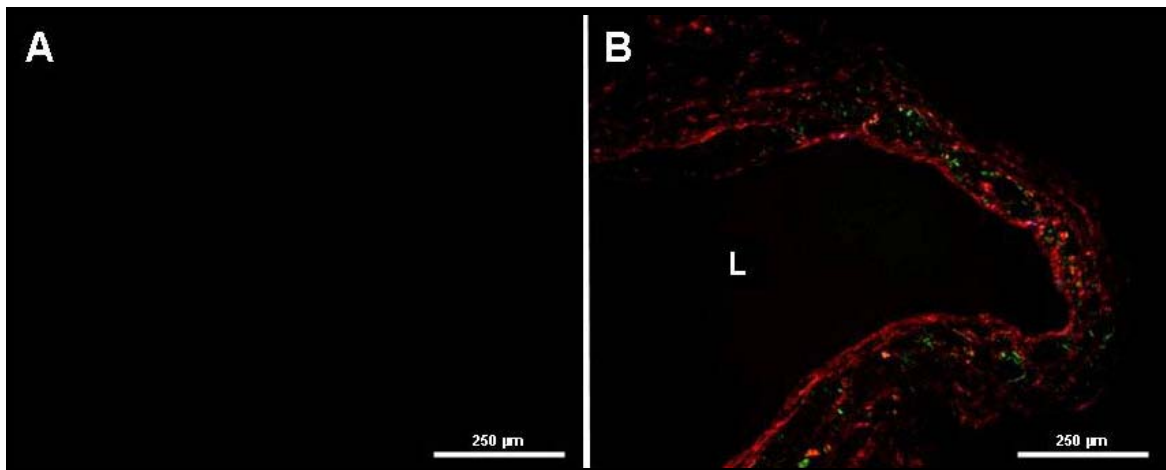


**Figure 4-7: PSR staining of sections of uSMC-populated TEUW cultured for 5 days (A) and native urethra (B). Red/orange = mature collagen fibers, green/yellow = immature collagen. These are representative images.**

#### 4.2.4 Mechanical testing

Mechanical testing yielded various mechanical parameters including pressure-diameter, compliance, and burst pressure values. Each of these is discussed below.

#### 4.2.4.1 Pressure-diameter relationship

The pressure-diameter profile of the native urethra (**Figure 4-8**) shows a non-linear, sigmoidal-shaped curve. This is a characteristic of a soft tissue in which the tissue acts stiff initially, but gradually becomes more compliant with increased pressures, before reaching a stiffness plateau, during which the diameter does not increase with the increase in pressure. Both uSMC- and stem-cell based TEUWs [31] lacked this sigmoidal shape, but still displayed non-linear curves, which are typical of soft-tissues. They display compliant characteristics during the initial pressure increments and continue to behave in this manner with subsequent increases in pressure. The slope of the pressure-diameter curves of the TEUWs and native urethra also appear to come closer to each other at higher pressures than the lower pressures. In comparing the two TEUW groups, no significant differences ( $p = 0.83$ ) were found.

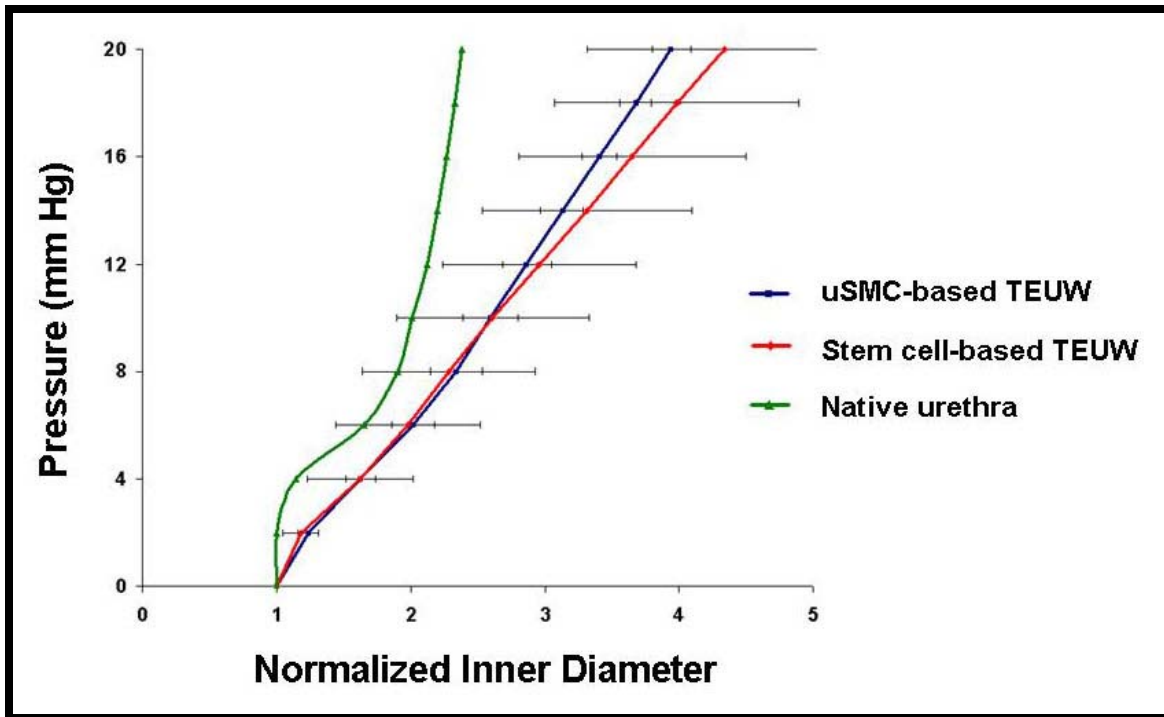


Figure 4-8: Pressure-diameter response curves for uSMC-based TEUWs (n = 4), stem cell-based TEUWs (n = 4), and native urethra (n = 1). Stem cell-based TEUW and native urethra data was obtained from [31].

#### 4.2.4.2 Compliance

The implications of the pressure-diameter trend may be illustrated in the plot of incremental compliance versus pressure (**Figure 4-9**). Both TEUW groups display greater compliance than the native urethra during the initial increase in intraluminal pressure. With further increases in pressure, the native urethra remains less compliant (more stiff) than both of the TEUW groups. There were no significant differences ( $p = 0.78$ ) found when the TEUW groups were compared.

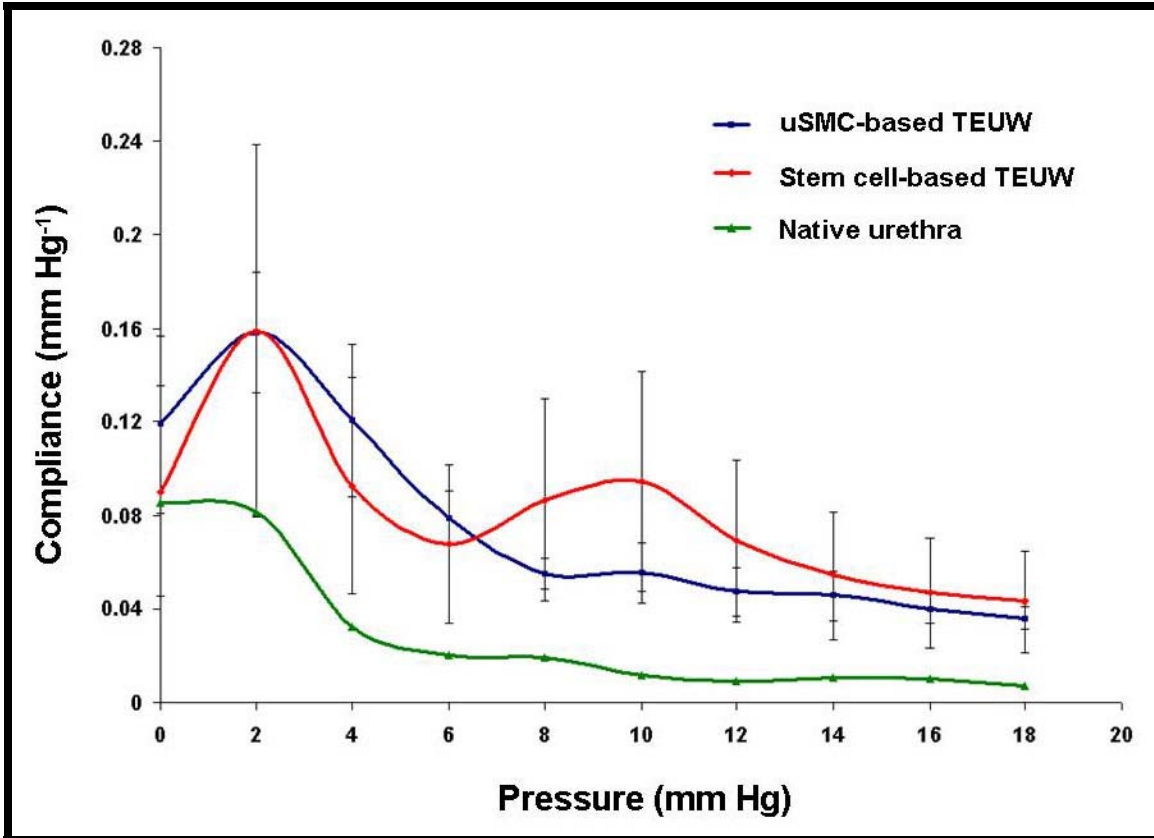


Figure 4-9: Compliance for uSMC-based TEUWs (n = 4), stem cell-based TEUWs (n = 4), and native urethra (n = 1). Stem cell-based TEUW and native urethra data was obtained from [31].

#### 4.2.4.3 Burst pressure

Burst pressure results (**Figure 4-10**) reveal no statistical difference ( $p = 0.76$ ) between the uSMC- and stem-cell based TEUW groups, which employed the same seeding density ( $1 \times 10^6$  cells per mL of fibrin) using the same culture method (spinner-flask) and time (5 days).

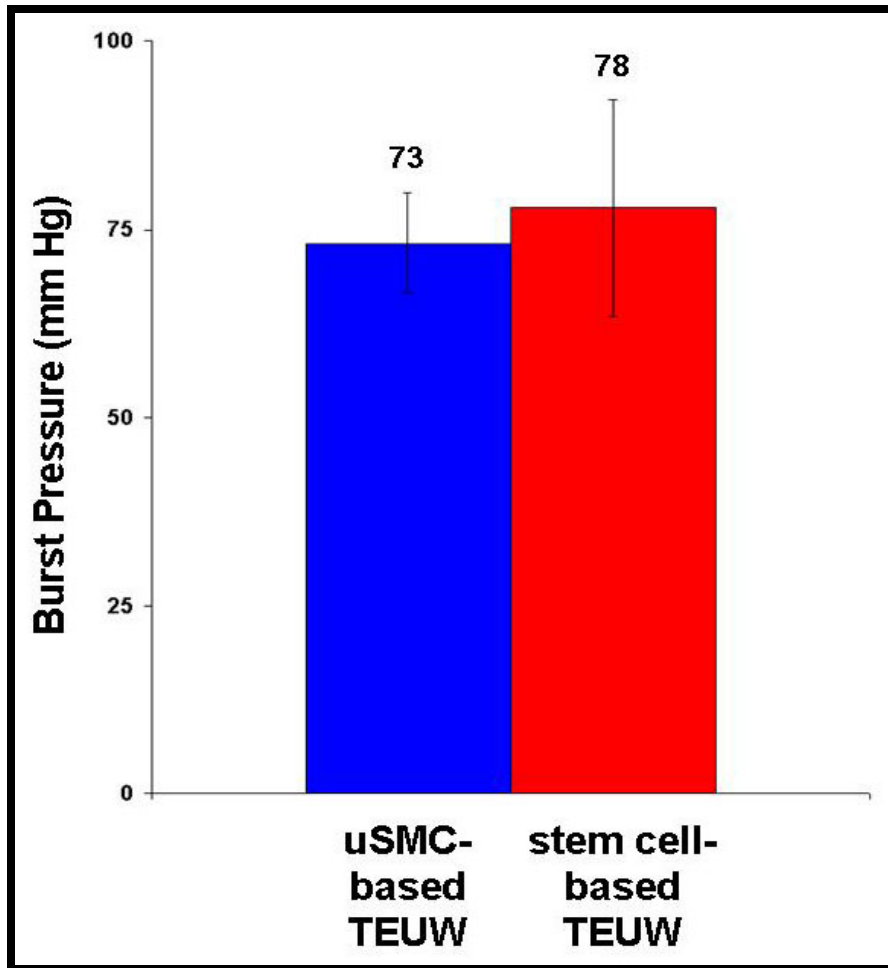


Figure 4-10: Burst pressure values for uSMC-based TEUWs (n = 4), and stem cell-based TEUWs (n = 3). Stem cell-based TEUW data was obtained from [31].

### 4.3 DISCUSSION

For engineering tissues, generally a greater degree of gel compaction is desired for stronger, more robust mechanical properties [99, 146]. uSMCs-TEUWs exhibited decreased stiffness (indicated by compliance and pressure-diameter profiles) compared to the native urethra. The burst pressure values, while comparable to stem-cell based TEUW, were much lower than that required of native soft tissues [147]. This could be due to the lower amount of compaction seen

in our TEUWs ( $\approx 1.81 \pm 0.09$  % of initial volume) versus published result on fibrin gels containing SMCs ( $\approx 4.6 \pm 0.83$  %) [99]. One way to achieve greater mechanical strength is by employing a higher cell seeding density relevant to native physiology [146]. However, it is difficult to achieve such high cell numbers given the lengthy cell expansion time. Instead, longer culture duration could prove to be a viable alternative to bringing our constructs closer to the mechanical characteristics of a healthy native urethra.

One function of extracellular matrix (ECM) fibrils (e.g., collagen, elastin) is to provide strength to the native tissues [11]. Therefore, with hopes of generating ECM deposition and thereby increasing the mechanical strength of our constructs, we enhanced the TEUW culture media within the spinner-flask by supplementing it with ascorbic acid. Ascorbic acid is well-known to stimulate the synthesis of collagen [148], the most abundant protein found in the urethra responsible for urethra's tensile strength [95]. Despite the presence of ascorbic acid in the culture media, TEUWs showed lack of collagen deposition indicated by the Masson's trichrome and picrosirius red staining. These results can be attributed to a relatively short-culture period of 5 days compared to Kim *et al.*, who were successful in observing increased type I collagen deposition by seeding human aortic smooth muscle cells in their fibrinogen constructs during two-week culture [149].

Despite the results of mechanical testing and ECM deposition, this study has many encouraging aspects including the ease of producing TEUWs, maintenance of SMC phenotype (SMA and CALP) through its transition from use in 2D culture (**Section 3.2.2, Figure 3-5**) to a 3D construct (**Figure 4-3**) and uniform cell distribution within the constructs likely due to nutrient diffusion by use of a dynamic spinner-flask culture, and the lack of apoptosis, which suggested excellent *in vitro* biocompatibility for the uSMC-fibrin interactions. Additionally, the

use of fibrin gels offered immediate cellularity of the construct by way of cell entrapment due mechanical constraint of cell induced gel compaction, necessary for fabrication of tissue replacements [146].

Altering the culture duration and/or improving the ECM synthesis can enhance the properties and function of TEUWs. Further characterization will lead to insight, not only into urethral augmentation, but also for cell-matrix interactions and lower urinary tract biology. In the future, uSMC-based TEUWs could be placed in an animal model to test its efficacy as an acute structural support for the incontinent urethra. Such implantation could lead to natural degradation of the fibrin construct, and positive remodeling through the synthesis of new collagen, resulting in improved mechanical characteristics of the new tissue.

There are several limitations of this study that must be taken into consideration. The lack of measurement such as ultimate tensile strength (UTS) is one shortcoming of this work. In hindsight, it would have been useful to corroborate the burst pressure results by measuring UTS using ring tests. Secondly, the application of pressure in small increments was performed using a calibrated ring stand. More than likely, there was a slight error in such increments. The use of an automatic computer-controlled system can address this shortcoming and even aid in making our testing process faster. Thirdly, as discussed previously, implementing longer culture duration in the presence of supplements such as ascorbic acid might help improve the current mechanical properties of the TEUWs due to increased compaction and ECM deposition. Lastly, cell viability and proliferation assays were not included in this study due to time constraints. However, cell viability assays such as the Live/Dead<sup>®</sup> assay require that the unfixed cells are cultured in a 96-well plate. In the future, such cell population can be recovered from the fibrin gels by digesting the gels after the spinner flask culture using tris/calcium acetate, EDTA-free trypsin, and

collagenase as previously described [150]. After recovering uSMCs from fibrin, performing the Live/Dead<sup>®</sup> assay would convert the non-fluorescent, cell-permeable calcein acetoxymethyl to fluorescent calcein (green color) in live cells. The dead cells, which would have damaged membranes, would allow the entry and binding of ethidium homodimer-1 to the nucleic acids, resulting in bright red fluorescence. For assessing cell proliferation, future studies can include uSMC labeling with DNA precursors such as BrdU at least twenty-four hours prior to the proliferation assay. The cells that divide would incorporate BrdU into their DNA during the S phase of synthesis and replication. The incorporated DNA could then be detected using antibodies against BrdU. In the current study, the cell nuclei from the DAPI nuclear stain during the apoptosis assay appear intact and not damaged (**Figure 4-4**), but the inclusion of cell viability and proliferation would have served as additional pieces of evidence in providing a more complete picture on any damage suffered by the uSMCs once incorporated within the fibrin gel [95]. Despite the lack of such assays, we have some evidence from a previous study (stem-cell based TEUW) in our laboratory, which suggests that the cells incorporated within similar fibrin gel, culture duration, and method (spinner-flask) as used in this study, were metabolically active in reducing yellow tetrazole dye to purple during the calorimetric MTT assay [90].

## 5.0 FUNCTIONALITY OF ISOLATED URETHRAL SMOOTH MUSCLE CELLS AND DIFFERENTIATED SMOOTH MUSCLE CELLS

A focal requirement of tissue engineering is that cells should be able to recapitulate full functional tissue capability when placed within an appropriate architecture or scaffold. Creating such functional tissue constructs require a thorough understanding of the native tissue composition and structure.

Smooth muscle cells (SMCs) are of prime importance in creating a variety of functional tissues that require contraction to control vascular tone, as well as facilitate movement of material into, out of, and within the body [6]. The contractile function of SMCs is dependent on the expression of proteins such as  $\alpha$ -smooth muscle actin (SMA), calponin (CALP), and myosin heavy chain (MHC). From our own laboratory, Dr. Timothy Maul demonstrated the expression of SMA, CALP, and MHC in by differentiating bone marrow-derived mesenchymal stem cells (BMMSCs) via physiologically relevant mechanical stimulation (such as cyclic stretch) [91]. Such differentiated smooth muscle cells (dSMCs) are of great interest because of their clinical adaptability. dSMCs provide a valuable cell source for creating SMC-populated biologic substitutes for a specific target tissue. Even though expression of smooth muscle proteins *in vitro* has been demonstrated, both in isolated and differentiated stem cells, the functional characteristics such as intracellular calcium activity and contraction remain questionable [91, 93, 151-153].

This study strived to examine the functional properties of two populations of SMCs, namely: isolated urethral smooth muscle cells (uSMCs) and differentiated smooth muscle cells (dSMCs) obtained from mechanical stimulation (cyclic stretch) BMMSCs [90, 91, 152]. We studied calcium signaling and *in vitro* contraction of uSMCs, dSMCs, and undifferentiated BMMSCs.

## 5.1 METHODS

### 5.1.1 Cell source and characterization

uSMCs were isolated from adult, female Sprague-Dawley rats (240-310 g, 9-15 wks of age; Charles Rivers Laboratories, Wilmington, MA) and expanded as described in **Chapter 3.1.3**.

Lewis rat BMMSCs were obtained from the Tulane Center for Gene Therapy under a material transfer agreement. The Tulane Center for Gene Therapy is a NIH-funded organization to provide well-characterized BMMSCs to investigators to reduce the variability within the results of different researchers from different cell sourcing techniques. The BMMSCs were harvested from the femurs of adolescent Lewis rats and characterized as CD90+ and CD59+ stem cells [154]. The BMMSCs were expanded in alpha modified Eagle's media ( $\alpha$ -MEM, Invitrogen, Carlsbad, CA) supplemented with 20% fetal bovine serum (FBS, Atlanta Biologicals, Atlanta, GA), 1% antibiotic/antimicotic (Invitrogen, Carlsbad, CA) and 10 mM L-glutamine (Invitrogen, Carlsbad, CA).

### 5.1.2 Cyclic stretch apparatus

Briefly, mechanical stimulation of BMMSCs via cyclic stretch was done exactly as previously described by Maul *et al* [91]. Forty-eight hours before the beginning of cyclic stretch mechanical stimulation (**Figure 5-1**), BMMSCs were seeded (200 cells/cm<sup>2</sup>) onto type I collagen coated BioFlex<sup>®</sup> plates (Flexcell International, Hillsborough, NC), which have a flexible growth surface. Cells were subjected to 10% uniaxial strain at 1 Hz (cyclic stretch group, CS) for 5 days using a FX-4000 strain unit (Flexcell International, Hillsborough, NC). The control group (CTRL) was statically cultured on the same plates for the same duration.

The Flexcell system has been well established to impose cyclic stretch on cell monolayers [91, 152, 155-157]. Briefly, the system works by applying a vacuum underneath the culture plates, causing membrane deformation with negligible shear stress and hydrostatic pressure. A rigid arc tangent loading post positioned under the membrane provides a uniaxial stretch to the membranes. Computer control over the vacuum regulating valves allows for user specific stretch regimens such as 10% strain at 1 Hz frequency in this study.

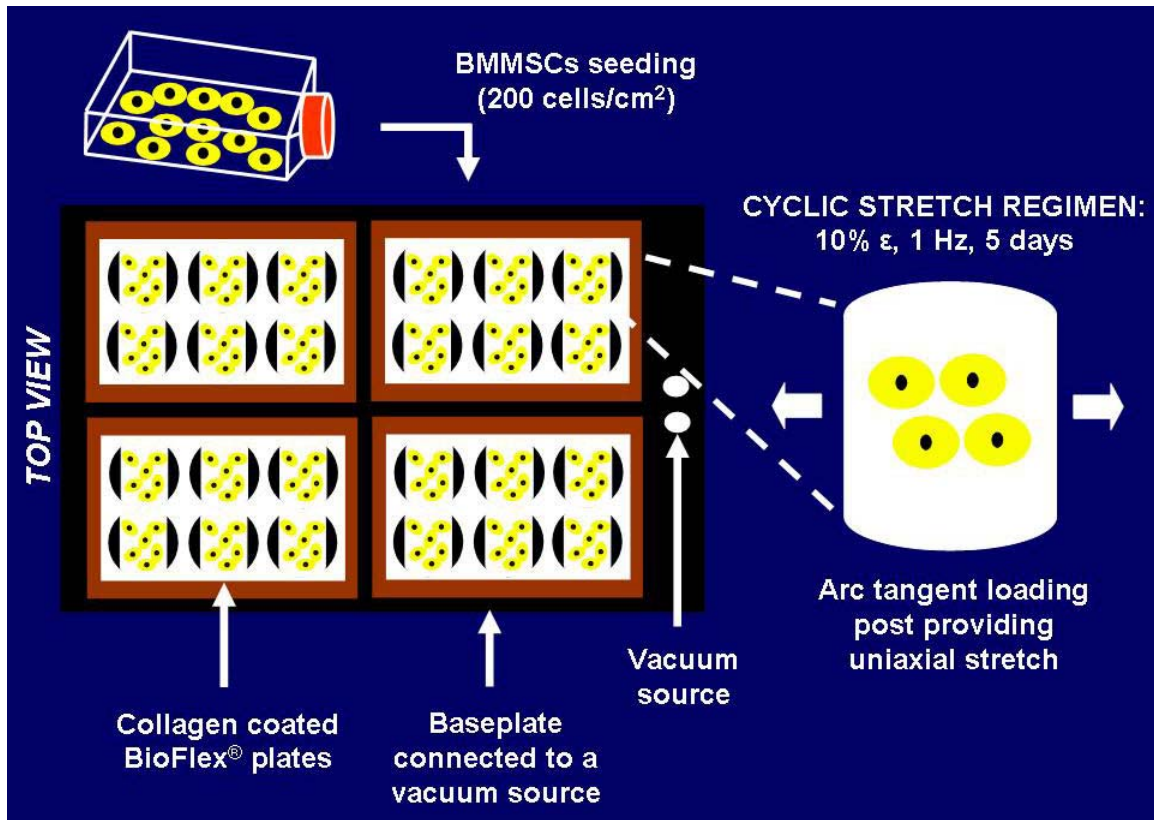


Figure 5-1: Schematic illustrating cyclic stretch 5 day mechanical stimulation of BMMSCs at 10% strain and 1 Hz frequency. Cells not shown to scale.

### 5.1.3 Morphology

In order to evaluate cell alignment following mechanical stimulation (cyclic stretch), Coomassie Brilliant Blue R-250 (Pierce, Rockford, IL) was used for a total protein stain (to enhance contrast). The designated samples for CTRL and CS groups were fixed with 4% paraformaldehyde (USB Corporation, Cleveland, OH) for 5 minutes and washed 3 times with phosphate buffered saline (PBS, Sigma-Aldrich, St. Louis, MO). Next, the samples were incubated with Coomassie Brilliant Blue R-250 for 5 minutes, followed by 5 washes with PBS. Samples were viewed under brightfield microscopy (Nikon Eclipse E800, Glenshaw, PA), and images were qualitatively evaluated.

#### 5.1.4 Immunofluorescence

At the termination of the mechanical stimulation (cyclic stretch), designated samples for CTRL and CS groups were fixed with 4% paraformaldehyde for 5 minutes and washed 3 times with PBS. Next, samples were assessed for SMC phenotype by immunofluorescence as described in **Chapter 3.1.4** (see **Table 3-3** for details on the antibodies used).

#### 5.1.5 Calcium imaging

Ionized calcium is the most common signal transduction element associated with SMC contraction. For signal transduction,  $\text{Ca}^{2+}$  ions enter the cytoplasm, either from the sarcoplasmic reticulum or the extracellular space across the plasma membrane [7, 20, 139, 158]. These two motifs for  $\text{Ca}^{2+}$  signaling were studied via calcium imaging performed in the Department of Pharmacology in collaboration with Dr. William deGroat.

Prior to the start of calcium imaging, monolayers of uSMCs, dSMCs (CS group), and undifferentiated BMMSCs (CTRL) were cultured on collagen-coated coverslips in serum-free conditions for twenty-four hours. Calcium imaging was performed as previously described [159]. Briefly, the coverslips were loaded with 5  $\mu\text{M}$  fura-2 (Molecular Probes, Eugene, OR) for 30 minutes at 37°C, 5%  $\text{CO}_2$ . Fura-2 was dissolved in bath solution containing HBSS; in mM: 138 NaCl, 5 KCl, 0.3  $\text{KH}_2\text{PO}_4$ , 4  $\text{NaHCO}_3$ , 2  $\text{CaCl}_2$ , 1  $\text{MgCl}_2$ , 10 HEPES, 5.6 glucose, pH 7.4, to which BSA was added (5 mg/ml; Sigma-Aldrich, MO) to promote loading. Coverslips were placed on an inverted epifluorescence microscope (Olympus IX70, Melville, NY) and continuously perfused with HBSS (flow rate  $\approx$  2 mL/min). Fura-2 was excited alternately with ultraviolet light at 340 and 380 nm and the fluorescence emission was detected at 510 nm.

Agonists were bath applied through gravity-driven perfusion system (flow rate  $\approx$  2 mL/min) by manually switching a valve from the container holding HBSS to the container holding the agonist dissolved at the desired concentration. See **Table 5-1** for details on agonists used in the study. For measuring calcium activity in the absence of extracellular calcium ( $[Ca^{2+}]_{ex}$ ), HBSS was used as described above, but without  $CaCl_2$ . Each agonist was applied for approximately 60 seconds followed by HBSS perfusion before another agonist application.

**Table 5-1: Agonists used during calcium imaging studies.**

<b>Chemical</b>	<b>Concentration</b>	<b>Catalog Number</b>	<b>Manufacturer</b>
ATP	100 $\mu$ M	A9187	Sigma-Aldrich, St.Louis, MO
KCl	80 mM	P3911	Sigma-Aldrich, St.Louis, MO
Phenylephrine	100 $\mu$ M	P6126	Sigma-Aldrich, St.Louis, MO

Wavelength selection, excitation timing, and acquisition of images were controlled using C-Imaging software (Compix, Irvine, CA). During image analysis, background was subtracted to minimize camera dark noise and tissue autofluorescence. An area of interest was drawn around each cell, and the average value of all pixels included in this area was taken as one measurement. Data analysis was performed using Excel (Microsoft, Redmond, WA). Intracellular calcium ( $[Ca^{2+}]_{in}$ ) was determined from the average measurement of 10-15 cells obtained before and after agonist application. The results are given as changes in  $[Ca^{2+}]_{in}$  reported as Ratio (340/380), before and after agonist application in the presence and absence of  $[Ca^{2+}]_{ex}$  over time. uSMCs used were at passage 5, while CS and CTRL cells were at passage 6

### 5.1.6 Contraction assessment

Extensive use of measuring cell traction started almost 30 years ago, when Harris *et al.* cultured cells on thin sheets of silicon fluid cross-linked using a flame. Adhered cells exerted compressive forces causing wrinkles on the substratum, which were visible under the light microscope [160]. Over the years, several new optimization schemes and methods have been introduced to better assess cell traction during events such as contraction [161-165]. One such method is the use of contemporary optical microscopy and fluorescent molecules in live cells to investigate contraction or dilation perfected by Drs. Claudette St. Croix and Simon Watkins at the Center for Biologic Imaging [166].

Contraction assessment was performed in collaboration with them by making a few changes to their previously described protocol [166]. Briefly, uSMC, dSMCs (CS group), and undifferentiated BMSCs (CTRL) monolayers were cultured on collagen coated dishes (MatTek Corporation, Ashland, MA) in serum-free conditions for twenty-four hours. To obtain CS and CTRL cells, at the end of cyclic stretch mechanical stimulation and static culture, designated samples were exposed to trypsin-EDTA (Invitrogen, Carlsbad, CA).

Following the initial twenty-four hour culture on MatTek dishes, cells were imaged in a closed, thermocontrolled (37°C) stage using MetaMorph (Molecular Devices, Sunnyvale, CA) and an inverted microscope (Nikon Eclipse TE-2000E, Glenshaw, PA). Periodic images were taken (every 30 seconds) when cells were sequentially exposed to baseline (serum-free media), agonist (see **Table 5-2**) and recovery (serum-free media) conditions. Each condition was examined for approximately 15-20 minutes. After each agonist condition, a PBS wash was performed to ensure complete removal of previous agonist. Following data acquisition, images and time-lapsed videos were used for qualitative assessment using MetaMorph. Briefly, time-

lapsed videos were constructed by first loading the images using the *apps* function under the *base files* option on the toolbar in MetaMorph. Briefly, cells of interest were selected using the *ROI* (region of interest) function. The region of interest was then duplicated using the *duplicate* function to zoom in and adjust the *auto-scale* for enhanced contrast between cells and the underlying collagen-coated substrate. In order to display time and the treatment (media, agonist, or recovery) that the cell monolayers were exposed to, the *text* and *elapsed time* functions were chosen under the *display/graphics* tool. Periodically imaged stacks were tagged together to form one cohesive movie using the *make movie* function. uSMCs used were at passage 5, while CS and CTRL cells were at passage 6

**Table 5-2: Agonists used during contraction assessment.**

<b>Chemical</b>	<b>Concentration</b>	<b>Catalog Number</b>	<b>Manufacturer</b>
ATP	100 $\mu$ M	A9187	Sigma-Aldrich, St.Louis, MO
KCl	80 mM	P3911	Sigma-Aldrich, St.Louis, MO
Phenylephrine	50-100 $\mu$ M	P6126	Sigma-Aldrich, St.Louis, MO

## 5.2 RESULTS

### 5.2.1 Morphology

From qualitative assessment of **Figure 5-2**, it appears that the stretched cells within the CS group show a tendency to elongate and align perpendicular to the direction of stretch. Whereas,

statically cultured cells within the CTRL group display random cell long axis and orientation in the absence of external strain. This finding is consistent with those found previously for these cells [91].

For striking comparisons with the origin of this mechanobiology work in our laboratory, **Figures 5-3 and 5-5** have been borrowed from Dr. Timothy M. Maul's dissertation [91]. Qualitatively speaking, the trends for cell shape and alignment remain similar in both of our studies (**Figures 5-2 and 5-3**). In **Figure 5-3B**, it appears that the cyclic strain causes cessation of cell proliferation in **Figure 5-3B**. This trend in cell proliferation appears to be present in the current work as well, but it is much less pronounced (**Figure 5-2B**).

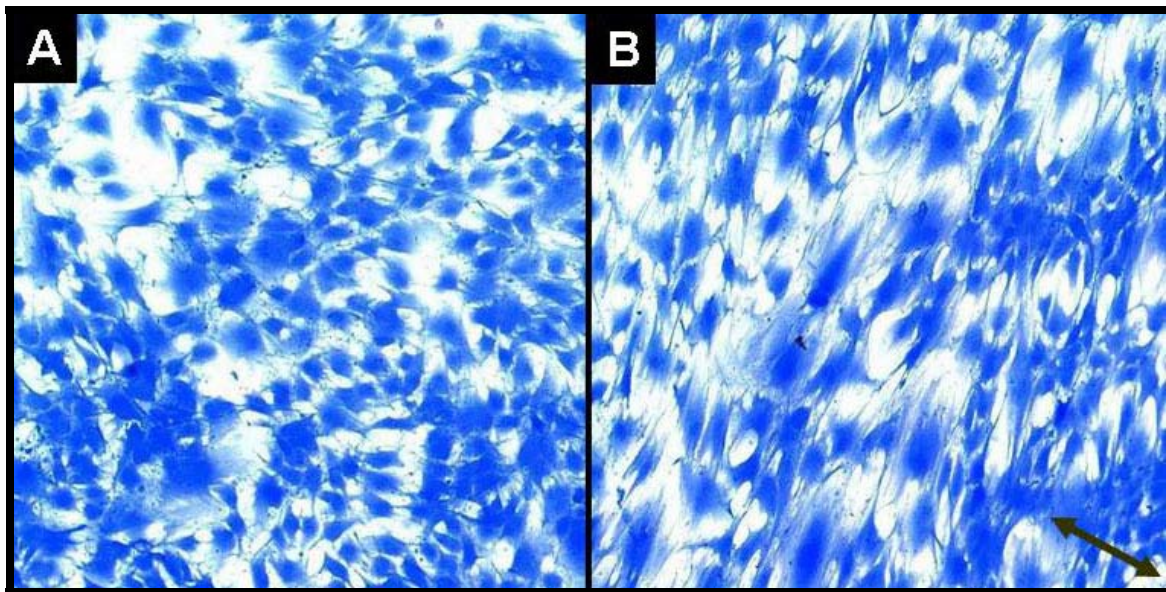


**Figure 5-2: Coomassie brilliant blue stained BMMSCs in CTRL (A, static culture) and CS groups (B: cyclic stretch). Arrow indicated the direction of stretch. These are representative images taken at 10x.**

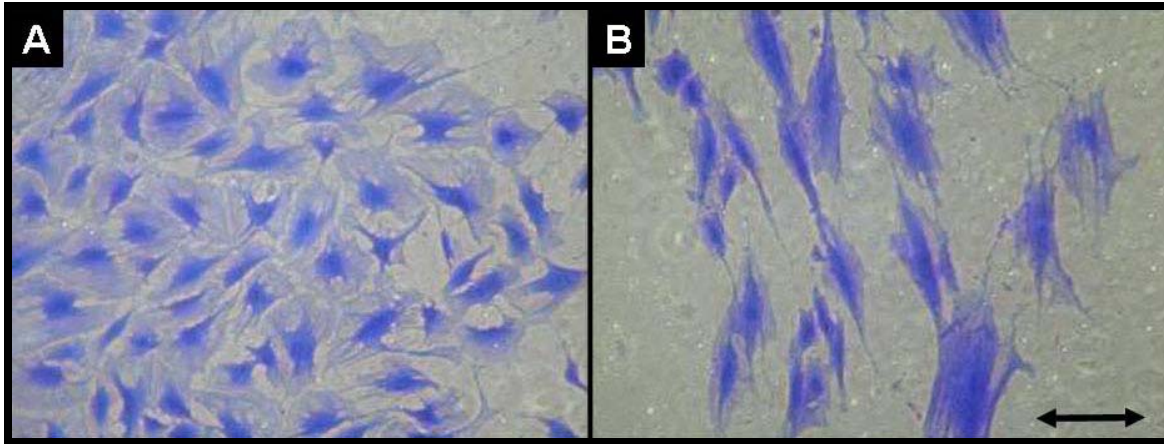


**Figure 5-3:** Coomassie brilliant blue stained BMMSCs in CTRL (A, static culture) and CS groups (B: cyclic stretch). Arrow indicates the direction of stretch. These images were obtained from [91], taken at 10x.

## 5.2.2 Immunofluorescence

**Figure 5-4** shows that some BMMSCs stained positive for SMA and CALP after 5 days of 10% cyclic stretch (heterogeneous result). Neither protein could be detected in static cultures. MHC was not found in either stretched or control cultures.

SMA and CALP expression was also seen in Maul's work (**Figure 5-5, D-E**). He was successful in finding MHC expression in his stretched cultures, as well (**Figure 5-5F**). Moreover, he found positive staining for SMA, CALP and MHC in all (homogeneous result) of the cells (**Figure 5-5, D-F**), and not just a few (**Figure 5-5, D-E**). Judging from the lower nuclear count, it is obvious that Maul's cyclic stretch caused cessation of cell proliferation. Again, this trend is visible in my study, but much less profound. Finally, qualitative assessment of protein filaments confirms the perpendicular cell alignment to the direction of stretch.

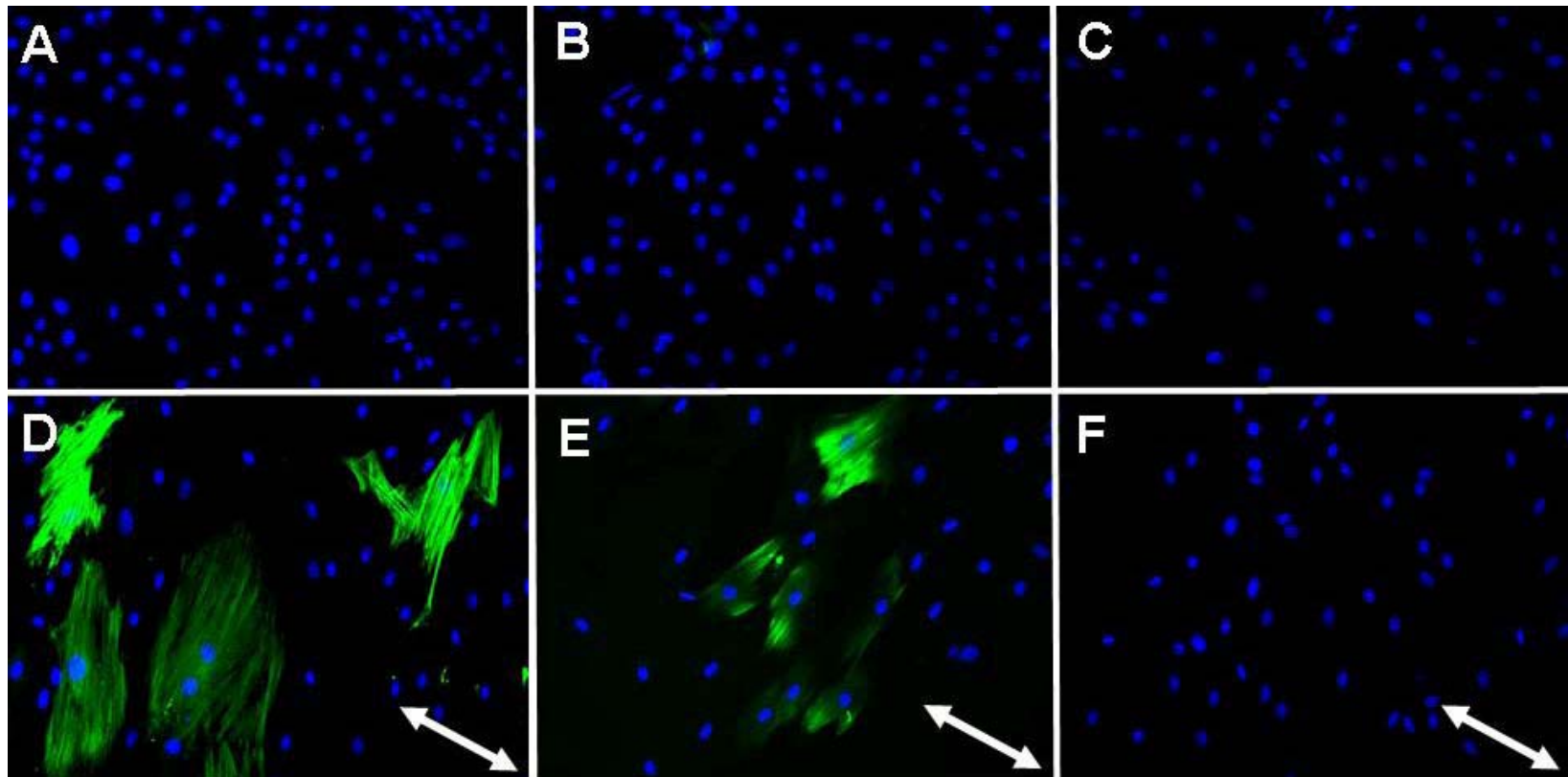


**Figure 5-4: Immunofluorescence staining of smooth muscle markers SMA (A, D), CALP (B, E), and MHC (C, F) on BMMSCs in CTRL (A-C, static culture) and CS groups (D-F, dSMCs). Arrow indicates the direction of stretch. Green = protein, blue = nuclei. These are representative images taken at 20x.**

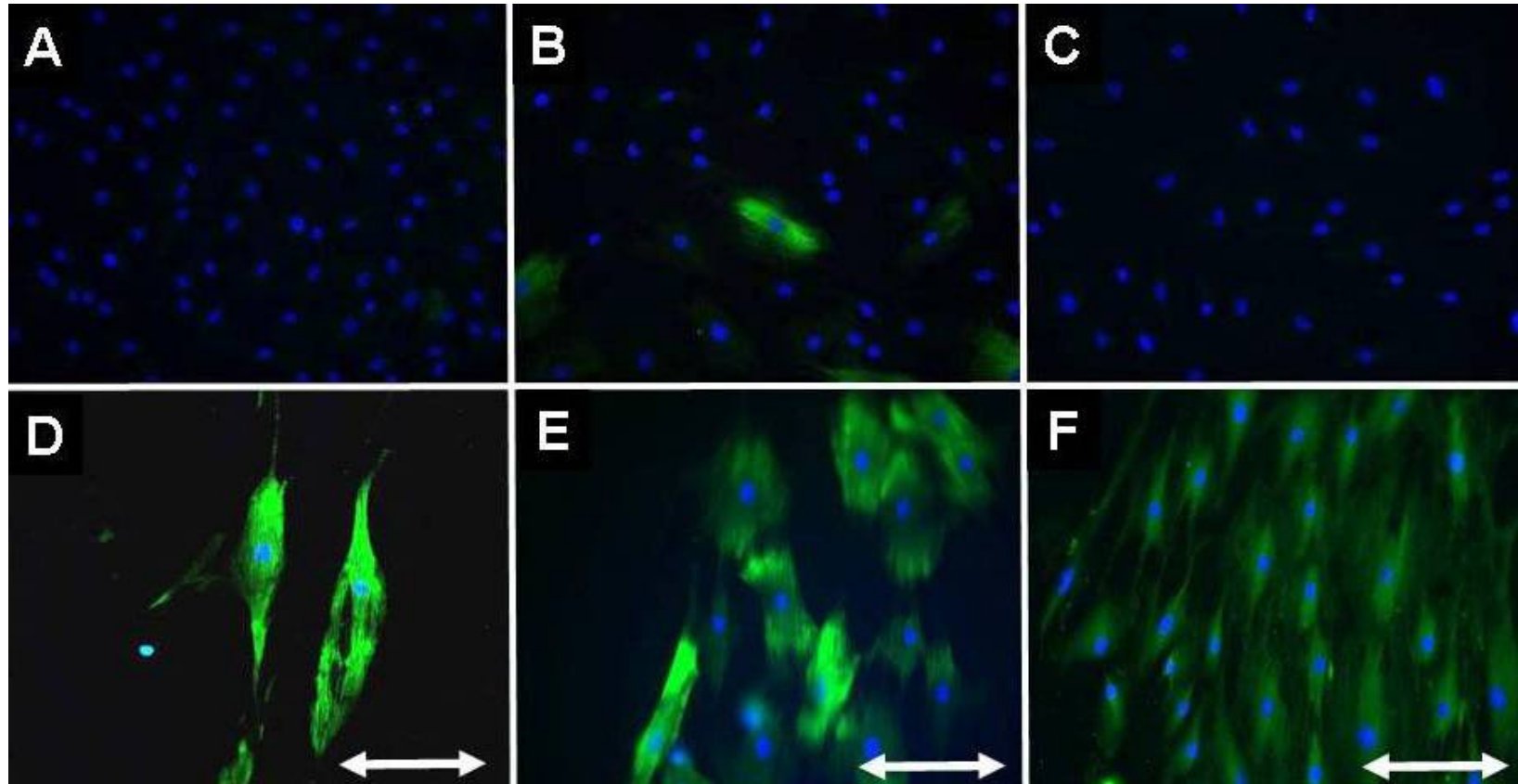


**Figure 5-5: Immunofluorescence staining of smooth muscle markers SMA (A, D), CALP (B, E), and MHC (C, F) on BMMSCs in CTRL (A-C, static culture) and CS groups (D-F, dSMCs). Arrow indicates the direction of stretch. Green = protein, blue = nuclei. These images were obtained from [91], taken at 20x.**

### 5.2.3 Calcium imaging

During fura-2 calcium imaging, both uSMCs (**Figure 5-6**) and dSMCs (**Figure 5-7**) respond positively to ATP in the presence and absence of  $[Ca^{2+}]_{ex}$  showing  $[Ca^{2+}]_{in}$  activity. However, they fail to respond to other physiologically important agonists such as phenylephrine (PE) and potassium chloride (KCl). BMMSCs obtained from static cultures also respond to ATP in the presence of  $[Ca^{2+}]_{ex}$ , but not in its absence (**Figure 5-8**). They fail to respond to PE and KCl, as well.

For any of the above-mentioned positive responses, the magnitude of  $[Ca^{2+}]_{in}$  activity (measured by the dimensionless y-axis) is worth noting. It varies amongst the different cell populations being greatest in uSMCs, mediocre in dSMCs, and lowest in BMMSCs obtained from static cultures.

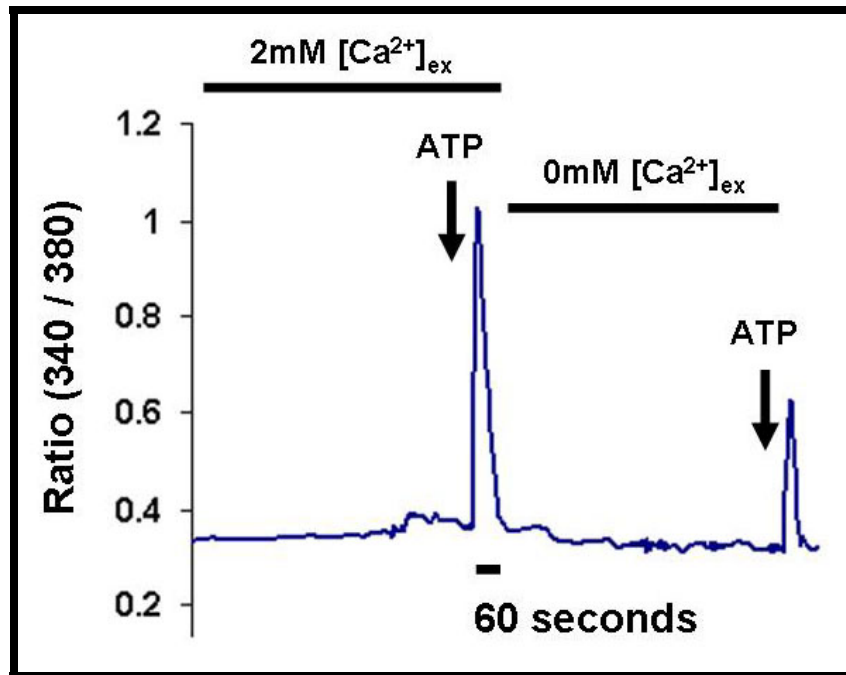


**Figure 5-6:** ATP-evoked  $Ca^{2+}$  response in the presence ( $\approx 1.05$ ) and absence ( $\approx 0.62$ ) of extracellular  $Ca^{2+}$  for uSMC monolayers. Averaged data from  $n = 12$  cells.

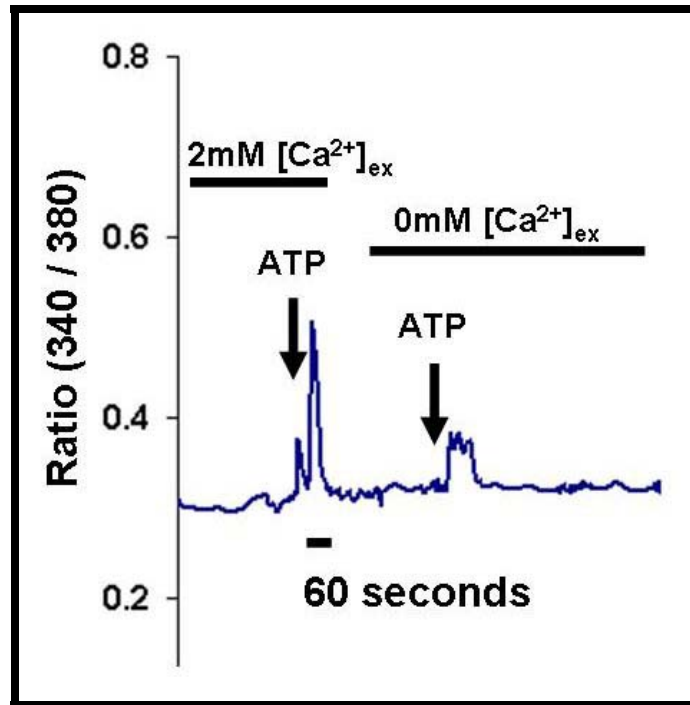


Figure 5-7: ATP-evoked  $\text{Ca}^{2+}$  response in the presence ( $\approx 0.50$ ) and absence ( $\approx 0.37$ ) of extracellular  $\text{Ca}^{2+}$  for BMMSC monolayers obtained from stretched cultures (dSMCs). Averaged data from  $n = 13$  cells.

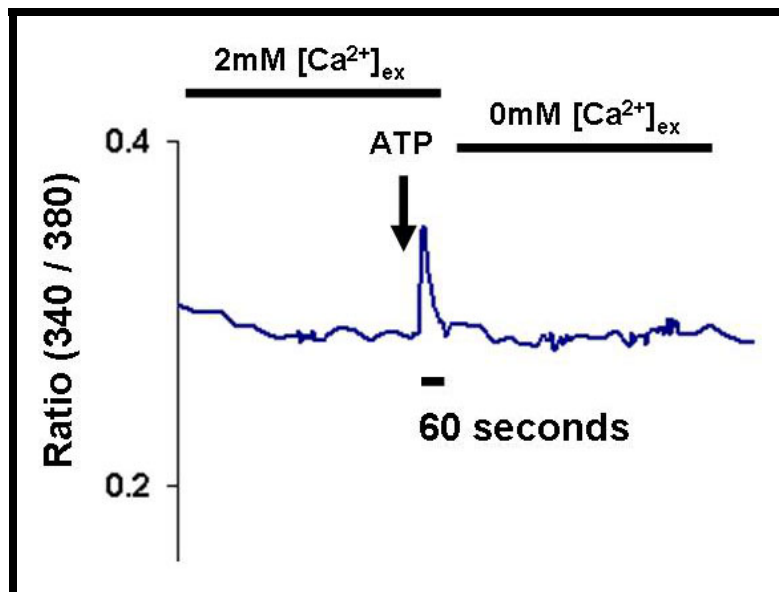
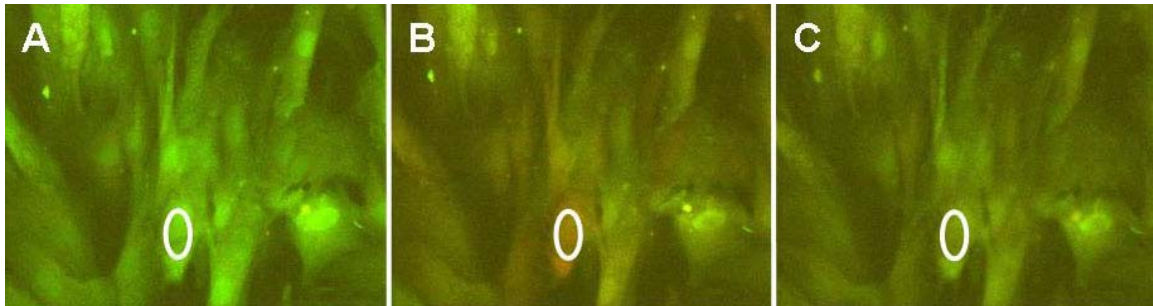


Figure 5-8: ATP-evoked  $\text{Ca}^{2+}$  response in the presence ( $\approx 0.35$ ) of extracellular  $\text{Ca}^{2+}$  (but not absence) for BMMSC monolayers obtained from static cultures. Averaged data from  $n = 8$  cells.

Fura-2 loading efficiency was high as seen in **Figure 5-9**, which also offers a qualitative look at the calcium imaging principle. The ratio of emissions at fura-2 excitation wavelength 340 and 380 nm changes with a change in  $[Ca^{2+}]_{in}$  uptake over time. In the case of **Figure 5-9**, ATP causes this change.



**Figure 5-9: Representative images illustrating the change in spectral properties of fura-2 bound to intracellular  $Ca^{2+}$  ions (pointed out in one cell with circles) before (A: baseline HBSS perfusion) and after (C: recovery using HBSS perfusion) an ATP-elicited response (B).**

#### 5.2.4 Contraction assessment

uSMCs, dSMCs, and BMMSCs obtained from static cultures showed no contraction in response to individually applied chemical stimulation using ATP, PE, and KCl. **Figure 10** shows the absence of change in the cell morphology after the exposure to various stimuli.

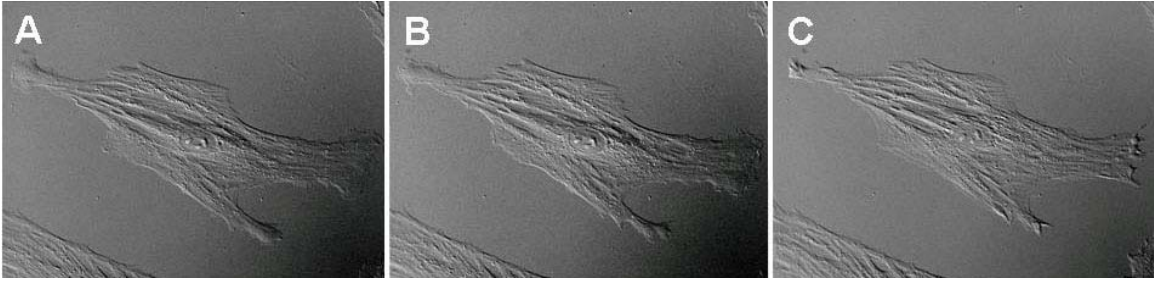


**Figure 5-10: Montage (A: baseline media, B: agonist, C: recovery using media) illustrating failure of cells to contract in response to various agonists. This a representative montage for results obtained examining uSMCs, dSMCs, and BMMSCs obtained from static cultures. Images taken at 40x.**

### 5.3 DISCUSSION

SMCs dominate the walls of internal organs (viscera) such as the esophagus, blood vessel and urethra. They play an essential role in angiogenesis, vessel maintenance, regulation of blood pressure, and they generate force to move material through the lumen of the organ. SMCs embody many contractile elements including actin-myosin cross-bridges, sarcoplasmic reticulum with  $\text{Ca}^{2+}$  release channels, and a  $\text{Ca}^{2+}$  signals that initiate the contraction process. Therefore, we established different objectives including phenotypic characterization, calcium imaging, and contraction assays to create a “complete model” for studying SMC functionality, which can be very useful in tissue engineering applications.

Characterization of SMCs is often done by demonstrating the presence of SMA, whose transient expression in non-SMCs cannot be ruled out [143]. Therefore, the presence of CALP in addition to SMA in uSMCs (**Chapter 3**) and dSMCs is increasingly SMC-restrictive. However, the absence of MHC in this shows evidence that they are not mature SMCs by virtue of phenotypic characterization. At the very least, the expression of SMA and CALP confirm that mechanical forces such as cyclic strain can result in differentiation of stem cells into SMCs [91,

152]. The differences in cell proliferation and heterogeneous nature of differentiation between this study and that of Maul may be due to the possibility of unknown differences in serum lots and errors in initial cell seeding density [91]. Elucidating the exact mechanism causing differentiation of BMMSCs towards SMC lineage on account of cyclic stretch was beyond the scope of this work. One possible cause could be the activation of mitogen-activated protein kinases (MAPK), such as extracellular signal-regulated kinase (ERK) and c-jun amino terminal kinase (JNK) in the presence of external mechanical stimuli, as previously suggested [167].

Aside from phenotypic characterization, intracellular (cytoplasmic) calcium is also a major determinant in SMC contraction, warranting its assessment in uSMCs and dSMCs using unstretched BMMSCs as controls. Calcium imaging studies reveal that the uSMCs and dSMCs appear to generate cytoplasmic calcium activity by calcium release from internal stores such as sarcoplasmic reticulum (in the absence of extracellular  $\text{Ca}^{2+}$  within HBSS perfusion buffer) as well as calcium influx from extracellular milieu (in the presence of 2 mM  $\text{Ca}^{2+}$  within HBSS perfusion buffer), both of which are vital for full SMC function [7]. Higher  $[\text{Ca}^{2+}]_{\text{in}}$  measurements in uSMCs over dSMCs and controls suggest greater ion channel activity in those cells. However, the absence of a reaction to PE and KCl suggests that these SMC populations are not mature because as they might lack the necessary receptors required for ligand-gated ion channel activity stimulated by agonists like PE and KCl. Finally, the low  $[\text{Ca}^{2+}]_{\text{in}}$  measurements for dSMCs and controls in the absence and presence of  $[\text{Ca}^{2+}]_{\text{ex}}$ , respectively, might not imply true physiologic activity. One way of identifying this problem in the future is by performing multiple experiments on a different batch of cells and tracking the baseline  $[\text{Ca}^{2+}]_{\text{in}}$  measurements among the same cell population (uSMC and dSMCs).

Contraction assessment of uSMCs and dSMCs also displayed the lack of a response to various agonists, which further suggests the immature nature of these SMCs. This result of uSMCs and dSMCs is not surprising given the absence of myosin filaments, which form the basis for actin-myosin cross-bridge cycling necessary for contraction. Future studies should focus on the *in vitro* maturation of these SMCs under different conditions, including the use of alternative culture media [151], electrophysiological stimulation [151], cell culture in native matrix-like substrates [132, 141, 142], and chemical stimulation using growth factors and hormones [144].

Collective results of phenotypic characterization, calcium imaging and contraction assay establish that the isolated uSMCs and dSMCs at the current differentiation stage are not fully functional. However, this study represents an important step in the broader picture of investigating functionality of SMCs with implications in tissue engineering.

One limitation of this study is the exclusion of voltage-gated ion channel activity assessment from our objectives mentioned above. The SMC contraction mechanism becomes activated either due to voltage- or receptor-operated ion channels demanding the need to assess the former. To address this limitation, the conventional patch-clamp technique could be used [151] in the future. This would allow experimental control of the membrane potential for characterizing the voltage dependence of membrane currents in uSMCs and dSMCs. In using specific agonists such as purinergic blockers during the patch-clamp technique experiments can help identify specific calcium and potassium channels that are ubiquitously found in SMCs [138].

After systematic examination of *in vitro* maturation of both uSMCs and dSMCs as mentioned above; fura-2 calcium imaging, live-cell contraction assessment, as well as patch-

clamp experiments should be pursued to study the functional characteristics of SMCs. Selective use of electrical stimulations and chemical agonists (both contractile and relaxing agents), in such studies can help identify voltage- and ion- gated channel activities that are specific to SMCs [20, 138, 151]. Inclusion of such items would make our model of SMC functionality assessment more complete.

## 6.0 CONCLUSIONS

Smooth muscle cells (SMCs) are a functionally critical component for an array of tissues located within the cardiovascular, gastrointestinal, respiratory and urinary systems. Millions of people suffer from diseases related to SMC deficiency in these tissues. Clinically, these tissues are treated with organ transplantation or with the use of synthetic substitutes. However, organ transplantation is limited by a shortage of donor tissue suitable for transplantation, and synthetic options rarely replace the entire function of the original tissue and often carry a substantial risk of infection, graft necrosis, inadequate blood supply, lack of peristaltic activity, and other complications. This has motivated us to explore the promising field of tissue engineering to treat these types of diseases without the limitations of current therapies.

With that broader picture in mind, the purpose of this project was to create a tubular-shaped tissue engineered urethral wrap (TEUW) using isolated urethral smooth muscle cells (uSMCs), for providing therapy for urethral dysfunctions such as stress urinary incontinence, which can often be caused by SMC abnormality within the urethra. This study also investigated the functional aspect of uSMCs and differentiated SMCs (dSMCs) obtained from mechanical stimulation of bone marrow-derived mesenchymal stem cells.

The work presented in this thesis suggests that isolated uSMCs positively express smooth muscle markers such as  $\alpha$ -actin and calponin. However, they do not express myosin heavy chain, a highly definitive smooth muscle contractile marker. Nonetheless, the isolation purity marked

by the absence of other cell types, which are also present in the urethra, was an important step toward the development of uSMC-populated TEUWs. The TEUWs failed to synthesize extracellular matrix (ECM) proteins such as collagen over a 5-day culture period in the presence of a stimulant such as ascorbic acid. They also show greater compliance than the native urethra. The lack of ECM deposition and stiffness can be addressed by employing longer culture periods such as two weeks and/or biochemical stimulants such as transforming growth factor- $\beta$  [149]. For functionality assessment, isolated uSMCs and dSMCs were subjected to calcium imaging and live-cell contraction assays. During calcium imaging, the use of ATP was able to produce  $\text{Ca}^{2+}$  transients in uSMCs and dSMCs, suggesting that it may be functional in the activation of the SMC contraction mechanism. However, neither cell population responded to other agonists such as phenylephrine and potassium chloride, implying underdeveloped ligand-gated ion channels. Not surprisingly, contraction assays did not show any morphological change in both uSMCs and dSMCs in response to different chemical stimuli. This result is most likely due to two factors: the absence of myosin filaments required for contractile assembly of actin and myosin, and the lack of specific receptors on cell's plasma membrane to which agonists can bind and stimulate the contraction mechanism. Despite these results, both calcium imaging and live-cell contraction assessment are valuable tools in measuring cytosolic  $\text{Ca}^{2+}$  levels and assessing contraction, respectively, warranting the need for ongoing exploration of these techniques in the future.

In conclusion, this work has provided significant information that may be valuable for the development of an experimental model to study smooth muscle characteristics. The knowledge obtained from such a model may ultimately lead to new clinical therapies for the large number of diseases compromising SMC-containing tissue including, but not limited to the urethra.

Additionally, this study may also lead to an elevated understanding of biological mechanisms, which need to be deciphered in order to successfully create engineered tissue equivalents containing functional smooth muscle.

## 7.0 FUTURE WORK

This work has several facets that would be very interesting to expand upon. First, it is imperative that we facilitate the generation of contractile smooth muscle cell (SMC) markers such as myosin heavy chain. This can be achieved by individual or synergistic contributions of cell culture in basement membrane matrices such as Matrigel, electrical stimulation relevant to SMC physiology, and exposure to growth factors and neurotransmitters that are essential to SMC contractile activity. Systematic evaluation of these factors can assist with *in vitro* development of myosin filaments that are crucial for actin-myosin cross-bridges responsible for smooth muscle contraction.

In addition to phenotypic characterization of smooth muscle contractile markers, it is important to further expand upon the current functionality assay. A wide range of contractile as well as relaxation agonists relevant to *in vivo* physiology could be used to demonstrate full SMC functionality. Action potentials may also activate the SMC contraction mechanism, demanding the need to assess electrical properties of smooth muscle cells to obtain a more complete understanding. This can be achieved by using the conventional patch-clamp technique in the whole-cell configuration. Additionally, studying gap-junction proteins such as the family of connexins would also be beneficial. The presence of gap junctions in the urethral smooth muscle for instance, allows it to contract more effectively while expelling urine.

Longer culture durations together with supplements of growth factors such as transforming growth factor- $\beta$  could be used to assess SMC-mediated compaction in our TEUWs to bring them closer to the characteristics of native tissues. More so, differentiated SMCs could also be used to fabricate tubular constructs, as this cell source offers a more practical approach, benefiting clinical translation for end-stage organ replacements.

Finally, future work will need to assess the effectiveness of such SMC-populated tubular constructs *in vivo* using an animal model. The body is the ultimate bioreactor and an essential tool for diagnosing the effectiveness of our solution, which is developed by means of *in vitro* tissue engineering.

The challenges that remain in creating a fully functional tissue construct are many. Yet, in spite of these challenges, the continuation of interdisciplinary interactions can facilitate the creation of an effective therapy that “guides” the damaged tissues through an autonomous regeneration process.

## APPENDIX A

### CALCULATIONS FOR COMPACTION OF FIBRIN-BASED TISSUE ENGINEERED URETHRAL WRAPS AS A PERCENT OF THEIR INITIAL VOLUME BEFORE CULTURE

Fibrin-based tissue engineered urethral wraps (TEUWs) were fabricated using urethral smooth muscle cells as described in **Section 4.1.1**. The following equation was used to calculate the volume of such cylindrical constructs:

$$V = \pi * (R^2 - r^2) * L$$

where  $R$  is the outer radius,  $r$  is the inner radius,  $L$  is the length,  $V$  is the volume of the construct.

Before the 5-day spinner flask culture, the day 0 dimensions of uSMC-based TEUW were assumed equal from construct to construct as were measured by estimating the three-dimensional mold used to fabricate TEUW using vernier calipers. The measured values were  $R = 5\text{mm}$ ,  $r=1.25\text{mm}$ ,  $L=50\text{mm}$ , and  $V=3681.445\text{mm}^3$  or  $V_{day0}=3681.445\text{mm}^3$ .

Following the 5-day spinner flask culture, the dimensions of compacted TEUWs were estimated in this manner:  $R$  was recorded as half the loaded outer diameter recorded during intraluminal pressure of 0 mmHg prior to the start of mechanical testing;  $r$  was determined as half the inner diameter at zero pressure as described in **Section 4.1.5**;  $L$  was measured using

vernier calipers by placing the TEUW in a media-filled Petri dish prior to mounting within the bathing chamber for mechanical testing. The individual and average R, r, L, and volume measurements ( $V_{day5}$ ) with standard errors of means (SEM) for TEUWs after the 5-day spinner flask culture (n=4) are provided below:

	R (mm)	r (mm)	L (mm)	$V_{day5}$ (mm <sup>3</sup> )
TEUW 1:	1.4050	0.4450	12.8	71.4183
TEUW 2:	1.2155	0.3162	13.4	57.9860
TEUW 3:	1.2671	0.2671	13.5	65.0655
TEUW 4:	1.2724	0.1724	14.5	72.3925
Average $\pm$ SEM	1.29 $\pm$ 0.02	0.30 $\pm$ 0.03	13.55 $\pm$ 0.18	66.72 $\pm$ 1.67

The following formula was used to calculate compaction of TEUWs after the spinner flask culture as a percentage of its initial volume (3681.445mm<sup>3</sup>):

$$\% V = \left( \frac{V_{day5}}{V_{day0}} \right) * 100$$

where  $V_{day5}$  and  $V_{day0}$  are the TEUW volumes after and before 5-day spinner flask culture, respectively. The individual and average values for the TEUW volume as a percentage of the original volume before the 5-day spinner flask culture are provided below.

	% V
TEUW 1	1.94
TEUW 2	1.58
TEUW 3	1.77
TEUW 4	1.97
Average $\pm$ SEM	1.81 $\pm$ 0.09

## APPENDIX B

### PROPOGATION OF ERROR ASSOCIATED WITH PRESSURE AND OUTER DIAMETER MEASUREMENTS

The following error analysis was performed as previously described [168]. Before measuring the propagation of error in calculated quantities, the uncertainty in the measured parameters such as pressure and outer diameter was first estimated. The mechanical testing system was set up using a piece of Penrose™ rubber tube (Ref# 0912010, C.R.Bard Inc., Covington, GA) tied onto the tees of the *in vitro* testing apparatus described in **Section 4.1.5**. Using the hydrostatic fluid reservoir, static pressure was increased and the outer diameter of the rubber tube during inflation was measured using the laser micrometer. Values for both pressure and outer diameter were averaged and standard deviations were computed. This was repeated 3 times. The uncertainty was taken as two standard deviations for 95% confidence limits and given by:

$$\sigma = 2 * 1.96 * \sigma_{\text{measured}}$$

where  $\sigma$  is the uncertainty value and  $\sigma_{\text{measured}}$  is the standard deviation of the pressure or outer diameter. These uncertainty values for pressures (0, 6, 12, 20 mm Hg) and corresponding diameters are provided below:

$$\sigma_{P0}: 0.0154, \sigma_{D0}: 0.0990;$$

$$\sigma_{P6}: 4.4495, \sigma_{D6}: 0.0771;$$

$$\sigma_{P12}: 4.5038, \sigma_{D12}: 0.0442;$$

$$\sigma_{P20}: 0.1455, \sigma_{D20}: 0.0188.$$

Before calculating the propagation of errors for compliance over 0-6 mm Hg (low), 6-12 mm Hg (mid) and 12-20 mm Hg (high), the following calculations were performed:

$$\sigma_{\Delta P} = \sqrt{\sigma_{P_{\max}} + \sigma_{P_{\min}}}$$

$$\sigma_{\Delta D} = \sqrt{\sigma_{D_{\max}} + \sigma_{D_{\min}}}$$

where  $\sigma_{P_{\max}}$  and  $\sigma_{P_{\min}}$  are the uncertainty values for maximum and minimum pressures, and  $\sigma_{D_{\max}}$  and  $\sigma_{D_{\min}}$  are the uncertainty values for maximum and minimum outer diameters. The percentage of error for compliance was calculated by using the following equation:

$$\% \sigma_C = \sqrt{(\% \sigma_{\Delta P})^2 + (\% \sigma_{\Delta D})^2 + (\% \sigma_{D_{\min}})^2}$$

where  $\% \sigma_{\Delta P} = \sigma_{\Delta P} / \Delta P$  and  $\% \sigma_{\Delta D} = \sigma_{\Delta D} / \Delta D$ , i.e., uncertainty values divided by measured differences in values. The resulting propagation errors for compliance over 0-6 mm Hg (low), 6-12 mm Hg (mid) and 12-20 mm Hg (high) are listed shown below:

$$\sigma_{\text{low } C} = 0.79\%;$$

$$\sigma_{\text{mid } C} = 1.53\%;$$

$$\sigma_{\text{high } C} = 1.73\%.$$

## BIBLIOGRAPHY

1. Atala, A., *Tissue engineering and regenerative medicine: concepts for clinical application*. Rejuvenation Res, 2004. **7**(1): p. 15-31.
2. Brading, A.F., *Smooth muscle research: from Edith Bulbring onwards*. Trends Pharmacol Sci, 2006. **27**(3): p. 158-65.
3. Murphy, R.A., *Muscle Cells of Hollow Organs*. News Physiol Sci, 1988. **3**: p. 124-28.
4. Nikolovski, J. and D.J. Mooney, *Smooth muscle cell adhesion to tissue engineering scaffolds*. Biomaterials, 2000. **21**(20): p. 2025-32.
5. Owens, G.K., *Regulation of differentiation of vascular smooth muscle cells*. Physiol Rev, 1995. **75**(3): p. 487-517.
6. Silverthorne, D.U., *Human physiology: an integrated approach*. 3 ed. 2003: Benjamin Cummings.
7. Webb, R.C., *Smooth muscle contraction and relaxation*. Adv Physiol Educ, 2003. **27**(1-4): p. 201-6.
8. Langer, R. and J.P. Vacanti, *Tissue engineering*. Science, 1993. **260**(5110): p. 920-6.
9. L'Heureux, N., et al., *A completely biological tissue-engineered human blood vessel*. Faseb J, 1998. **12**(1): p. 47-56.
10. Niklason, L.E., et al., *Functional arteries grown in vitro*. Science, 1999. **284**(5413): p. 489-93.
11. Ratner, B.D., et al., *Biomaterials science: an introduction to materials in medicine*. 2 ed. 2004.
12. Atala, A., *Tissue engineering in urology*. Curr Urol Rep, 2001. **2**(1): p. 83-92.
13. Brading, A.F., *The physiology of the mammalian urinary outflow tract*. Exp Physiol, 1999. **84**(1): p. 215-21.

14. Vandekerckhove, J. and K. Weber, *The complete amino acid sequence of actins from bovine aorta, bovine heart, bovine fast skeletal muscle, and rabbit slow skeletal muscle. A protein-chemical analysis of muscle actin differentiation.* Differentiation, 1979. **14**(3): p. 123-33.
15. Fatigati, V. and R.A. Murphy, *Actin and tropomyosin variants in smooth muscles. Dependence on tissue type.* J Biol Chem, 1984. **259**(23): p. 14383-8.
16. Darby, I., O. Skalli, and G. Gabbiani, *Alpha-smooth muscle actin is transiently expressed by myofibroblasts during experimental wound healing.* Lab Invest, 1990. **63**(1): p. 21-9.
17. Cintonino, M., et al., *Expression of alpha-smooth-muscle actin in stromal cells of the uterine cervix during epithelial neoplastic changes.* Int J Cancer, 1991. **47**(6): p. 843-6.
18. Winder, S.J., C. Sutherland, and M.P. Walsh, *Biochemical and functional characterization of smooth muscle calponin.* Adv Exp Med Biol, 1991. **304**: p. 37-51.
19. Frid, M.G., et al., *Myosin heavy-chain isoform composition and distribution in developing and adult human aortic smooth muscle.* J Vasc Res, 1993. **30**(5): p. 279-92.
20. Chamley-Campbell, J., G.R. Campbell, and R. Ross, *The smooth muscle cell in culture.* Physiol Rev, 1979. **59**(1): p. 1-61.
21. Miano, J.M., et al., *Smooth muscle myosin heavy chain exclusively marks the smooth muscle lineage during mouse embryogenesis.* Circ Res, 1994. **75**(5): p. 803-12.
22. *eLibrary, Medicine.* [cited 2009 June 10]; Available from: [http://www.web-books.com/eLibrary/Medicine/Physiology/Urinary/urinary\\_system.jpg](http://www.web-books.com/eLibrary/Medicine/Physiology/Urinary/urinary_system.jpg).
23. Norton, P. and L. Brubaker, *Urinary incontinence in women.* Lancet, 2006. **367**(9504): p. 57-67.
24. Miller, K.L., *Stress urinary incontinence in women: review and update on neurological control.* J Womens Health (Larchmt), 2005. **14**(7): p. 595-608.
25. *Female Urinary Incontinence.* [cited 2009 July 4]; Available from: <http://www.uro.co.nz/articles/fui.html>.
26. Brading, A.F., et al., *Morphological and physiological characteristics of urethral circular and longitudinal smooth muscle.* Scand J Urol Nephrol Suppl, 2001(207): p. 12-8; discussion 106-25.
27. Dass, N., *Studies on the anatomy and autonomic innervation of the vesico-urethral junction and urethra.* 1997, Oxford University: Oxford, UK.

28. Macniel, H.F., W.H. Turner, and A.F. Brading, *The physiology of the pig urinary sphincter*. 1991. **10**: p. 351-2.
29. Thind, P., *The significance of smooth and striated muscles in the sphincter function of the urethra in healthy women*. *Neurourol Urodyn*, 1995. **14**(6): p. 585-618.
30. Bridgewater, M., J.R. Davies, and A.F. Brading, *Regional variations in the neural control of the female pig urethra*. *Br J Urol*, 1995. **76**(6): p. 730-40.
31. Haworth, D.J., et al. *Evaluation of a Tissue Engineered Urethral Wrap Following Implantation*. in *TERMIS North America*. 2008. San Diego, CA.
32. Abrams, P., S.K. Lowry, and A.J. Wein, *Consensus assessment and treatment of urinary incontinence*. *Lancet*, 2000. **355**: p. 2153-58.
33. Raja. *Urinary Incontinence*. [cited 2009 July 6]; Available from: <http://www.dilipraja.com/urinary-incon.htm>.
34. Rogers, R.G., *Clinical practice. Urinary stress incontinence in women*. *N Engl J Med*, 2008. **358**(10): p. 1029-36.
35. Grady, D., et al., *Postmenopausal hormones and incontinence: the Heart and Estrogen/Progestin Replacement Study*. *Obstet Gynecol*, 2001. **97**(1): p. 116-20.
36. Nygaard, I.E. and K.J. Kreder, *Pharmacologic therapy of lower urinary tract dysfunction*. *Clin Obstet Gynecol*, 2004. **47**(1): p. 83-92.
37. Ward, K.L. and P. Hilton, *A prospective multicenter randomized trial of tension-free vaginal tape and colposuspension for primary urodynamic stress incontinence: two-year follow-up*. *Am J Obstet Gynecol*, 2004. **190**(2): p. 324-31.
38. Lee, J.Y., et al., *The effects of periurethral muscle-derived stem cell injection on leak point pressure in a rat model of stress urinary incontinence*. *Int Urogynecol J Pelvic Floor Dysfunct*, 2003. **14**(1): p. 31-7; discussion 37.
39. Carr, L.K., et al., *1-year follow-up of autologous muscle-derived stem cell injection pilot study to treat stress urinary incontinence*. *Int Urogynecol J Pelvic Floor Dysfunct*, 2008. **19**(6): p. 881-3.
40. Chermansky, C.J., et al., *Intraurethral muscle-derived cell injections increase leak point pressure in a rat model of intrinsic sphincter deficiency*. *Urology*, 2004. **63**(4): p. 780-5.
41. Jack, G.S., et al., *Urinary bladder smooth muscle engineered from adipose stem cells and a three dimensional synthetic composite*. *Biomaterials*, 2009. **30**(19): p. 3259-70.

42. De Filippo, R.E., J.J. Yoo, and A. Atala, *Urethral replacement using cell seeded tubularized collagen matrices*. J Urol, 2002. **168**(4 Pt 2): p. 1789-92; discussion 1792-3.
43. Joslin Diabetes Center, U.o.C., Irvine Healthcare. [cited 2009 July 4]; Available from: <http://www.healthcare.uci.edu/dc.asp>.
44. Yang, Z., P.C. Dolber, and M.O. Fraser, *Diabetic urethropathy compounds the effects of diabetic cystopathy*. J Urol, 2007. **178**(5): p. 2213-9.
45. Andersson, K.E., *Neurotransmission and drug effects in urethral smooth muscle*. Scand J Urol Nephrol Suppl, 2001(207): p. 26-34; discussion 106-25.
46. de Groat, W.C., et al., *Neural control of the urethra*. Scand J Urol Nephrol Suppl, 2001(207): p. 35-43; discussion 106-25.
47. Watanabe, T., D.A. Rivas, and M.B. Chancellor, *Urodynamics of spinal cord injury*. Urol Clin North Am, 1996. **23**(3): p. 459-73.
48. *Spinal cord injury, Mayo Clinic*. [cited 2009 July 5]; Available from: <http://www.mayoclinic.com/health/spinal-cord-injury/DS00460>.
49. de Groat, W.C. and N. Yoshimura, *Pharmacology of the lower urinary tract*. Annu Rev Pharmacol Toxicol, 2001. **41**: p. 691-721.
50. Prantil, R.L., et al., *Ex vivo biomechanical properties of the female urethra in a rat model of birth trauma*. Am J Physiol Renal Physiol, 2007. **292**(4): p. F1229-37.
51. Cannon, T.W., et al., *Effects of vaginal distension on urethral anatomy and function*. BJU Int, 2002. **90**(4): p. 403-7.
52. Snooks, S.J., et al., *Effect of vaginal delivery on the pelvic floor: a 5-year follow-up*. Br J Surg, 1990. **77**(12): p. 1358-60.
53. Allen, R.E., et al., *Pelvic floor damage and childbirth: a neurophysiological study*. Br J Obstet Gynaecol, 1990. **97**(9): p. 770-9.
54. NIH. *Fact Sheet for Regenerative Medicine*. [cited 2009 July 6]; Available from: <http://www.nih.gov/about/researchresultsforthepublic/Regen.pdf>.
55. Saxena, A.K., et al., *Esophagus tissue engineering: hybrid approach with esophageal epithelium and unidirectional smooth muscle tissue component generation in vitro*. J Gastrointest Surg, 2009. **13**(6): p. 1037-43.
56. Baker, S.C. and J. Southgate, *Towards control of smooth muscle cell differentiation in synthetic 3D scaffolds*. Biomaterials, 2008. **29**(23): p. 3357-66.

57. Atala, A., *Recent developments in tissue engineering and regenerative medicine*. Curr Opin Pediatr, 2006. **18**(2): p. 167-71.
58. Opitz, F., et al., *Phenotypical plasticity of vascular smooth muscle cells-effect of in vitro and in vivo shear stress for tissue engineering of blood vessels*. Tissue Eng, 2007. **13**(10): p. 2505-14.
59. NIH, R.f.S.C.R. *The National Institutes of Health, Resource for Stem Cell Research. Stem Cell Basics* [cited 2009 July 7]; Available from: <http://stemcells.nih.gov/staticresources/info/basics/SCprimer2009.pdf>.
60. Pittenger, M.F., et al., *Multilineage potential of adult human mesenchymal stem cells*. Science, 1999. **284**(5411): p. 143-7.
61. Kuci, S., et al., *Adult stem cells as an alternative source of multipotential (pluripotential) cells in regenerative medicine*. Curr Stem Cell Res Ther, 2009. **4**(2): p. 107-17.
62. De Ugarte, D.A., et al., *Comparison of multi-lineage cells from human adipose tissue and bone marrow*. Cells Tissues Organs, 2003. **174**(3): p. 101-9.
63. Erickson, G.R., et al., *Chondrogenic potential of adipose tissue-derived stromal cells in vitro and in vivo*. Biochem Biophys Res Commun, 2002. **290**(2): p. 763-9.
64. Seo, M.J., et al., *Differentiation of human adipose stromal cells into hepatic lineage in vitro and in vivo*. Biochem Biophys Res Commun, 2005. **328**(1): p. 258-64.
65. Mizuno, H., et al., *Myogenic differentiation by human processed lipoaspirate cells*. Plast Reconstr Surg, 2002. **109**(1): p. 199-209; discussion 210-1.
66. Safford, K.M., et al., *Neurogenic differentiation of murine and human adipose-derived stromal cells*. Biochem Biophys Res Commun, 2002. **294**(2): p. 371-9.
67. Chen, R.B., et al., *[Differentiation of rat adipose-derived stem cells into smooth-muscle-like cells in vitro]*. Zhonghua Nan Ke Xue, 2009. **15**(5): p. 425-30.
68. Deasy, B.M., R.J. Jankowski, and J. Huard, *Muscle-derived stem cells: characterization and potential for cell-mediated therapy*. Blood Cells Mol Dis, 2001. **27**(5): p. 924-33.
69. Usas, A. and J. Huard, *Muscle-derived stem cells for tissue engineering and regenerative therapy*. Biomaterials, 2007. **28**(36): p. 5401-6.
70. Horwitz, E.M., et al., *Isolated allogeneic bone marrow-derived mesenchymal cells engraft and stimulate growth in children with osteogenesis imperfecta: Implications for cell therapy of bone*. Proc Natl Acad Sci U S A, 2002. **99**(13): p. 8932-7.

71. Huard, J., et al., *Muscle-derived cell-mediated ex vivo gene therapy for urological dysfunction*. Gene Ther, 2002. **9**(23): p. 1617-26.
72. Friedenstein, A.J., R.K. Chailakhyan, and U.V. Gerasimov, *Bone marrow osteogenic stem cells: in vitro cultivation and transplantation in diffusion chambers*. Cell Tissue Kinet, 1987. **20**(3): p. 263-72.
73. Quarto, R., et al., *Repair of large bone defects with the use of autologous bone marrow stromal cells*. N Engl J Med, 2001. **344**(5): p. 385-6.
74. Tateishi-Yuyama, E., et al., *Therapeutic angiogenesis for patients with limb ischaemia by autologous transplantation of bone-marrow cells: a pilot study and a randomised controlled trial*. Lancet, 2002. **360**(9331): p. 427-35.
75. Koc, O.N., et al., *Allogeneic mesenchymal stem cell infusion for treatment of metachromatic leukodystrophy (MLD) and Hurler syndrome (MPS-IH)*. Bone Marrow Transplant, 2002. **30**(4): p. 215-22.
76. Kassem, M., *Mesenchymal stem cells: biological characteristics and potential clinical applications*. Cloning Stem Cells, 2004. **6**(4): p. 369-74.
77. Johnstone, B., et al., *In vitro chondrogenesis of bone marrow-derived mesenchymal progenitor cells*. Exp Cell Res, 1998. **238**(1): p. 265-72.
78. Justesen, J., et al., *Maintenance of osteoblastic and adipocytic differentiation potential with age and osteoporosis in human marrow stromal cell cultures*. Calcif Tissue Int, 2002. **71**(1): p. 36-44.
79. Stenderup, K., et al., *Aging is associated with decreased maximal life span and accelerated senescence of bone marrow stromal cells*. Bone, 2003. **33**(6): p. 919-26.
80. Caplan, A.I., *Review: mesenchymal stem cells: cell-based reconstructive therapy in orthopedics*. Tissue Eng, 2005. **11**(7-8): p. 1198-211.
81. Bruder, S.P., D.J. Fink, and A.I. Caplan, *Mesenchymal stem cells in bone development, bone repair, and skeletal regeneration therapy*. J Cell Biochem, 1994. **56**(3): p. 283-94.
82. Ohgushi, H., V.M. Goldberg, and A.I. Caplan, *Repair of bone defects with marrow cells and porous ceramic. Experiments in rats*. Acta Orthop Scand, 1989. **60**(3): p. 334-9.
83. Allay, J.A., et al., *LacZ and interleukin-3 expression in vivo after retroviral transduction of marrow-derived human osteogenic mesenchymal progenitors*. Hum Gene Ther, 1997. **8**(12): p. 1417-27.
84. Alhadlaq, A., et al., *Adult stem cell driven genesis of human-shaped articular condyle*. Ann Biomed Eng, 2004. **32**(7): p. 911-23.

85. Walles, T., et al., *Experimental generation of a tissue-engineered functional and vascularized trachea*. J Thorac Cardiovasc Surg, 2004. **128**(6): p. 900-6.
86. Kadner, A., et al., *A new source for cardiovascular tissue engineering: human bone marrow stromal cells*. Eur J Cardiothorac Surg, 2002. **21**(6): p. 1055-60.
87. Perry, T.E., et al., *Thoracic Surgery Directors Association Award. Bone marrow as a cell source for tissue engineering heart valves*. Ann Thorac Surg, 2003. **75**(3): p. 761-7; discussion 767.
88. Shukla, D., et al., *Bone marrow stem cells for urologic tissue engineering*. World J Urol, 2008. **26**(4): p. 341-9.
89. Gong, Z. and L.E. Niklason, *Small-diameter human vessel wall engineered from bone marrow-derived mesenchymal stem cells (hMSCs)*. Faseb J, 2008. **22**(6): p. 1635-48.
90. Haworth, D.J., et al. *Implementation of a novel multi-chamber bioreactor for a tissue engineered urethral wrap*. in *International Conference on Mechanics in Medicine and Biology*. 2008. Pittsburgh, PA.
91. Maul, T.M., *Mechanobiology of Stem Cells: Implications for Vascular Tissue Engineering.*, in *Bioengineering*. 2007, University of Pittsburgh: Pittsburgh.
92. Narita, Y., et al., *Effects of transforming growth factor-beta 1 and ascorbic acid on differentiation of human bone-marrow-derived mesenchymal stem cells into smooth muscle cell lineage*. Cell Tissue Res, 2008. **333**(3): p. 449-59.
93. Nieponice, A., et al., *Mechanical stimulation induces morphological and phenotypic changes in bone marrow-derived progenitor cells within a three-dimensional fibrin matrix*. J Biomed Mater Res A, 2007. **81**(3): p. 523-30.
94. Godbey, W.T. and A. Atala, *In vitro systems for tissue engineering*. Ann N Y Acad Sci, 2002. **961**: p. 10-26.
95. Kim, B.S., A. Atala, and J.J. Yoo, *A collagen matrix derived from bladder can be used to engineer smooth muscle tissue*. World J Urol, 2008. **26**(4): p. 307-14.
96. Linnes, M.P., B.D. Ratner, and C.M. Giachelli, *A fibrinogen-based precision microporous scaffold for tissue engineering*. Biomaterials, 2007. **28**(35): p. 5298-306.
97. Wichterle, O. and D. Lim, *Hydrophilic gels for biological use*. Nature, 1960. **185**: p. 117-8.
98. Bootle-Wilbraham, C.A., et al., *Fibrin fragment E stimulates the proliferation, migration and differentiation of human microvascular endothelial cells in vitro*. Angiogenesis, 2001. **4**(4): p. 269-75.

99. Cummings, C.L., et al., *Properties of engineered vascular constructs made from collagen, fibrin, and collagen-fibrin mixtures*. *Biomaterials*, 2004. **25**(17): p. 3699-706.
100. Takei, A., et al., *Effects of fibrin on the angiogenesis in vitro of bovine endothelial cells in collagen gel*. *In Vitro Cell Dev Biol Anim*, 1995. **31**(6): p. 467-72.
101. Swartz, D.D., J.A. Russell, and S.T. Andreadis, *Engineering of fibrin-based functional and implantable small-diameter blood vessels*. *Am J Physiol Heart Circ Physiol*, 2005. **288**(3): p. H1451-60.
102. Rosso, F., et al., *Smart materials as scaffolds for tissue engineering*. *J Cell Physiol*, 2005. **203**(3): p. 465-70.
103. Dvorak, H.F., et al., *Fibrin containing gels induce angiogenesis. Implications for tumor stroma generation and wound healing*. *Lab Invest*, 1987. **57**(6): p. 673-86.
104. Rowe, S.L., S. Lee, and J.P. Stegemann, *Influence of thrombin concentration on the mechanical and morphological properties of cell-seeded fibrin hydrogels*. *Acta Biomater*, 2007. **3**(1): p. 59-67.
105. Pankajakshan, D. and L.K. Krishnan, *Design of fibrin matrix composition to enhance endothelial cell growth and extracellular matrix deposition for in vitro tissue engineering*. *Artif Organs*, 2009. **33**(1): p. 16-25.
106. Jockenhoevel, S., et al., *Fibrin gel -- advantages of a new scaffold in cardiovascular tissue engineering*. *Eur J Cardiothorac Surg*, 2001. **19**(4): p. 424-30.
107. Cho, S.W., et al., *Engineering of volume-stable adipose tissues*. *Biomaterials*, 2005. **26**(17): p. 3577-85.
108. Yoo, W.J., et al., *Implantation of perichondrium-derived chondrocytes in physeal defects of rabbit tibiae*. *Acta Orthop*, 2005. **76**(5): p. 628-36.
109. Dare, E.V., et al., *Differentiation of a fibrin gel encapsulated chondrogenic cell line*. *Int J Artif Organs*, 2007. **30**(7): p. 619-27.
110. Birla, R.K., et al., *Myocardial engineering in vivo: formation and characterization of contractile, vascularized three-dimensional cardiac tissue*. *Tissue Eng*, 2005. **11**(5-6): p. 803-13.
111. Bruns, H., et al., *Injectable liver: a novel approach using fibrin gel as a matrix for culture and intrahepatic transplantation of hepatocytes*. *Tissue Eng*, 2005. **11**(11-12): p. 1718-26.
112. Lee, A.C., et al., *Controlled release of nerve growth factor enhances sciatic nerve regeneration*. *Exp Neurol*, 2003. **184**(1): p. 295-303.

113. Taylor, S.J., J.W. McDonald, 3rd, and S.E. Sakiyama-Elbert, *Controlled release of neurotrophin-3 from fibrin gels for spinal cord injury*. J Control Release, 2004. **98**(2): p. 281-94.
114. Duchesne, B., H. Tahi, and A. Galand, *Use of human fibrin glue and amniotic membrane transplant in corneal perforation*. Cornea, 2001. **20**(2): p. 230-2.
115. Rama, P., et al., *Autologous fibrin-cultured limbal stem cells permanently restore the corneal surface of patients with total limbal stem cell deficiency*. Transplantation, 2001. **72**(9): p. 1478-85.
116. Hojo, M., et al., *Induction of vascular endothelial growth factor by fibrin as a dermal substrate for cultured skin substitute*. Plast Reconstr Surg, 2003. **111**(5): p. 1638-45.
117. Atala, A., L. Guzman, and A.B. Retik, *A novel inert collagen matrix for hypospadias repair*. J Urol, 1999. **162**(3 Pt 2): p. 1148-51.
118. Ozgok, Y., et al., *Use of bladder mucosal graft for urethral reconstruction*. Int J Urol, 2000. **7**(10): p. 355-60.
119. Bach, A.D., et al., *Fibrin glue as matrix for cultured autologous urothelial cells in urethral reconstruction*. Tissue Eng, 2001. **7**(1): p. 45-53.
120. Chen, F., J.J. Yoo, and A. Atala, *Experimental and clinical experience using tissue regeneration for urethral reconstruction*. World J Urol, 2000. **18**(1): p. 67-70.
121. Arakawa, E., et al., *A mouse bone marrow stromal cell line, TBR-B, shows inducible expression of smooth muscle-specific genes*. FEBS Lett, 2000. **481**(2): p. 193-6.
122. Caplice, N.M. and B. Doyle, *Vascular progenitor cells: origin and mechanisms of mobilization, differentiation, integration, and vasculogenesis*. Stem Cells Dev, 2005. **14**(2): p. 122-39.
123. Goodell, M.A., et al., *Stem cell plasticity in muscle and bone marrow*. Ann N Y Acad Sci, 2001. **938**: p. 208-18; discussion 218-20.
124. Jerareungrattan, A., M. Sila-asna, and A. Bunyaratvej, *Increased smooth muscle actin expression from bone marrow stromal cells under retinoic acid treatment: an attempt for autologous blood vessel tissue engineering*. Asian Pac J Allergy Immunol, 2005. **23**(2-3): p. 107-13.
125. Champy, C., *Quelques resultas de la method de culture des tissus. I. Generalities II. Le muscle lisse (note preliminaire)*. Arch Zool Exp Gen, 1913. **53**: p. 42-51.
126. Thyberg, J., *Differentiated properties and proliferation of arterial smooth muscle cells in culture*. Int Rev Cytol, 1996. **169**: p. 183-265.

127. Thyberg, J., et al., *Regulation of differentiated properties and proliferation of arterial smooth muscle cells*. Arteriosclerosis, 1990. **10**(6): p. 966-90.
128. Dai, J.M., et al., *Acetylcholine-induced asynchronous calcium waves in intact human bronchial muscle bundle*. Am J Respir Cell Mol Biol, 2007. **36**(5): p. 600-8.
129. Deng, H., et al., *Inhibition of glycogen synthase kinase-3beta is sufficient for airway smooth muscle hypertrophy*. J Biol Chem, 2008. **283**(15): p. 10198-207.
130. Watanabe, S., et al., *Expression of functional leukotriene B4 receptors on human airway smooth muscle cells*. J Allergy Clin Immunol, 2009. **124**(1): p. 59-65 e1-3.
131. Cheng, E.Y., et al., *Angiotensin II and basic fibroblast growth factor induce neonatal bladder stromal cell mitogenesis*. J Urol, 1996. **156**(2 Pt 2): p. 593-7.
132. Freeman, M.R., et al., *Heparin-binding EGF-like growth factor is an autocrine growth factor for human urothelial cells and is synthesized by epithelial and smooth muscle cells in the human bladder*. J Clin Invest, 1997. **99**(5): p. 1028-36.
133. Lau, C.L. and S. Chacko, *Identification of two types of smooth muscle cells from rabbit urinary bladder*. Tissue Cell, 1996. **28**(3): p. 339-55.
134. Persson, K., W.D. Steers, and J.B. Tuttle, *Regulation of nerve growth factor secretion in smooth muscle cells cultured from rat bladder body, base and urethra*. J Urol, 1997. **157**(5): p. 2000-6.
135. Hollywood, M.A., et al., *T- and L-type Ca<sup>2+</sup> currents in freshly dispersed smooth muscle cells from the human proximal urethra*. J Physiol, 2003. **550**(Pt 3): p. 753-64.
136. Sergeant, G.P., et al., *Spontaneous Ca<sup>2+</sup> activated Cl<sup>-</sup> currents in isolated urethral smooth muscle cells*. J Urol, 2001. **166**(3): p. 1161-6.
137. Jankowski, R.J., et al., *Development of an experimental system for the study of urethral biomechanical function*. Am J Physiol Renal Physiol, 2004. **286**(2): p. F225-32.
138. Cotton, K.D., et al., *Effect of purinergic blockers on outward current in isolated smooth muscle cells of the sheep bladder*. Am J Physiol, 1996. **270**(3 Pt 1): p. C969-73.
139. Chambers, P., D.E. Neal, and J.I. Gillespie, *Ca<sup>2+</sup> signalling in cultured smooth muscle cells from human bladder*. Exp Physiol, 1996. **81**(4): p. 553-64.
140. Ferreira, L.S., et al., *Vascular progenitor cells isolated from human embryonic stem cells give rise to endothelial and smooth muscle like cells and form vascular networks in vivo*. Circ Res, 2007. **101**(3): p. 286-94.

141. Rowlands, A.S. and J.J. Cooper-White, *Directing phenotype of vascular smooth muscle cells using electrically stimulated conducting polymer*. *Biomaterials*, 2008. **29**(34): p. 4510-20.
142. Song, J., et al., *Reorganization of structural proteins in vascular smooth muscle cells grown in collagen gel and basement membrane matrices (Matrigel): a comparison with their in situ counterparts*. *J Struct Biol*, 2001. **133**(1): p. 43-54.
143. Owens, G.K., M.S. Kumar, and B.R. Wamhoff, *Molecular regulation of vascular smooth muscle cell differentiation in development and disease*. *Physiol Rev*, 2004. **84**(3): p. 767-801.
144. Pepper, M.S., *Transforming growth factor-beta: vasculogenesis, angiogenesis, and vessel wall integrity*. *Cytokine Growth Factor Rev*, 1997. **8**(1): p. 21-43.
145. Hautmann, M.B., P.J. Adam, and G.K. Owens, *Similarities and differences in smooth muscle alpha-actin induction by TGF-beta in smooth muscle versus non-smooth muscle cells*. *Arterioscler Thromb Vasc Biol*, 1999. **19**(9): p. 2049-58.
146. Ross, J.J. and R.T. Tranquillo, *ECM gene expression correlates with in vitro tissue growth and development in fibrin gel remodeled by neonatal smooth muscle cells*. *Matrix Biol*, 2003. **22**(6): p. 477-90.
147. Magnan, M., et al., *Tissue engineering of a genitourinary tubular tissue graft resistant to suturing and high internal pressures*. *Tissue Eng Part A*, 2009. **15**(1): p. 197-202.
148. Davidson, J.M., et al., *Ascorbate differentially regulates elastin and collagen biosynthesis in vascular smooth muscle cells and skin fibroblasts by pretranslational mechanisms*. *J Biol Chem*, 1997. **272**(1): p. 345-52.
149. Kim, P.D., et al., *The influence of ascorbic acid, TGF-beta1, and cell-mediated remodeling on the bulk mechanical properties of 3-D PEG-fibrinogen constructs*. *Biomaterials*, 2009. **30**(23-24): p. 3854-64.
150. Losurdo, J.L., *Mechanically- and biochemically- induced differentiation of bone marrow-derived mesenchymal stem cells to smooth muscle cells in a three-dimensional fibrin matrix*, in *Bioengineering*. 2008, University of Pittsburgh: Pittsburgh.
151. Bonnet, P., et al., *Electrophysiological maturation of rat mesenchymal stem cells after induction of vascular smooth muscle cell differentiation in vitro*. *Stem Cells Dev*, 2008. **17**(6): p. 1131-40.
152. Hamilton, D.W., T.M. Maul, and D.A. Vorp, *Characterization of the response of bone marrow-derived progenitor cells to cyclic strain: implications for vascular tissue-engineering applications*. *Tissue Eng*, 2004. **10**(3-4): p. 361-9.

153. Ross, J.J., et al., *Cytokine-induced differentiation of multipotent adult progenitor cells into functional smooth muscle cells*. J Clin Invest, 2006. **116**(12): p. 3139-49.
154. Javazon, E.H., et al., *Rat marrow stromal cells are more sensitive to plating density and expand more rapidly from single-cell-derived colonies than human marrow stromal cells*. Stem Cells, 2001. **19**(3): p. 219-25.
155. Banes, A.J., et al., *Culturing cells in a mechanically active environment*. Am Biotechnol Lab, 1990. **8**(7): p. 12-22.
156. Sumpio, B.E. and A.J. Banes, *Prostacyclin synthetic activity in cultured aortic endothelial cells undergoing cyclic mechanical deformation*. Surgery, 1988. **104**(2): p. 383-9.
157. Sumpio, B.E., et al., *Modulation of endothelial cell phenotype by cyclic stretch: inhibition of collagen production*. J Surg Res, 1990. **48**(5): p. 415-20.
158. Clapham, D.E., *Calcium signaling*. Cell, 1995. **80**(2): p. 259-68.
159. Kullmann, F.A., et al., *Heterogeneity of muscarinic receptor-mediated Ca<sup>2+</sup> responses in cultured urothelial cells from rat*. Am J Physiol Renal Physiol, 2008. **294**(4): p. F971-81.
160. Harris, A.K., P. Wild, and D. Stopak, *Silicone rubber substrata: a new wrinkle in the study of cell locomotion*. Science, 1980. **208**(4440): p. 177-9.
161. Beningo, K.A. and Y.L. Wang, *Flexible substrata for the detection of cellular traction forces*. Trends Cell Biol, 2002. **12**(2): p. 79-84.
162. Burton, K. and D.L. Taylor, *Traction forces of cytokinesis measured with optically modified elastic substrata*. Nature, 1997. **385**(6615): p. 450-4.
163. Butler, J.P., et al., *Traction fields, moments, and strain energy that cells exert on their surroundings*. Am J Physiol Cell Physiol, 2002. **282**(3): p. C595-605.
164. Galbraith, C.G. and M.P. Sheetz, *A micromachined device provides a new bend on fibroblast traction forces*. Proc Natl Acad Sci U S A, 1997. **94**(17): p. 9114-8.
165. Iwadate, Y. and S. Yumura, *Molecular dynamics and forces of a motile cell simultaneously visualized by TIRF and force microscopies*. Biotechniques, 2008. **44**(6): p. 739-50.
166. Bernal, P.J., et al., *Nitric-oxide-mediated zinc release contributes to hypoxic regulation of pulmonary vascular tone*. Circ Res, 2008. **102**(12): p. 1575-83.

167. Reusch, H.P., et al., *Activation of JNK/SAPK and ERK by mechanical strain in vascular smooth muscle cells depends on extracellular matrix composition*. *Biochem Biophys Res Commun*, 1997. **237**(2): p. 239-44.
168. Prantil-Baun, R.L., *Biomechanics and function of the female rat urethra in stress urinary incontinence induced by birth trauma.*, in *Bioengineering*. 2007, University of Pittsburgh: Pittsburgh.